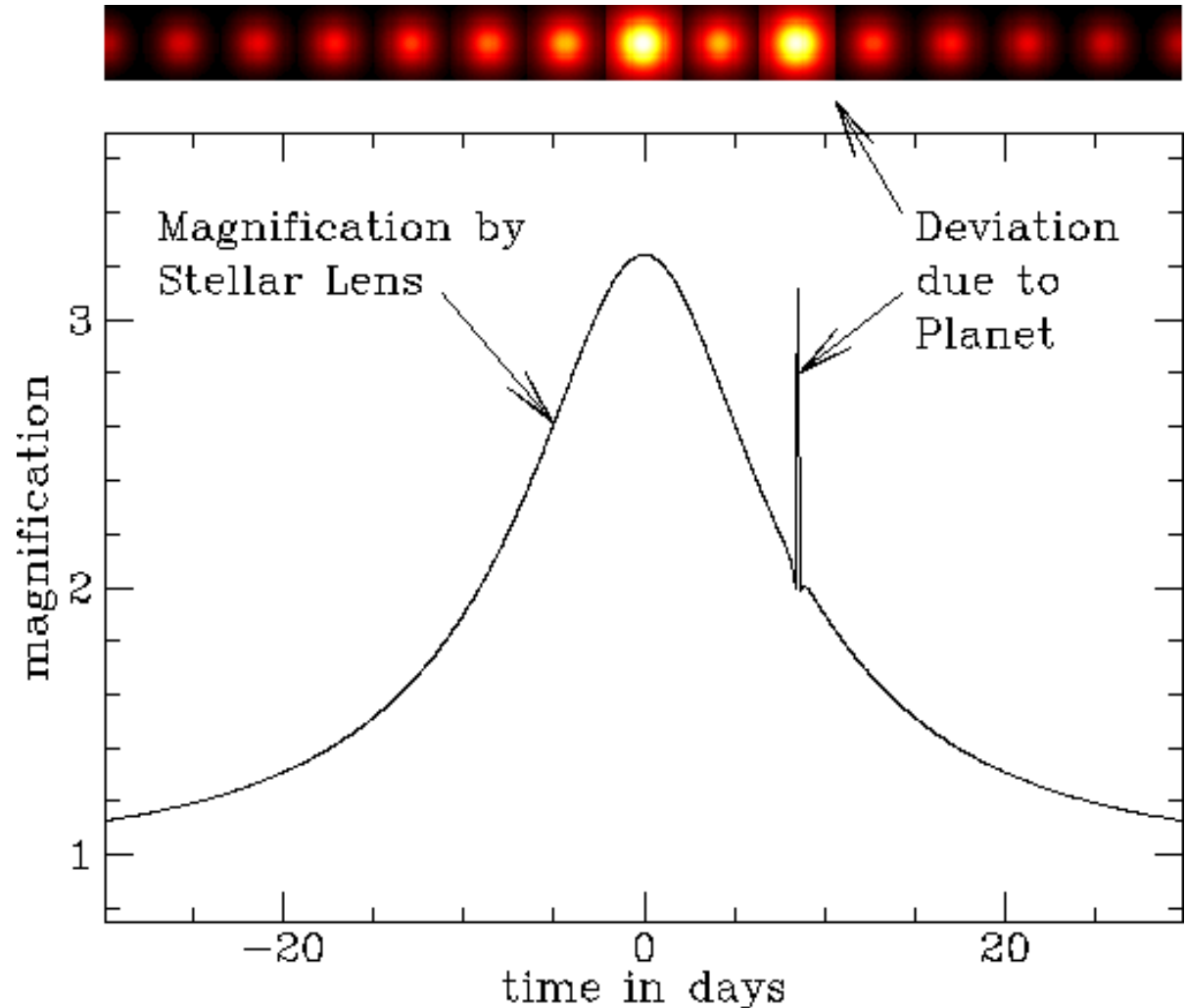


# Microlensing Events with Multiple Lens Masses and/or Multiple Source Stars

David Bennett

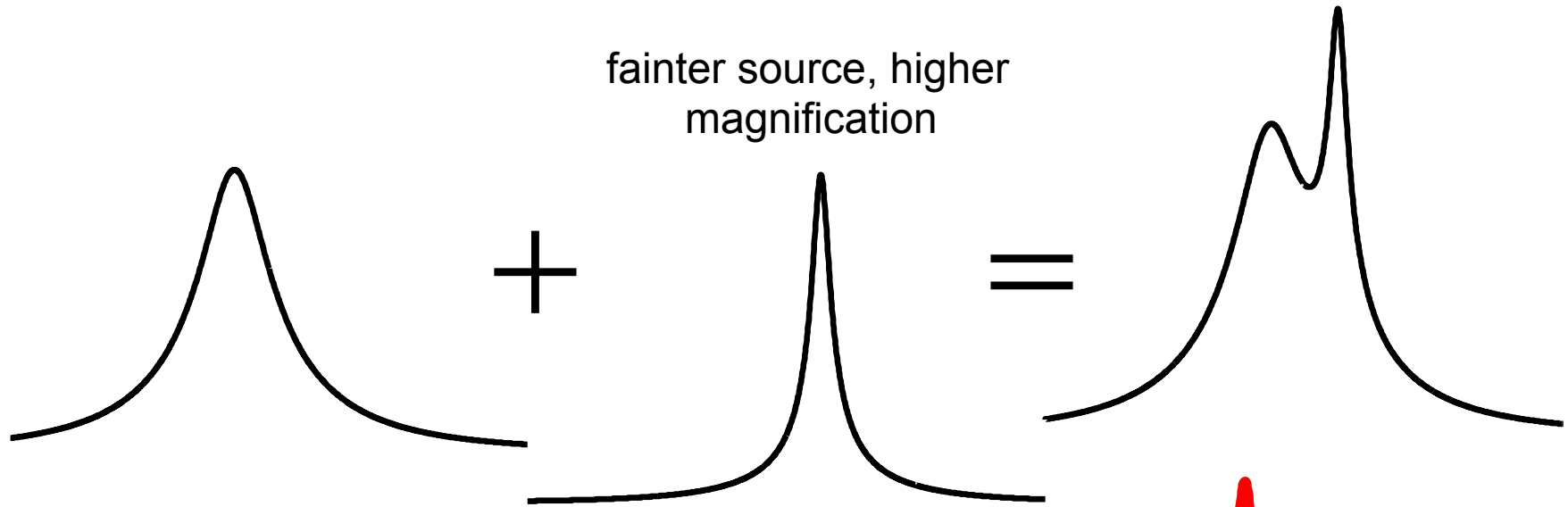
NASA Goddard Space  
Flight Center



# Talk Outline

- Quick slide on binary sources
- Binary lenses
  - Lens equation
  - Lens images
  - Caustics and Cusps
  - Magnification calculations for modeling
  - Calculation of light curves
- Binary Lens vs. Binary Source
  - False planetary events
  - Binary Lens Plus Binary Source
- Planetary events not easily identified by eye

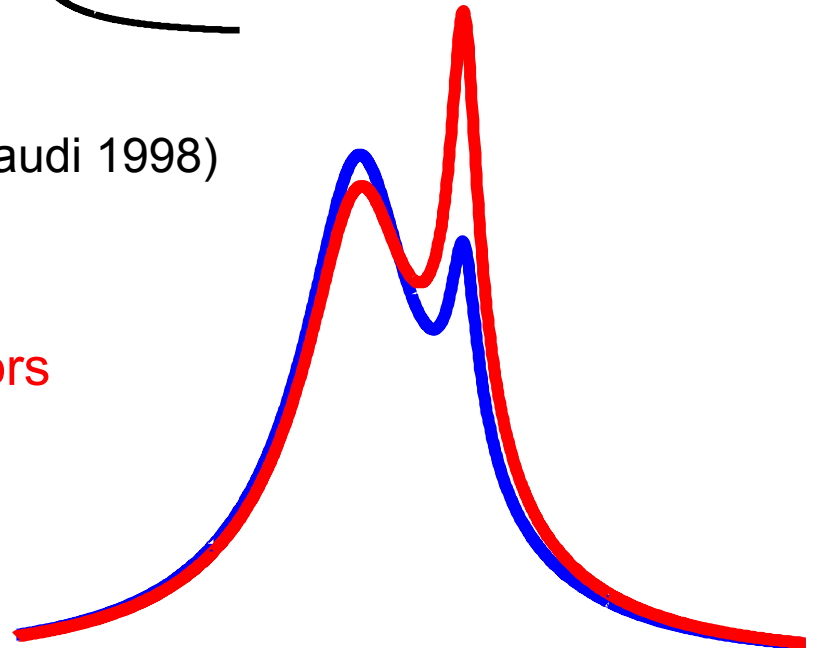
# Binary Source Events



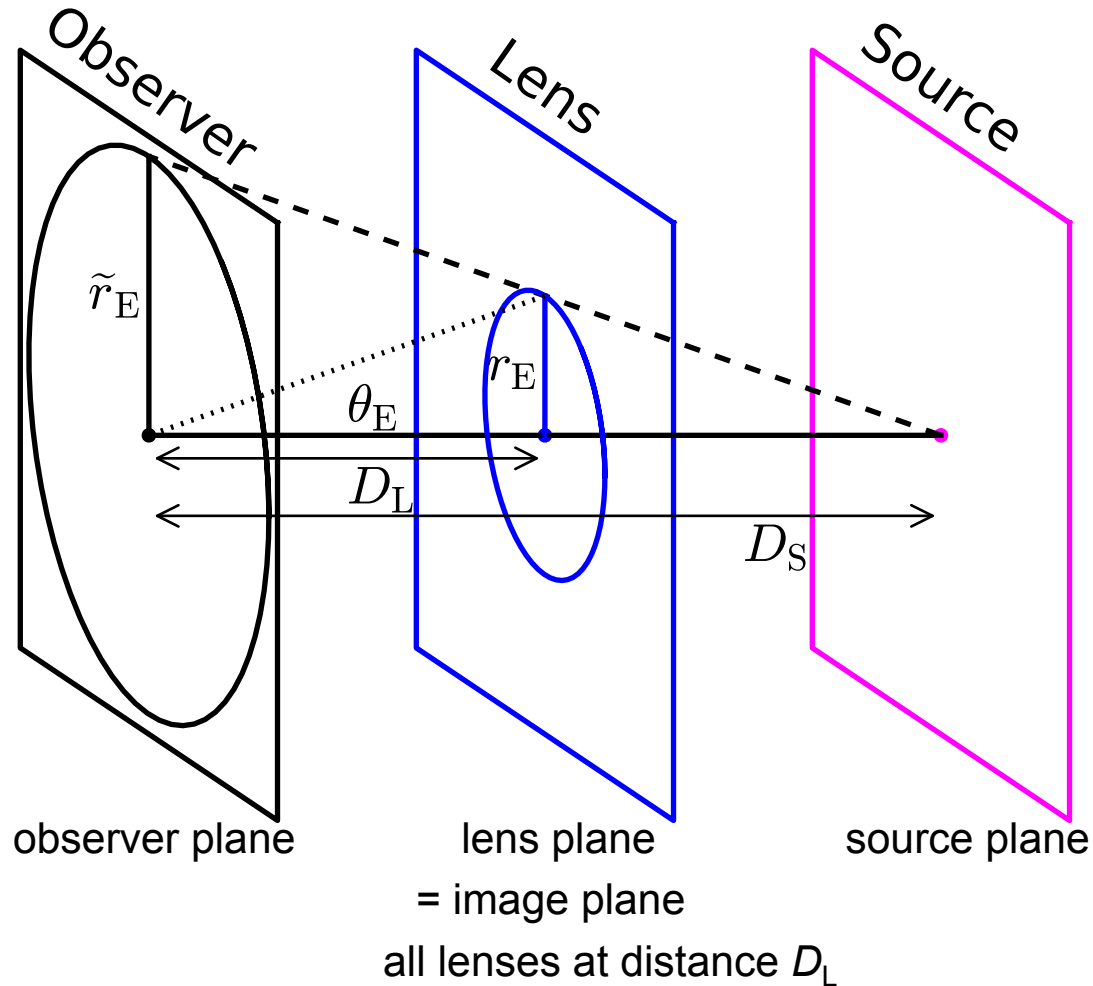
Possible ambiguity with planetary events (Gaudi 1998)

But, source stars have **different colors**

Binary companions cause orbital motion:  
“xallarap”, which can be confused with  
microlensing parallax



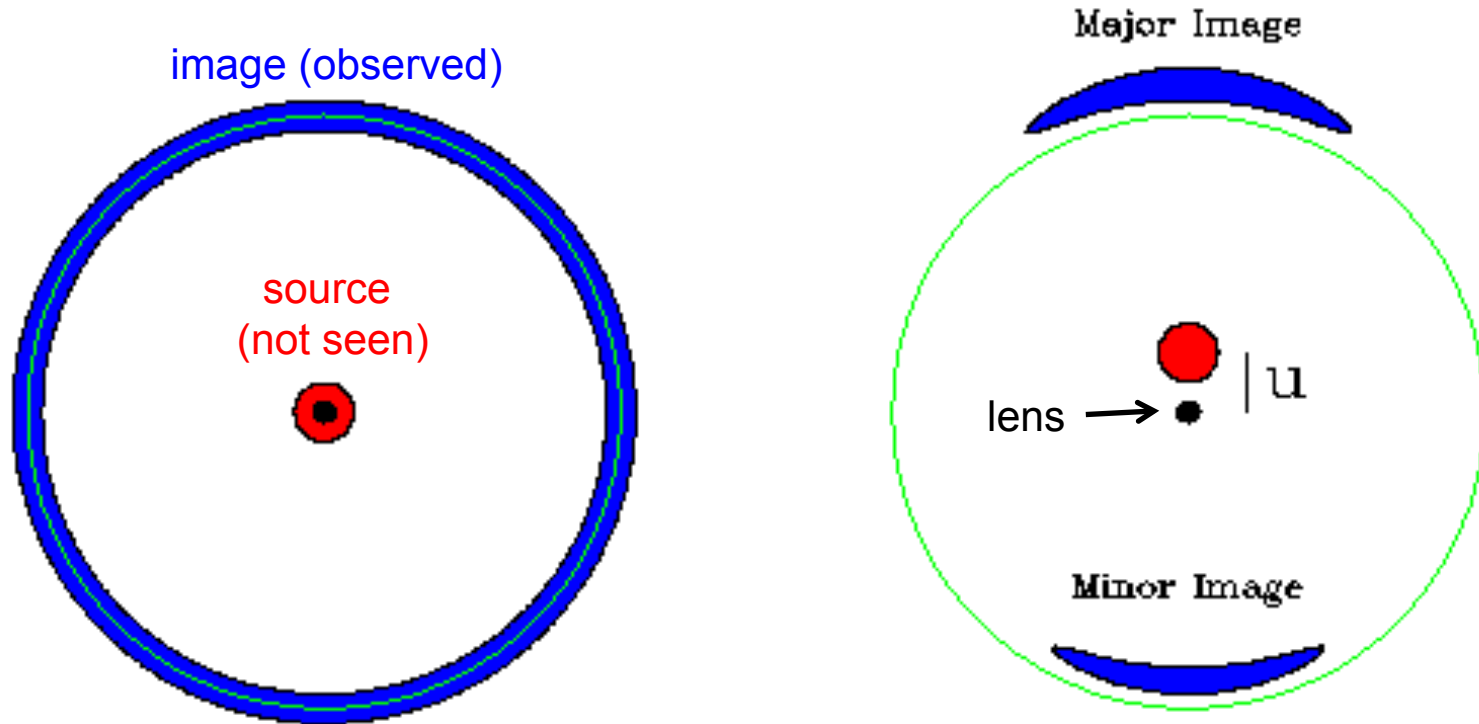
# Binary Lenses Are More Complicated



Gravitational bending angle in small angle approximation:

$$\alpha = \frac{4GM}{c^2 r}$$

# Lensed Images for a Single Lens Mass (Einstein 1936)



Perfect alignment gives an “Einstein Ring” image, and images are highly magnified near the Einstein ring when the alignment is nearly perfect. Planets are most easily detected near the Einstein ring (typically at 2-3 AU) when they distort one of the lensed images.

# Lens Equation

use angular coordinates  
or coordinates projected  
to the lens plane

lens equation with  
Cartesian coordinates

$w$  = source position

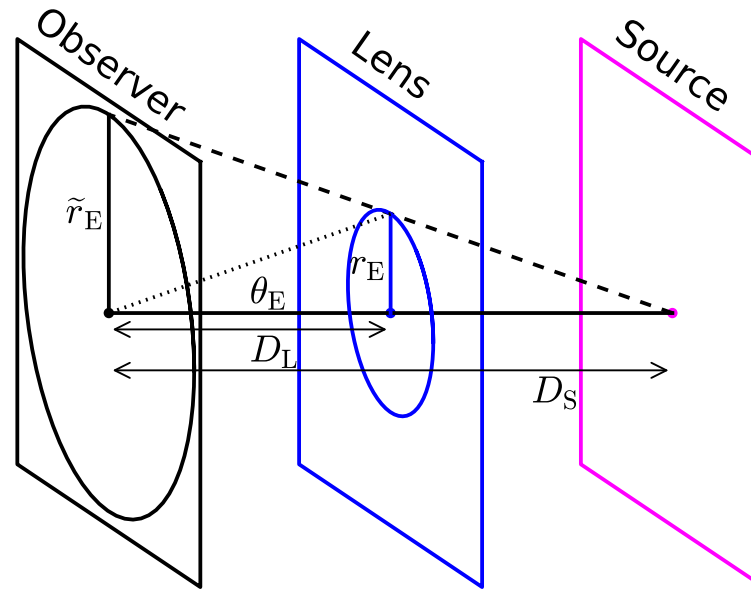
$z$  = image position

$x_i$  =  $i$ th lens mass position

Scale to angular Einstein  
radius

switch to complex  
notation

(Witt 1990, Rhie 1997)



$$\vec{z} - \vec{w} = \frac{4GM_1}{c^2} \frac{\vec{z} - \vec{x}_1}{|\vec{z} - \vec{x}_1|^2} + \frac{4GM_2}{c^2} \frac{\vec{z} - \vec{x}_2}{|\vec{z} - \vec{x}_2|^2} + \dots$$

$$\theta_E = 2\sqrt{\frac{GM}{c^2} \frac{D_S - D_L}{D_S D_L}} \quad D_S, D_L = \text{source, lens distances}$$

$$w = z - \sum_{i=1}^n \frac{\varepsilon_i}{\bar{z} - \bar{x}_i} \quad \text{for } n \text{ point masses}$$

$$\left(\text{where } \varepsilon_i = \frac{M_i}{\sum M_i} \text{ and } \bar{z} \text{ is complex conjugate of } z\right)$$

# Solve the Lens Equation: Inverse Ray Shooting

$$w = z - \sum_{i=1}^n \frac{\epsilon_i}{\bar{z}_i - \bar{x}_i}$$

- If we know the image position,  $z$ , then it is easy to solve for the source position,  $w$
- This is called inverse ray shooting (or inverse ray tracing)
  - + completely general; can be done for any lens configuration, i.e. > 4 masses, galaxies, galaxy clusters
  - very slow, because many rays must be shot
  - + basis of magnification map method for a brute force search for light curve models – this uses one magnification map for many calculations
  - many maps must be calculated to include lens orbital motion

# Solve the Lens Equation

- Take complex conjugate of lens equation to give equation for  $\bar{z}$
- eliminate  $\bar{z}$  to yield equation for only  $z$
- multiply by the denominators to clear the fractions and create a polynomial equation of order  $n^2 + 1$
- for  $n = 1$ , polynomial is a quadratic with 2 solutions
- for  $n = 2$ , polynomial is 5<sup>th</sup> order with 3 or 5 solutions
  - polynomial always has 5 solutions, but some are not solutions to the lens equation
- for  $n = 3$ , polynomial is 10<sup>th</sup> order with 4, 6, 8, or 10 solutions
- minimum number of solutions is  $n + 1 \rightarrow 1$  for each source and lens
  - when alignment is poor, there is 1 image direct from the source and very low magnification images bent by a large angle by each lens
- maximum number of images is  $5n - 5$  for  $n > 1$  (Rhie 2003; Khavinson & Neumann 2006)
  - Rhie constructed solutions with  $5n - 5$  solutions and Khavinson & Neumann proved that is the upper limit solving a pure math problem (extension of the fundamental theorem of algebra)

# Solve the Lens Equation (2)

- 3<sup>rd</sup> and 4<sup>th</sup> order polynomial equations have analytic solutions, but 5<sup>th</sup> order equations do not
- Recipe for lens equation solutions
  - Solve for image positions,  $z$ , numerically using standard root solving routines (or custom routines)
  - double precision is probably necessary for planetary binary events
  - quadruple precision is needed for many triple lens cases (available in most fortran implementations)
  - plug  $z$  values from polynomial solution back into lens eq. to find true lens eq. solutions
- Relate image positions to magnification
  - lensing doesn't change surface brightness
  - image brightness = [(image area)/(source area)] × (surface brightness)

$$w = z - \sum_{i=1}^n \frac{\epsilon_i}{\bar{z}_i - \bar{x}_i}$$

# Magnification from the Lens Equation

- (image area)/(source area) from lens equation:  $w = z - \sum_{i=1}^n \frac{\epsilon_i}{\bar{z}_i - \bar{x}_i}$
- The magnification for a point source can be derived from the Jacobian determinant of the lens equation:
$$J = \frac{\partial w}{\partial z} \frac{\partial \bar{w}}{\partial \bar{z}} - \frac{\partial w}{\partial \bar{z}} \frac{\partial \bar{w}}{\partial z} = 1 - \left| \frac{\partial w}{\partial \bar{z}} \right|^2$$
- Where  $\frac{\partial w}{\partial \bar{z}} = \sum_i \frac{\epsilon_i}{(\bar{z} - \bar{x}_i)^2}$
- This is the Jacobian determinant of the inverse mapping from the image to the source plane, so the magnification for each image is given by

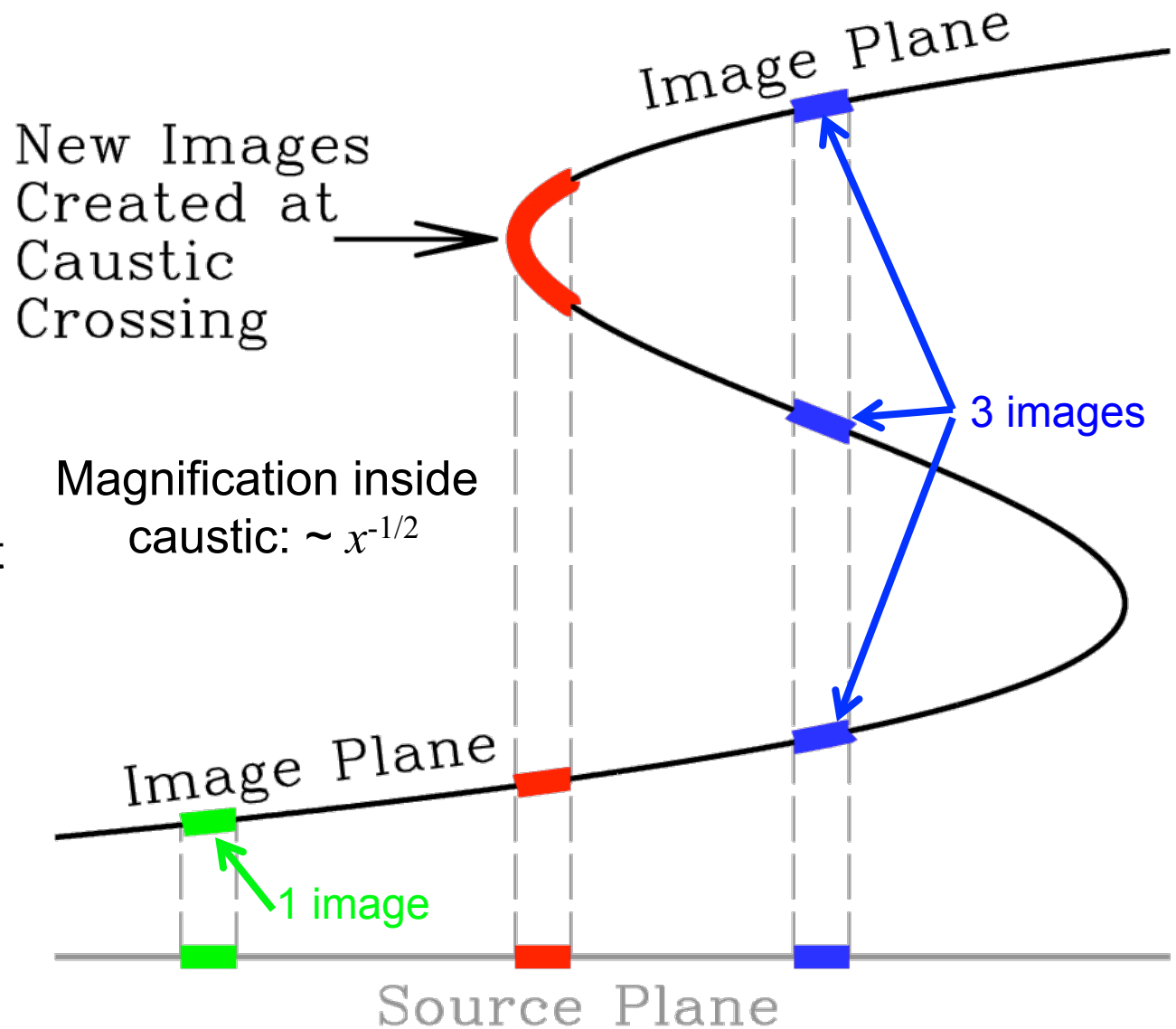
$$A = \frac{1}{|J|}$$

evaluated at the position of each image

- Critical curves are image locations where  $|J| = 0$ , i.e. infinite magnification
- Caustics are the corresponding source locations

# New Lens Image Pairs Appear on Caustics

- Lensing = smooth mapping from image plane to source plane
- Source plane = what we would see if there was no lens
- Image plane = what we really see
- Caustic crossings give 2 new images
- Infinite magnification for point sources



# Lensed images at $\mu$ arcsec resolution

lens star and planet =  
black •'s

blue • = source

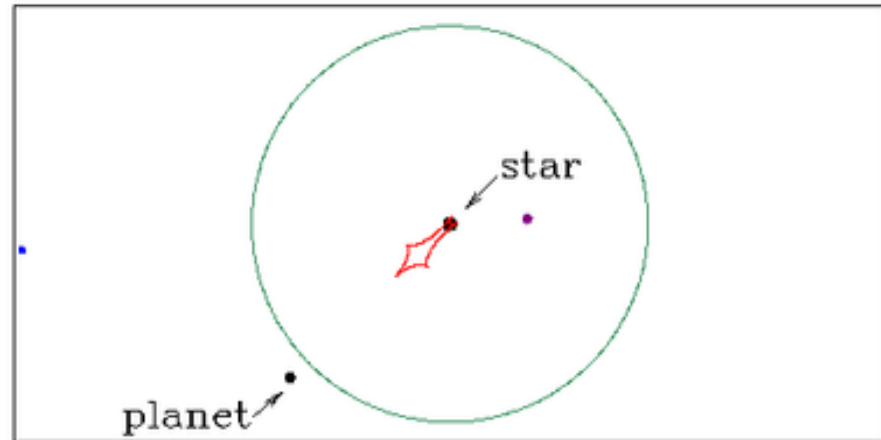
green ○ = Einstein ring

red curve = caustic

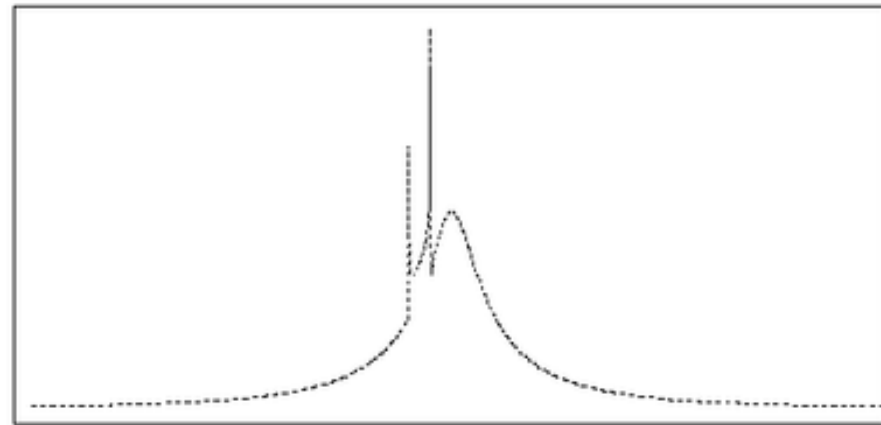
new images created or  
destroyed at **caustic**  
crossings

Highly magnified images  
near Einstein ring

View from telescope



Magnification

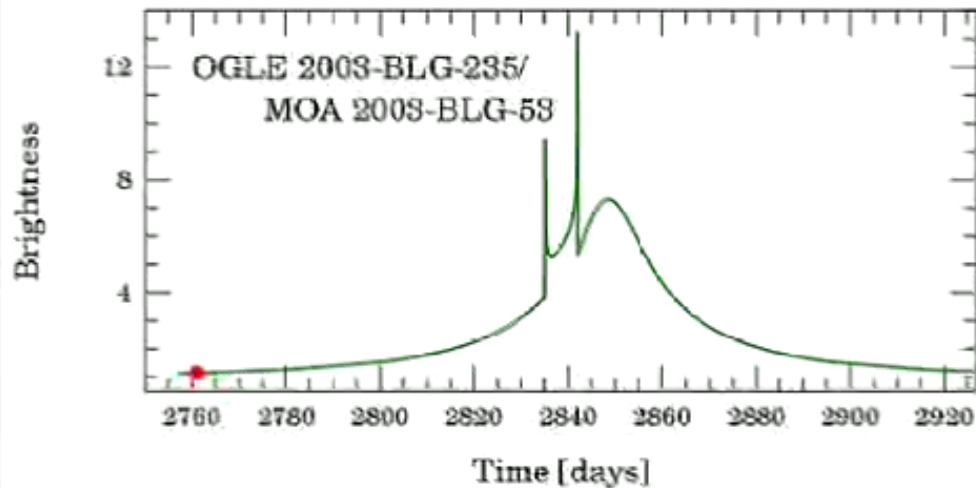
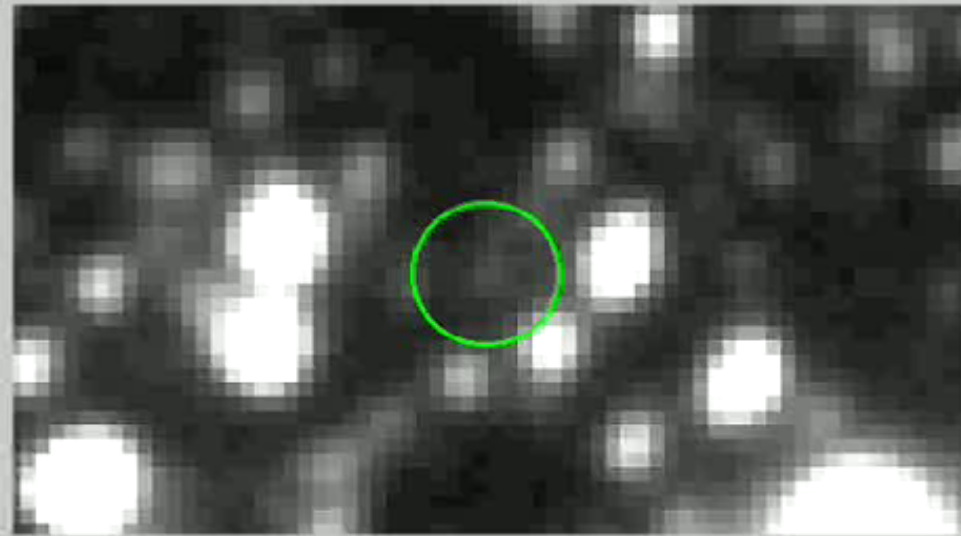


Time

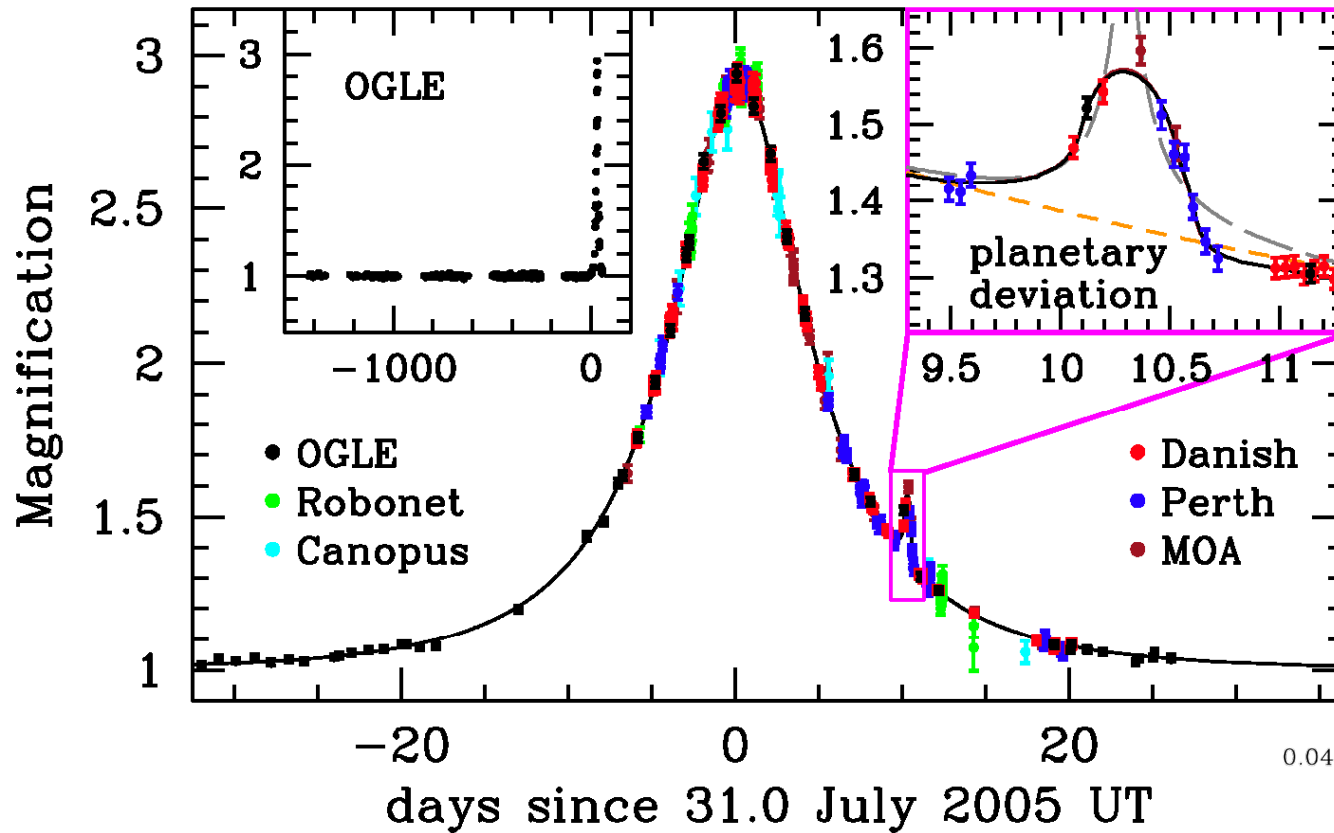
OGLE-2003-BLG-235 = 1<sup>st</sup> planetary microlensing event  
Bond et al. (2004)

# Simulated Lightcurve of 1st Planetary Event

Simulated version  
of actual data with  
~1" seeing



# OGLE-2005-BLG-390Lb - "lowest" mass exoplanet

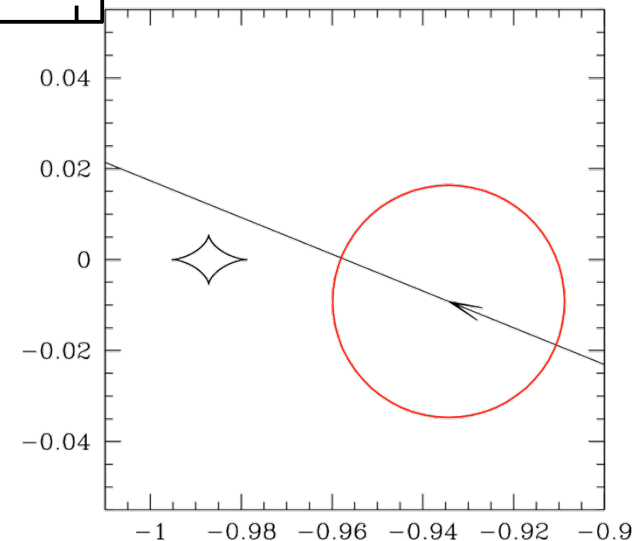


A  $5.5 M_{\oplus}$  planet discovered by microlensing: OGLE-2005-BLG-390Lb. The lowest mass planet discovered when announced in 2006.

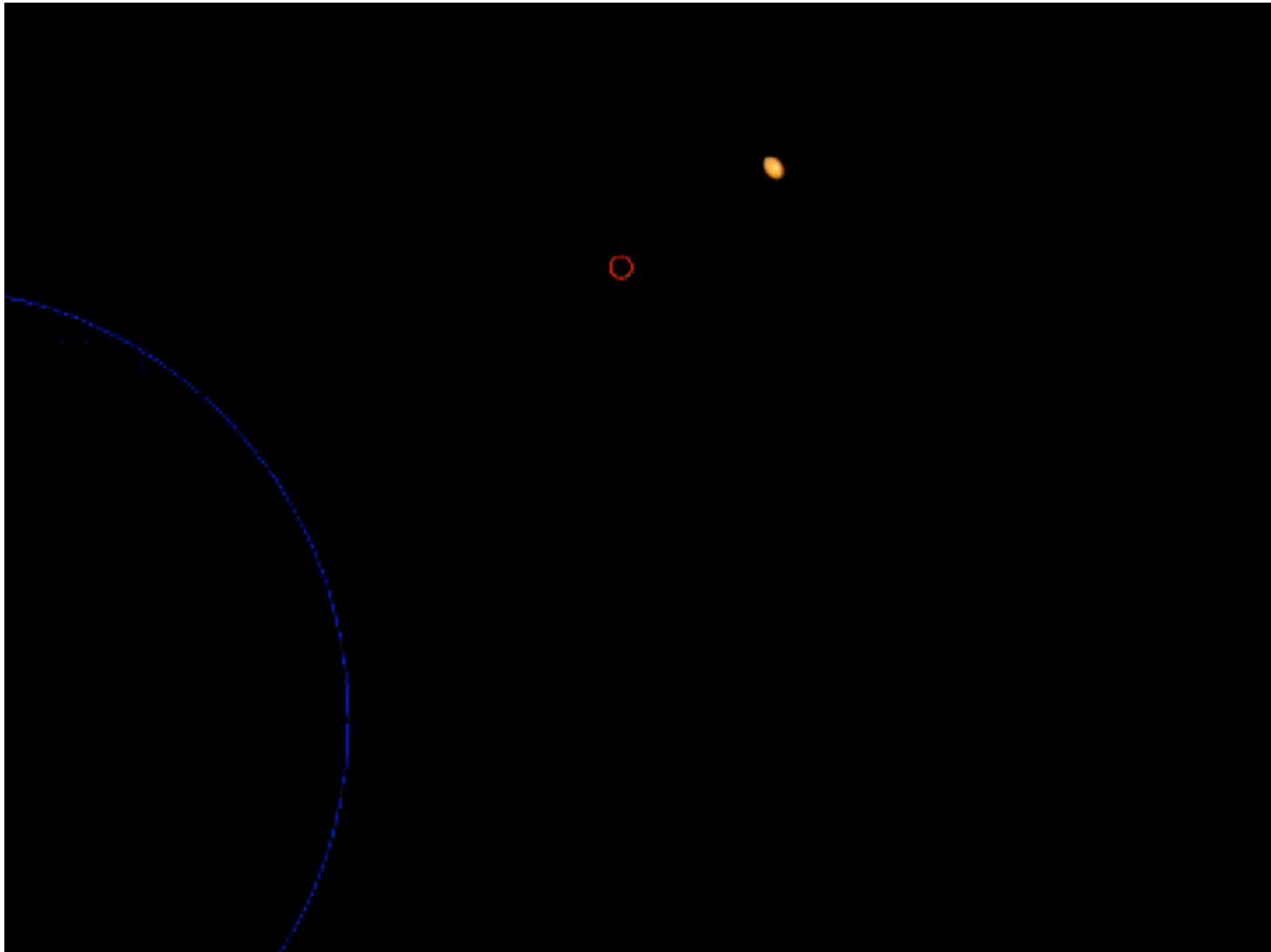
Source passes over caustic => significant finite source effect and clear measurement of  $t_*$

Giant source star means lens star detection will be difficult

PLANET, OGLE & MOA Collaborations  
Beaulieu et al. (2006)



# OGLE-2005-BLG-390Lb at high resolution

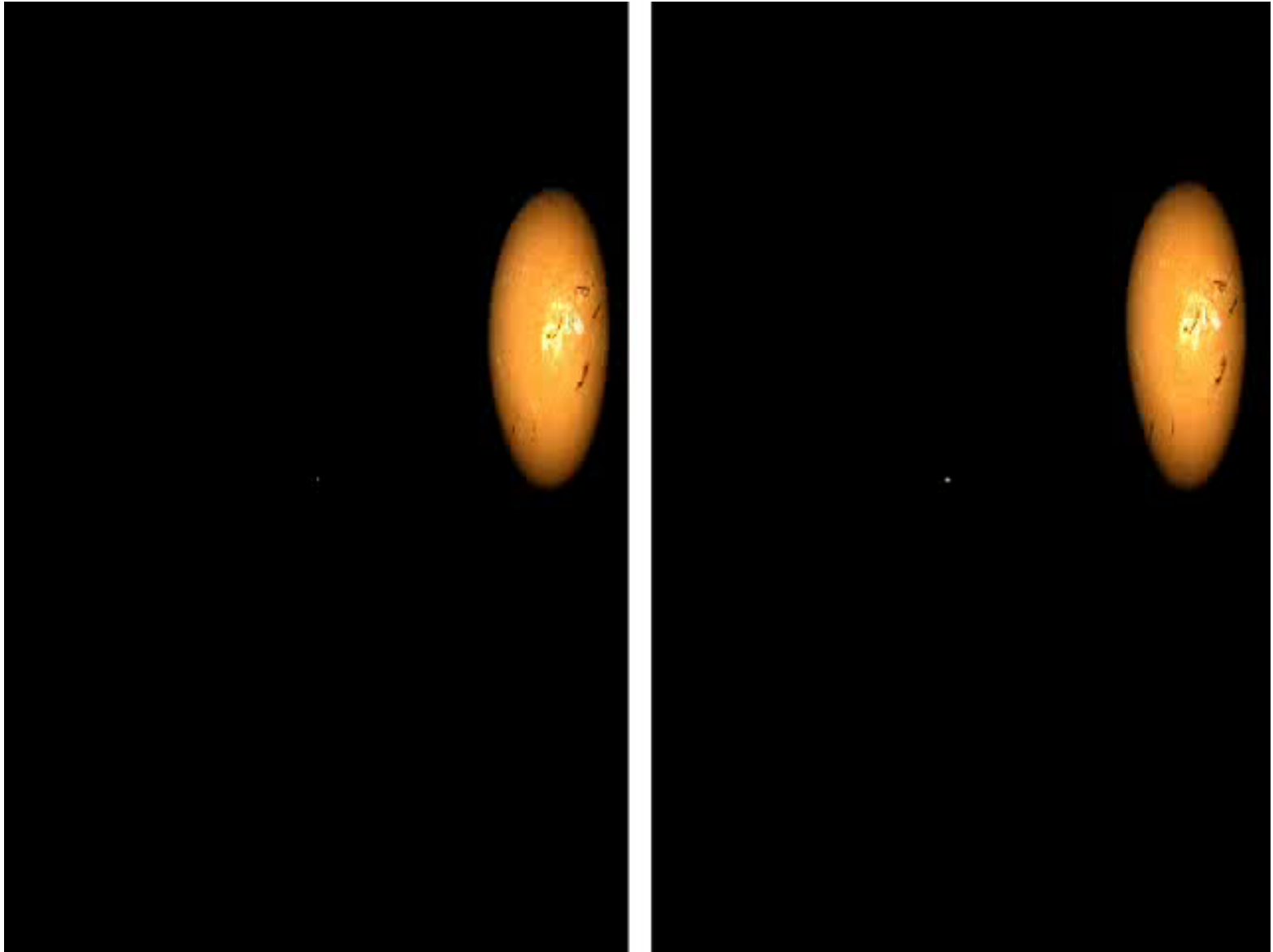


- Simulated view from 10,000 km aperture space telescope
- H- $\alpha$  filter Solar images generate cool videos! (videos by Bennett & Williams)

# Exoplanet lensing video



# OGLE-2005-BLG-390Lb at high resolution



5.5 Earth-mass planet vs. 16.5 Earth-mass planet.

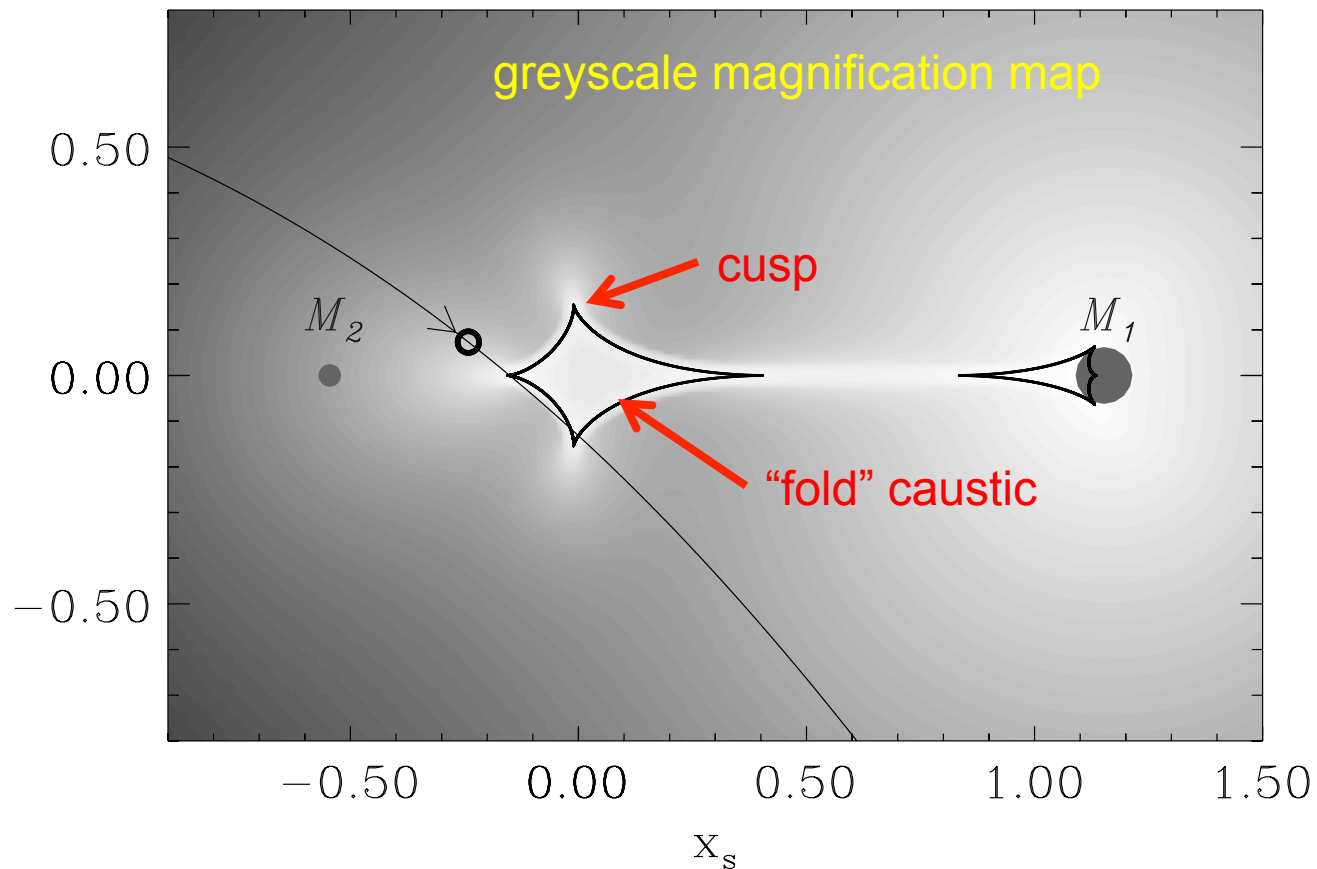
Only the total image area is observable. 5.5 Earth-mass is near limit for giant source.

# Caustics and Cusps Control Image Magnification

Lensing magnification is high just inside the caustic curve.

The sharp points on the caustic curves are called cusps. They indicate higher magnification not only inside but also outside the caustic

Most planetary light curve signals are due to caustic crossings and cusp approaches.

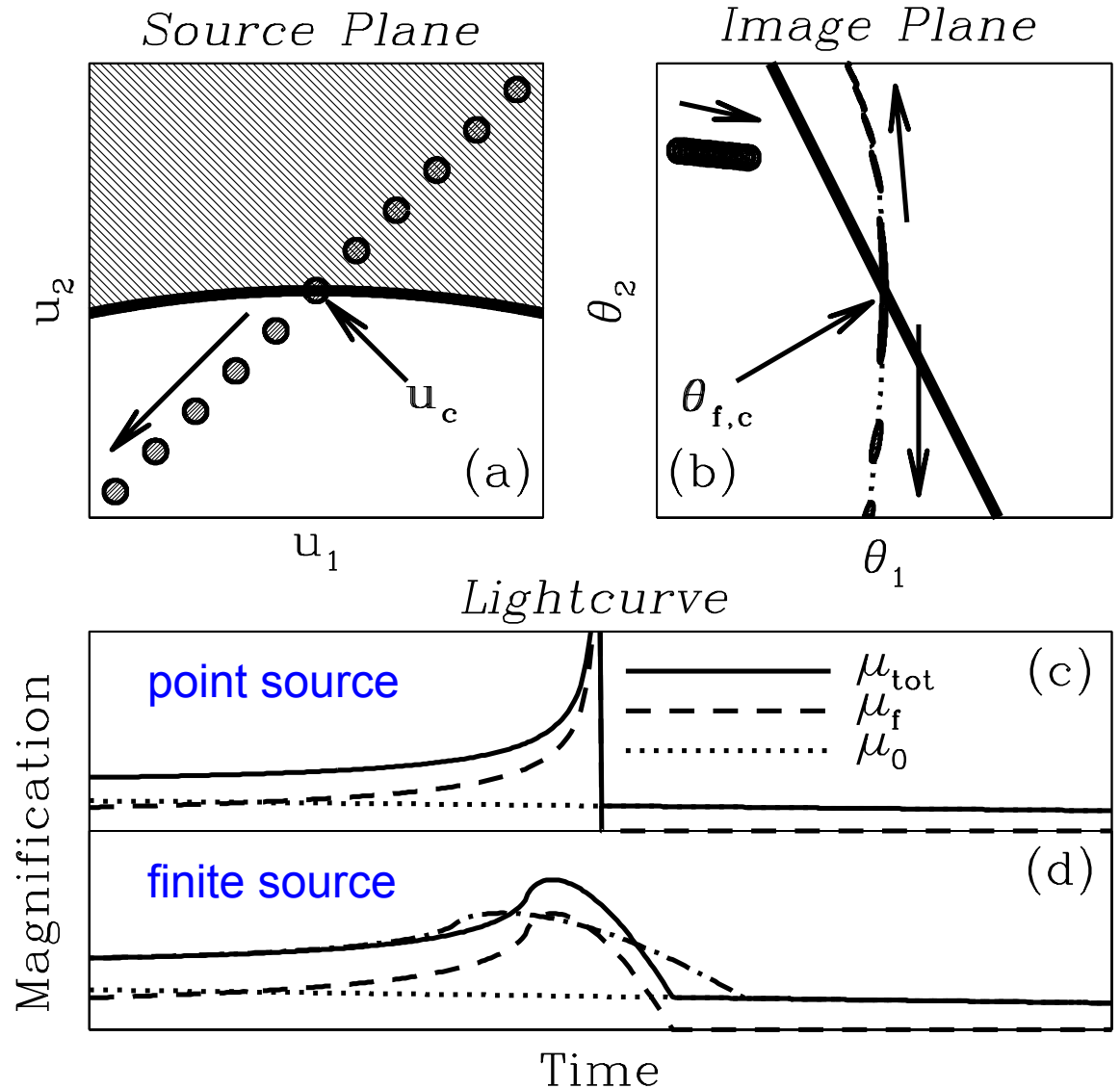


Major image caustic for  $s > 1$   
OGLE-2012-BLG-0358 example (Han et al. 2014)

# Fold Caustic

- 2 additional images are highly magnified with roughly equal magnification inside caustic
- images disappear outside caustic
- Magnification scales as:

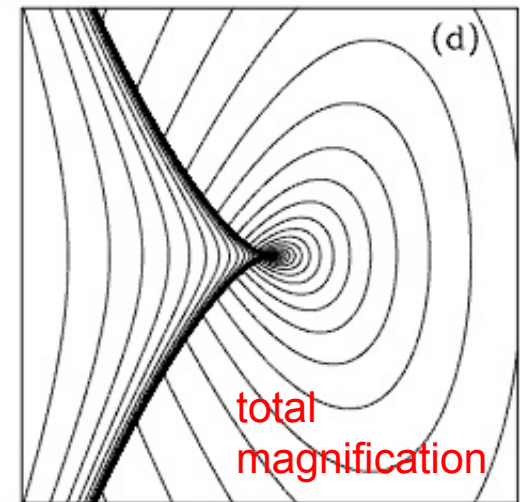
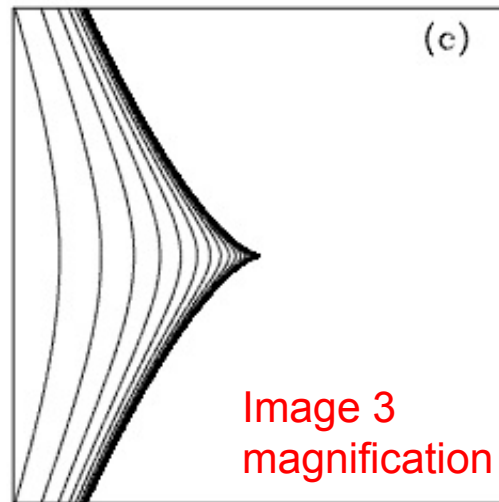
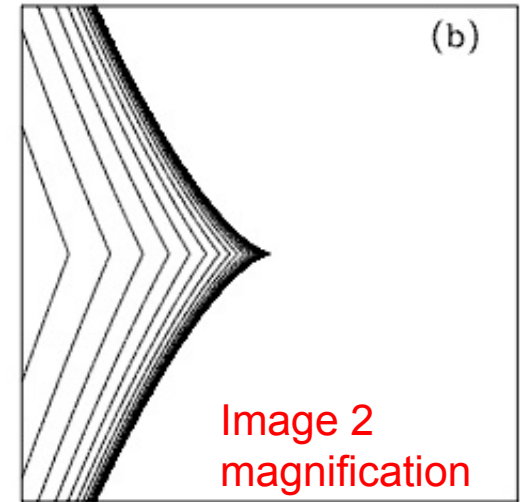
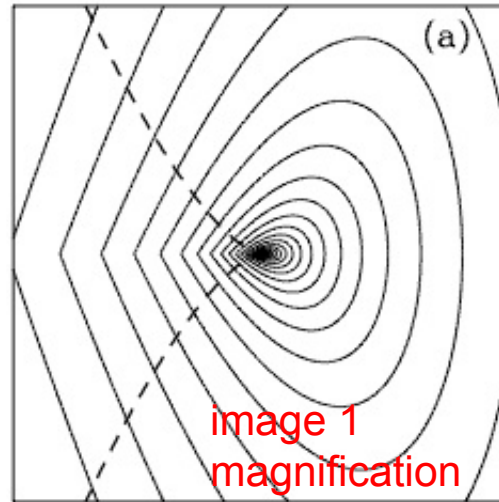
$$A \propto \Delta u_{\perp}^{-1/2} \Theta(\Delta u_{\perp})$$



(Gaudi & Petters 2002)

# Cusp of Caustic Curve

- Image 1 is continuous across the caustic
- Images 2 & 3 are divergent as the source approaches the caustic
- “Lobe” of high magnification just outside cusp due to image 1

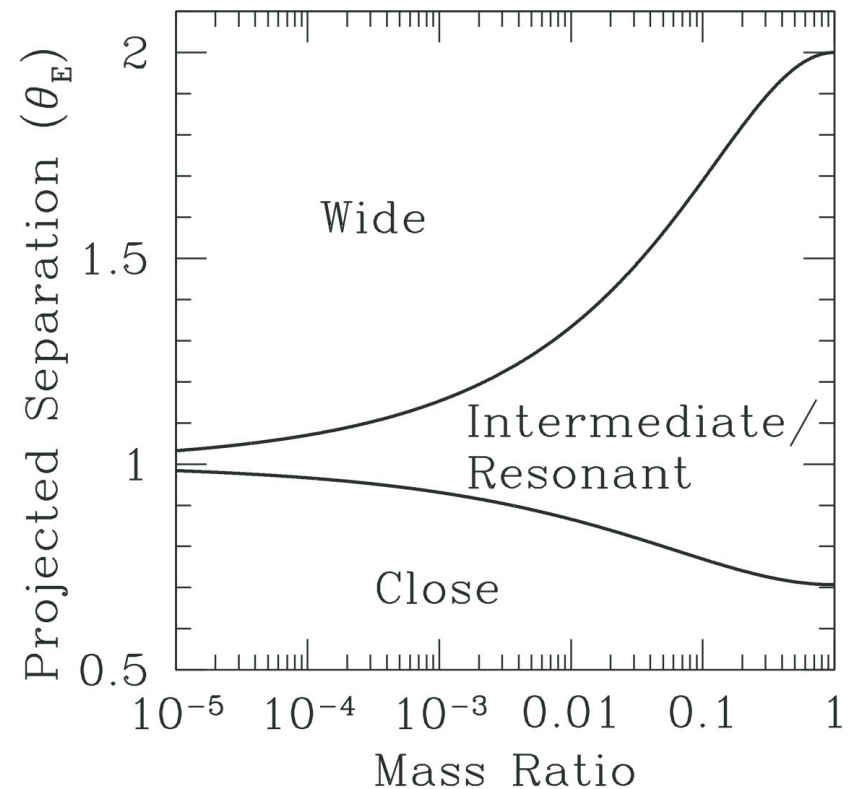


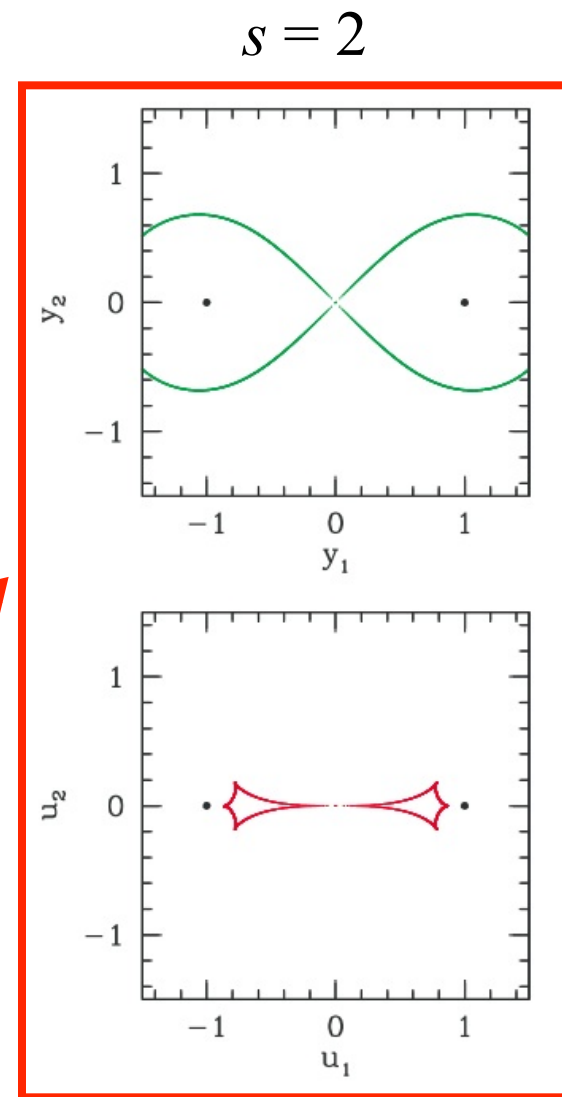
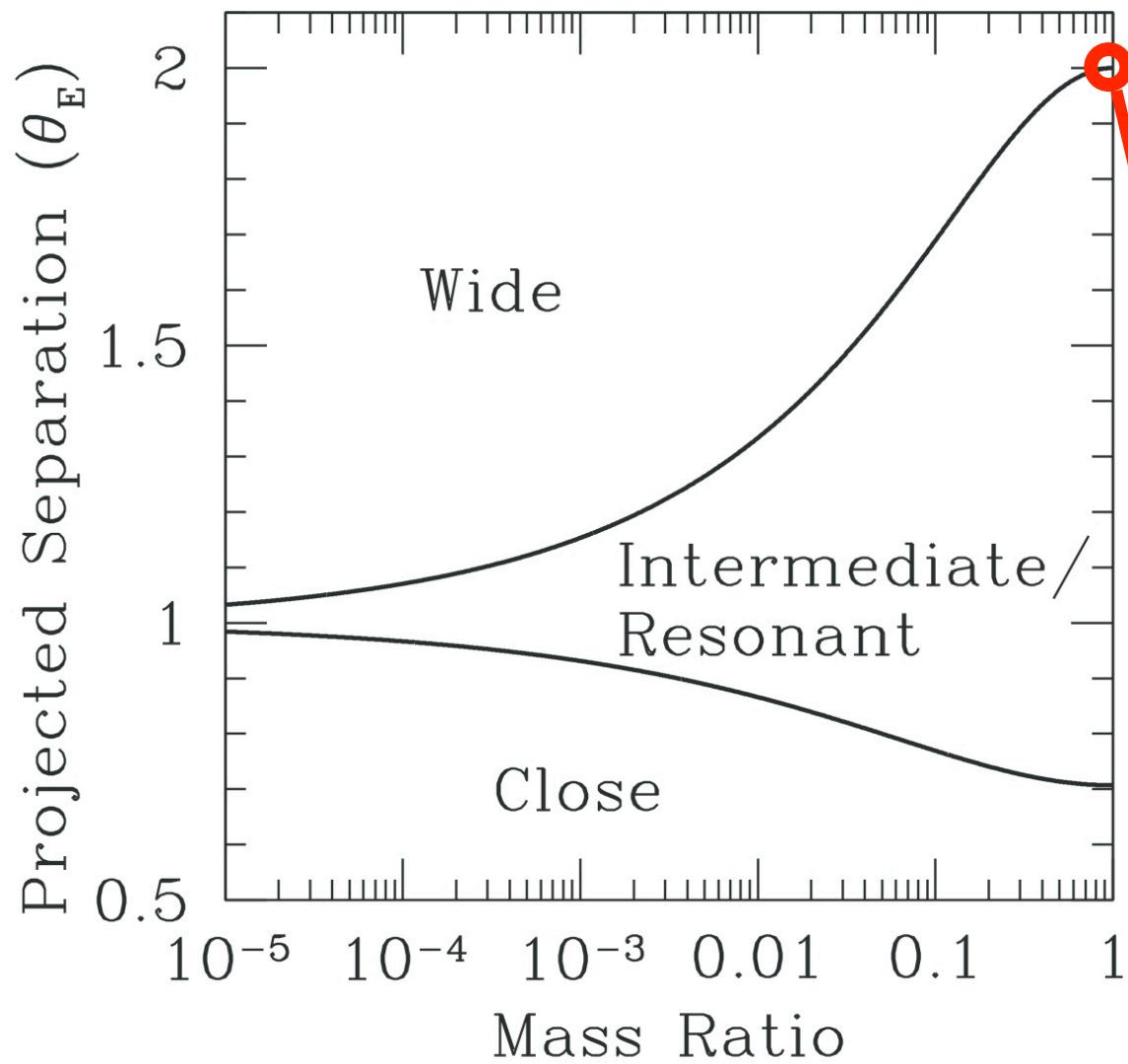
$u_2$

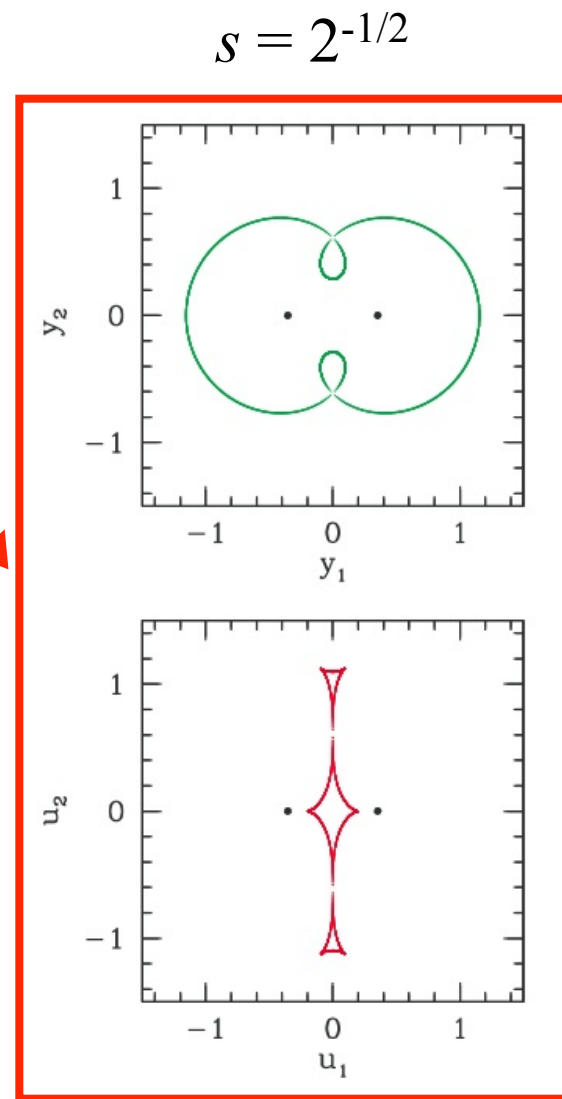
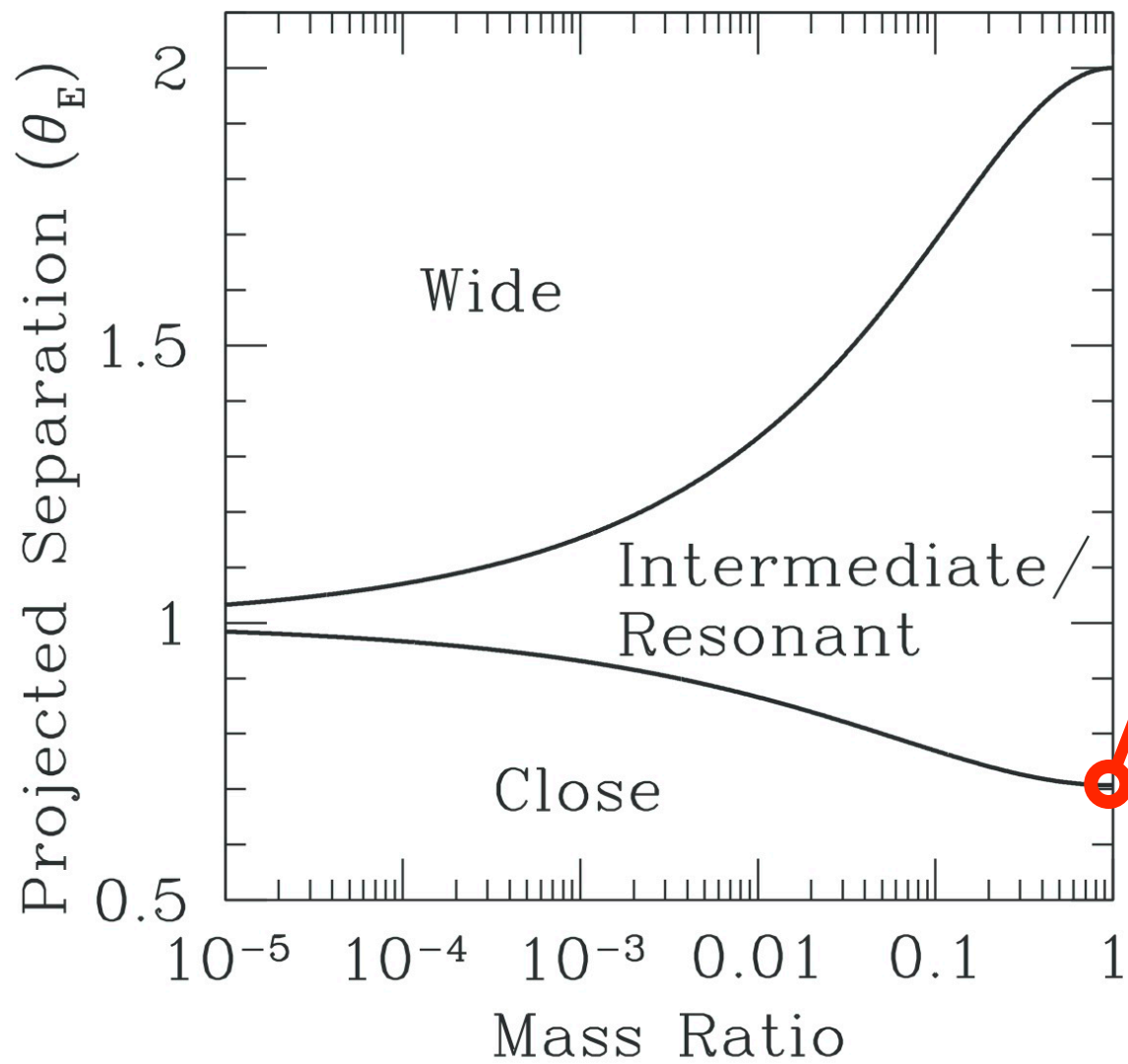
$u_1$

# Binary Lens Caustic Curve Morphology

- 3 different configurations with 1, 2, or 3 caustic curves.
- **Close** configuration – 3 separated caustic curves (2 are mirror images)
  - 4, 3, 3 cusps
- **Intermediate/resonant** configuration - 1 caustic
  - 6 cusps
- **Wide** configuration - 2 caustics.
  - 4 cusps each

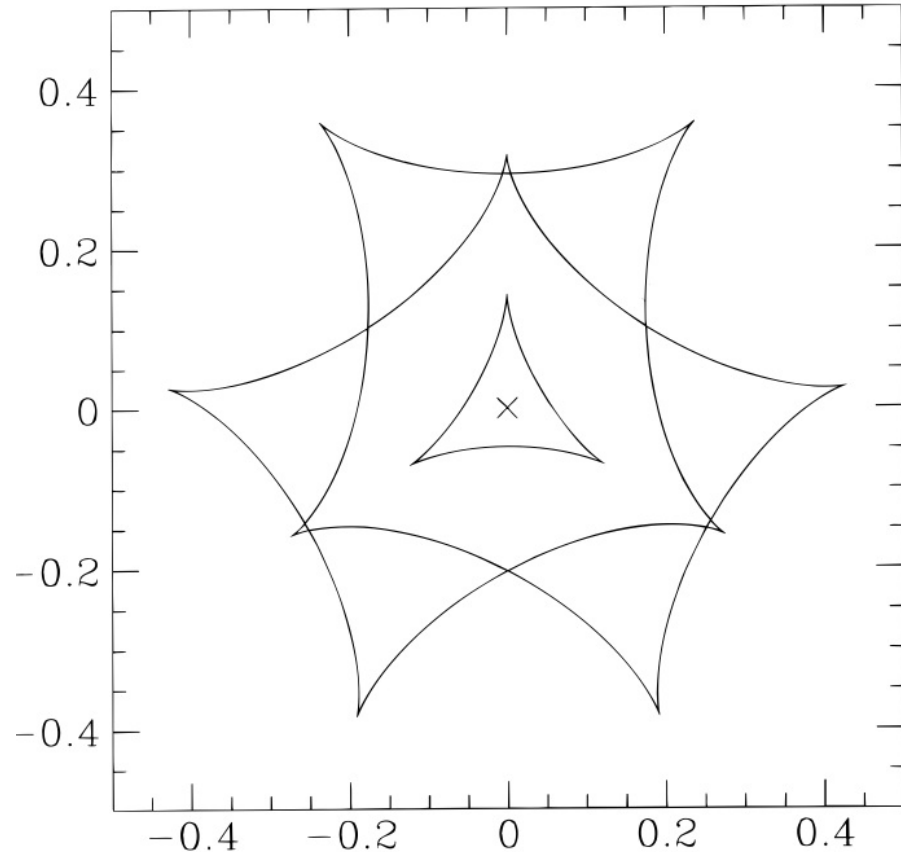




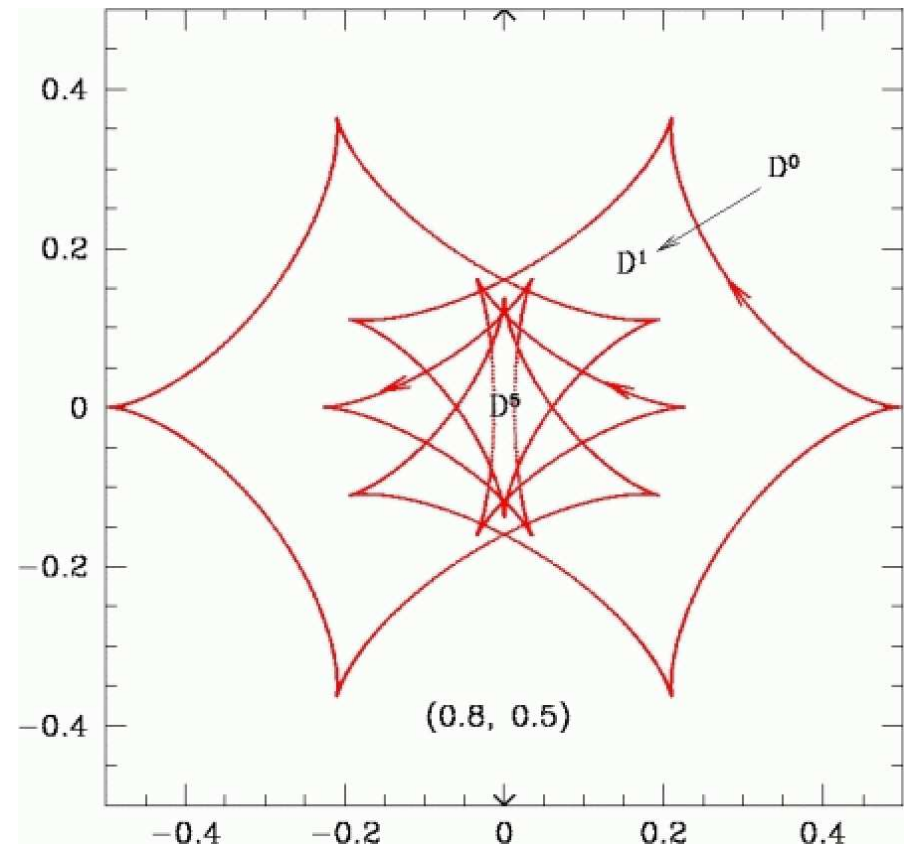


# Complicated Caustics with $> 2$ Lenses

Caustic curves are nested and self-intersecting

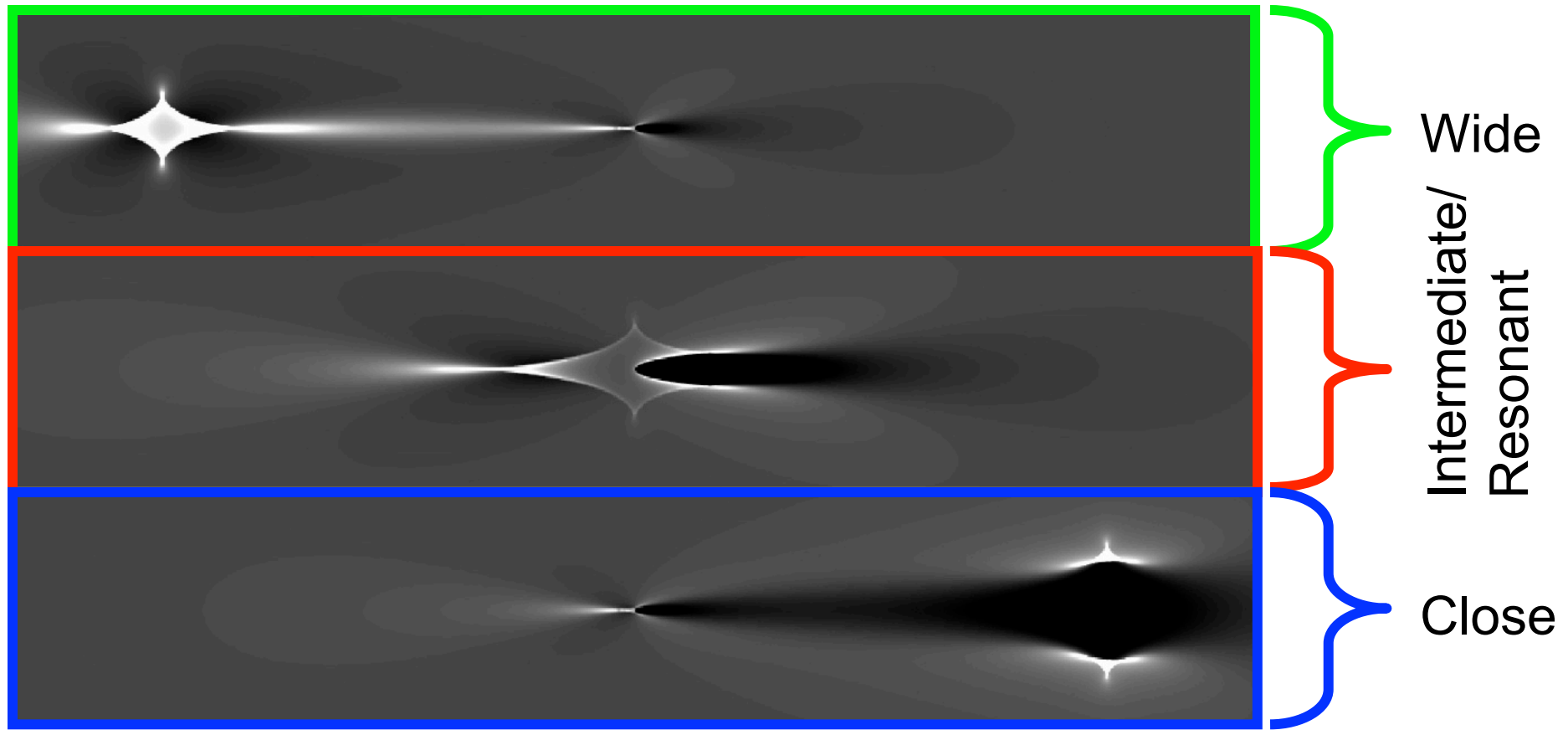


triple lens with 4, 6, 8 or 10 images  
 $n + 1$  to  $5n - 5$   
(Rhie 1997)



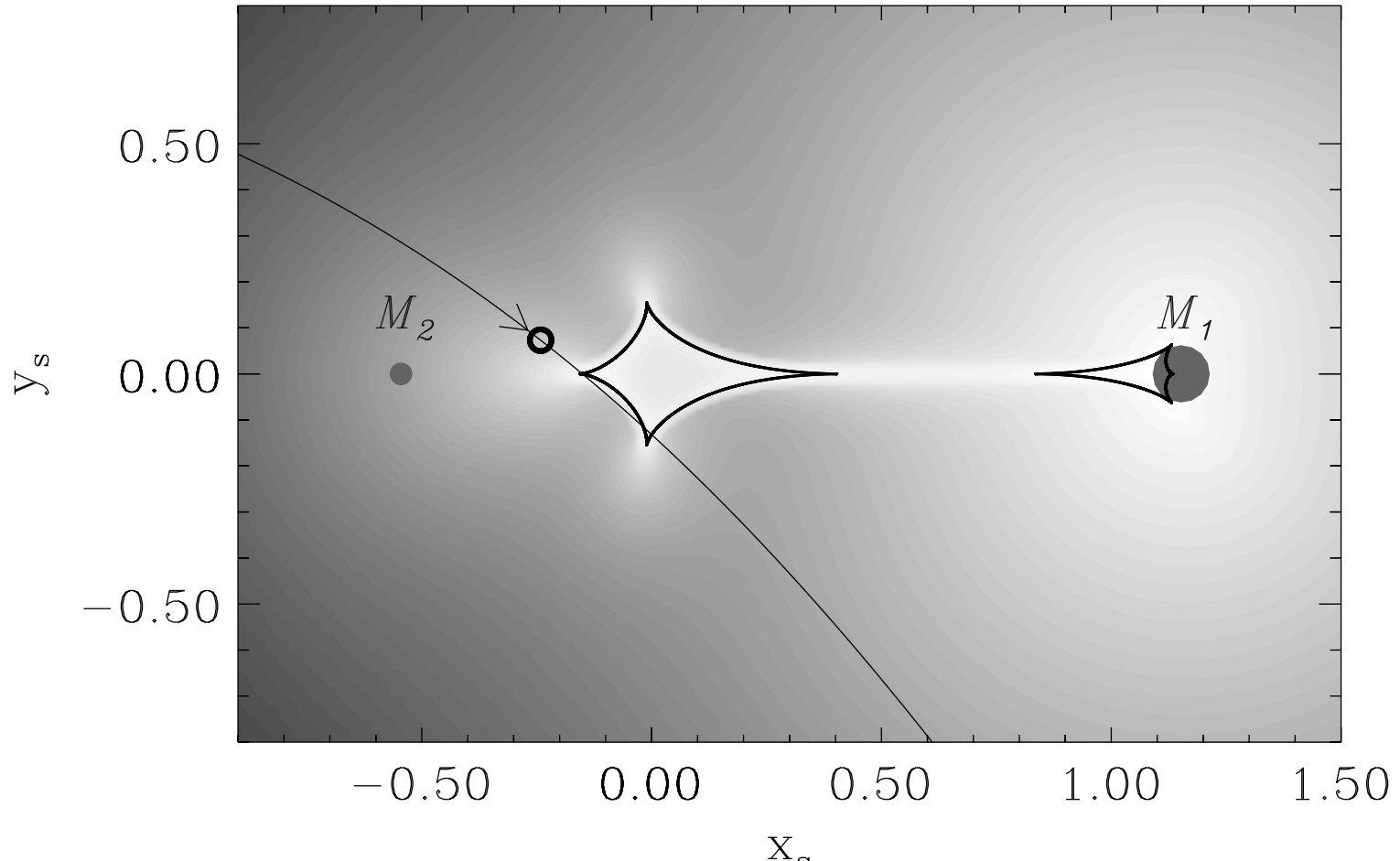
quadruple lens with 5, 7, 9, 11, 13 or 15 images  
 $n + 1$  to  $5n - 5$   
Rhie (2003)

# Relative Magnification Patterns for Planetary Mass Ratios



Planetary magnification pattern divided by single lens pattern

# Major Image Caustic



Mostly positive perturbation with slight demagnification outside caustics, away from cusps

OGLE-2012-BLG-0358 example (Han et al. 2014)

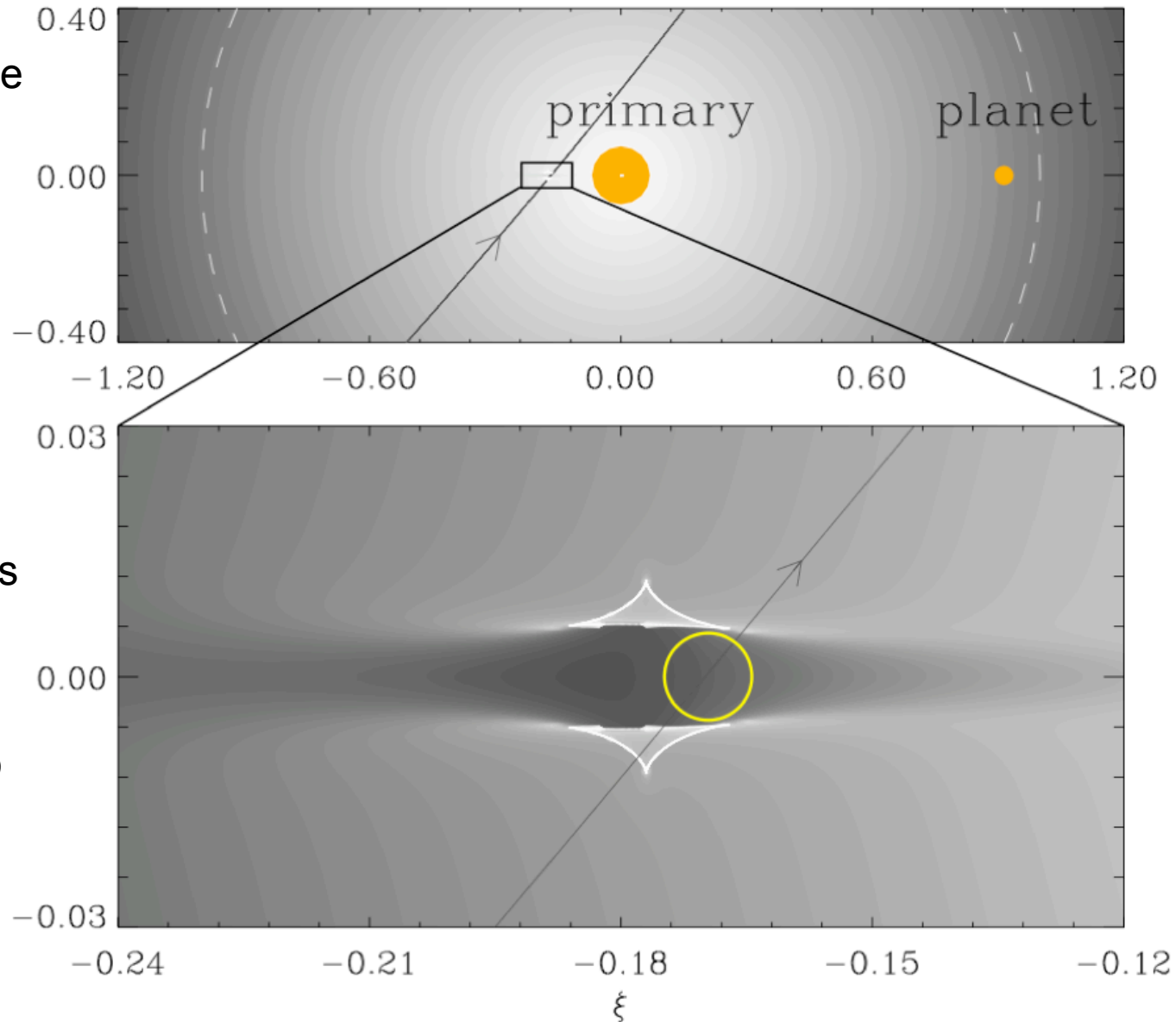
# Minor Image Caustic

For mass ratio  $q \ll 1$ ,  
triangular caustics come  
together

Large demagnification  
signal between two  
triangular caustics,  
where minor image  
is largely destroyed

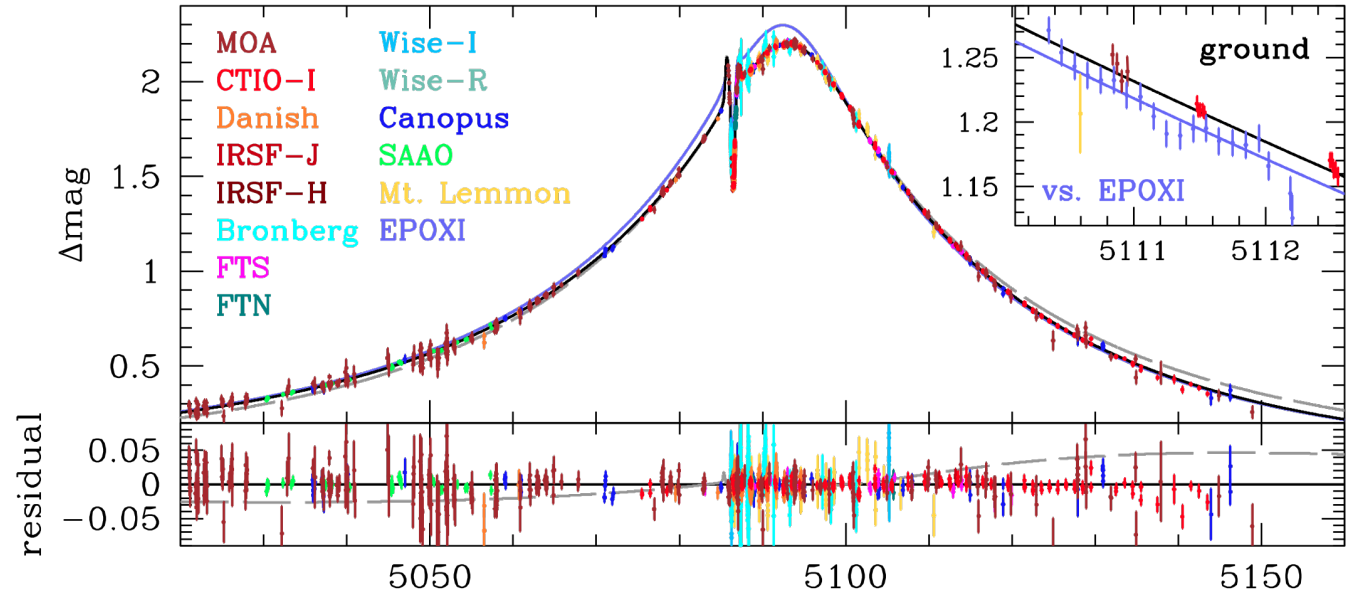
With spatial averaging,  
demagnification cancels  
magnification due to  
caustics

MOA-2009-BLG-266Lb  
example  
 $10 M_{\oplus}$  Planet

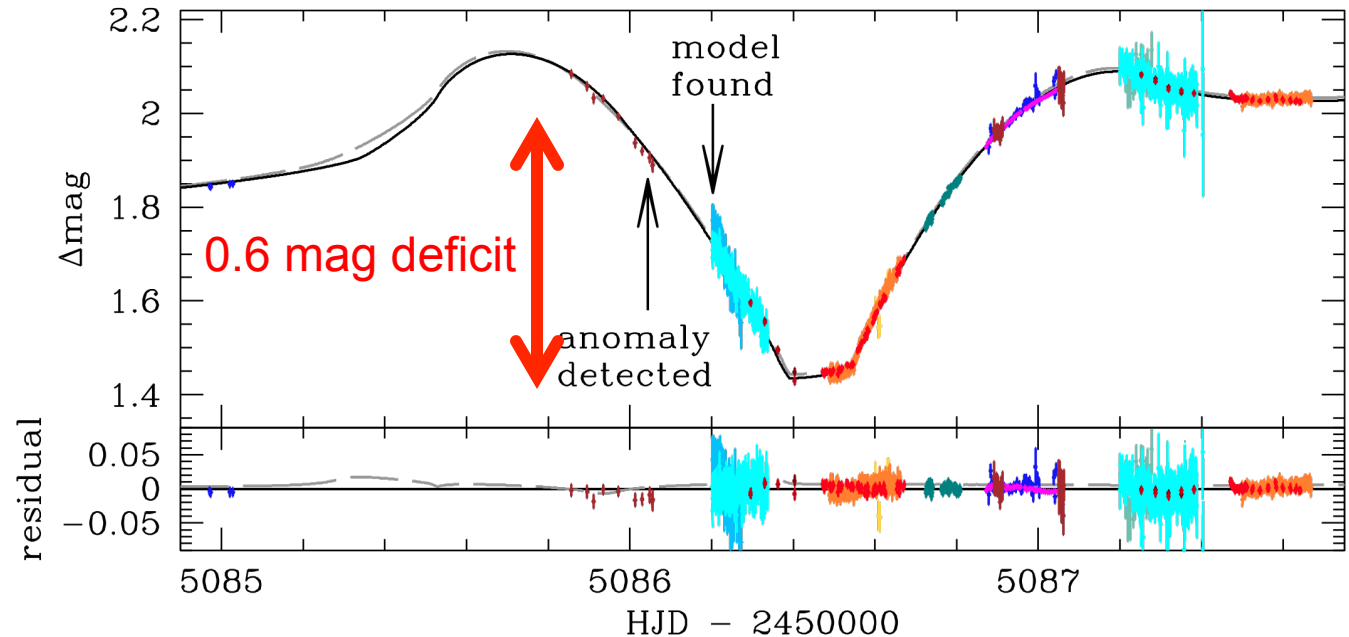


# MOA-2009-BLG-266Lb – $10 M_{\oplus}$ Planet

Cold,  
“failed Jupiter”

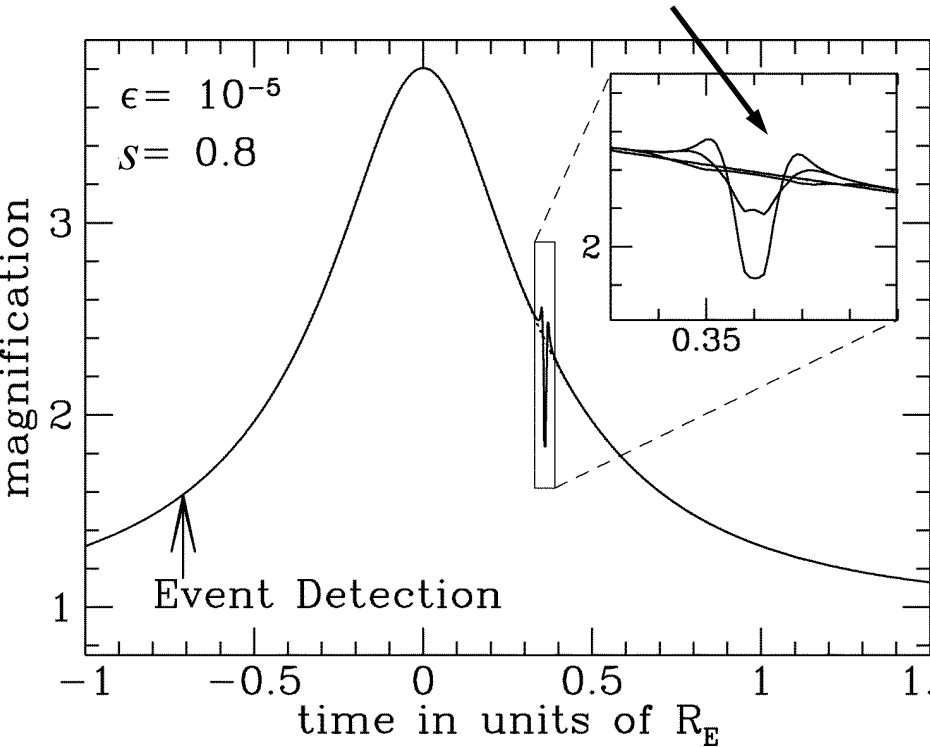


$$m_p = 10.4 \pm 1.7 M_{\oplus}$$
$$M_* = 0.56 \pm 0.09 M_{\odot}$$
$$a = 3.2^{+1.9}_{-1.5} \text{ AU}$$
$$D_L = 3.0 \pm 0.3 \text{ kpc}$$

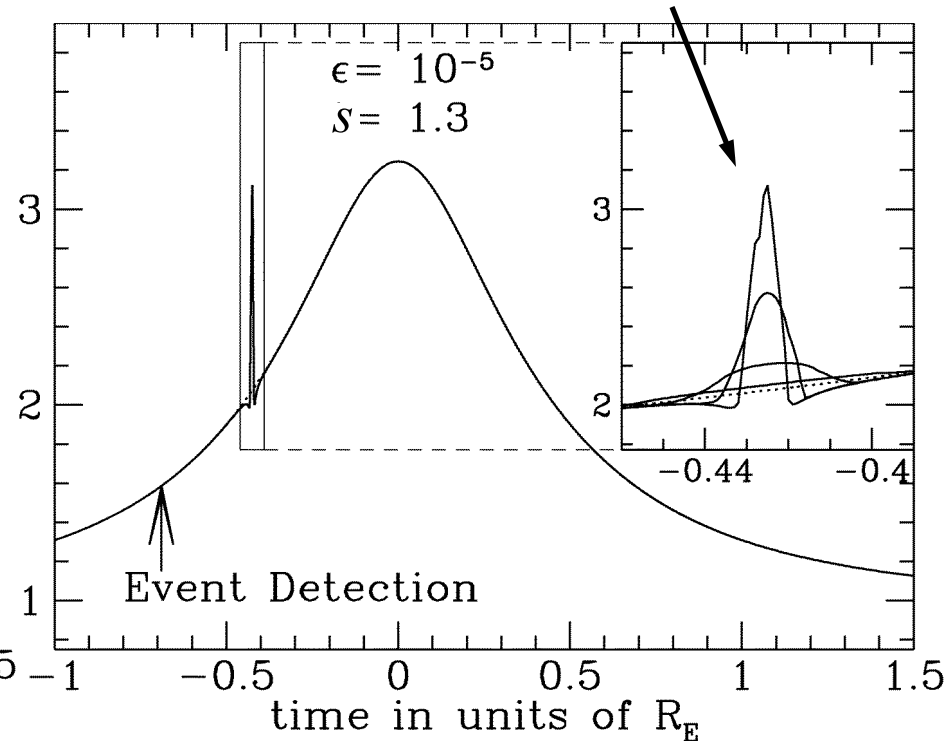


# Finite Source Effects

planet signal is washed out for  
giant source stars at  $s < 1$

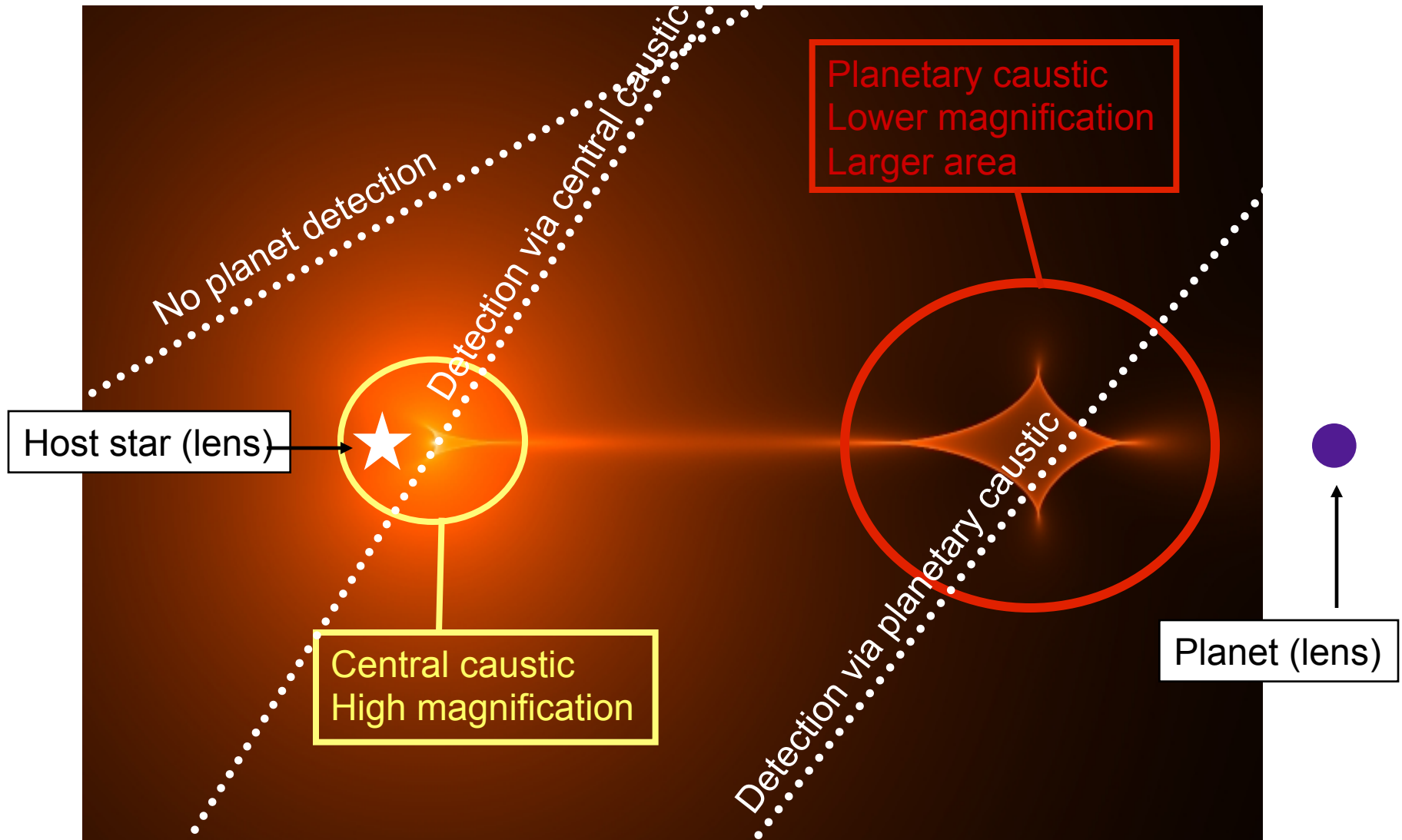


planet signal is smoothed for  
giant source stars at  $s > 1$



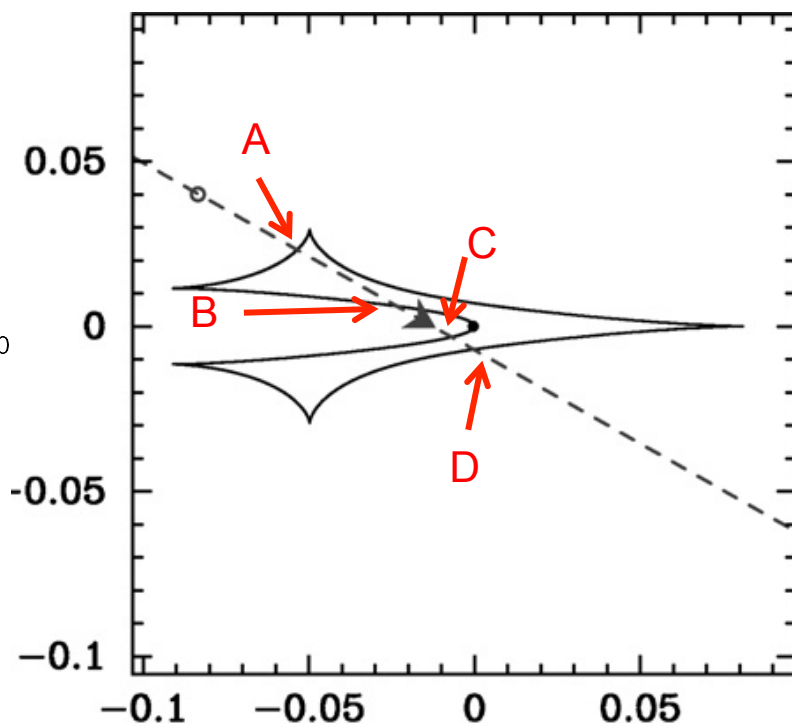
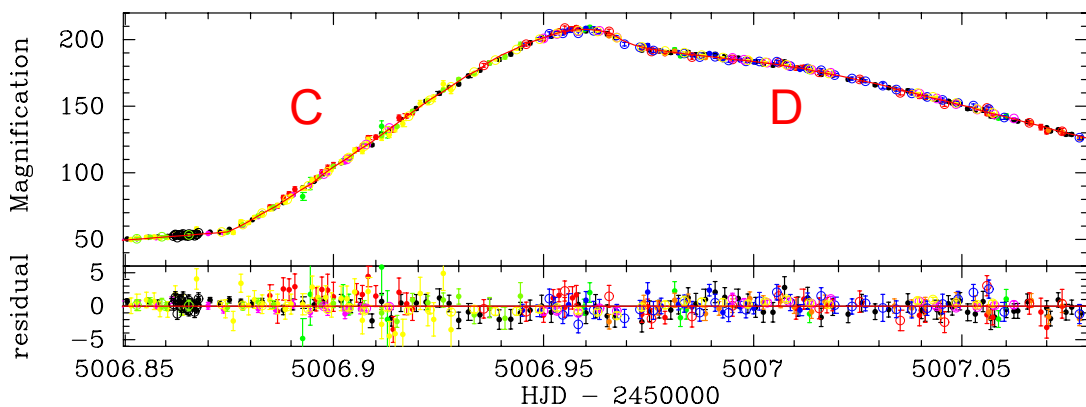
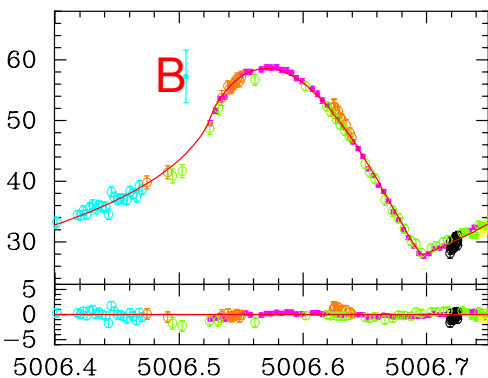
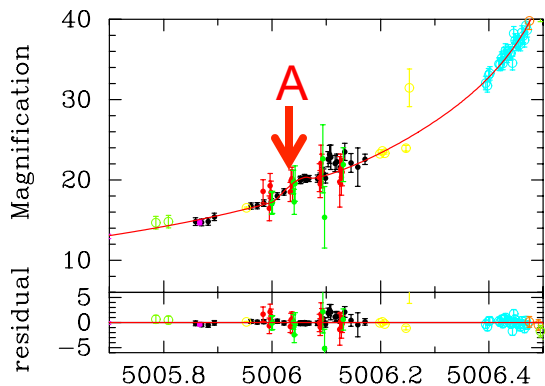
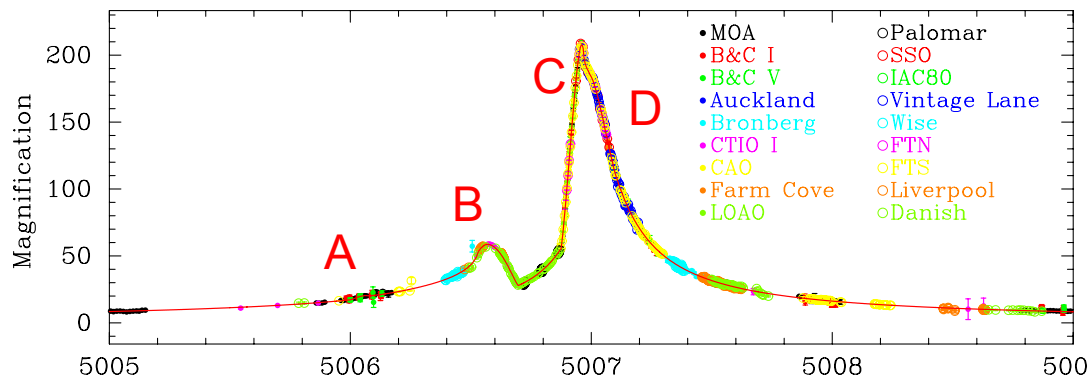
- If planetary Einstein Ring  $<$  source star disk: planetary microlensing effect is washed out (Bennett & Rhie 1996)
- For a typical bulge giant source star, the limiting mass is  $\sim 10 M_{\oplus}$
- For a bulge, solar type main sequence star, the limiting mass is  $\sim 0.1 M_{\oplus}$
- Main sequence stars can only be resolved at high magnification from the ground!

# Magnification Sampled Along Source Path



Deviation from single-lens is largely determined by “caustics”. Source plane plot

# Caustic Crossing Signals Are Not Equal



Exterior caustic crossings, **A** and **D** are weak; interior (back side) caustic crossings **B** and **C** are strong.

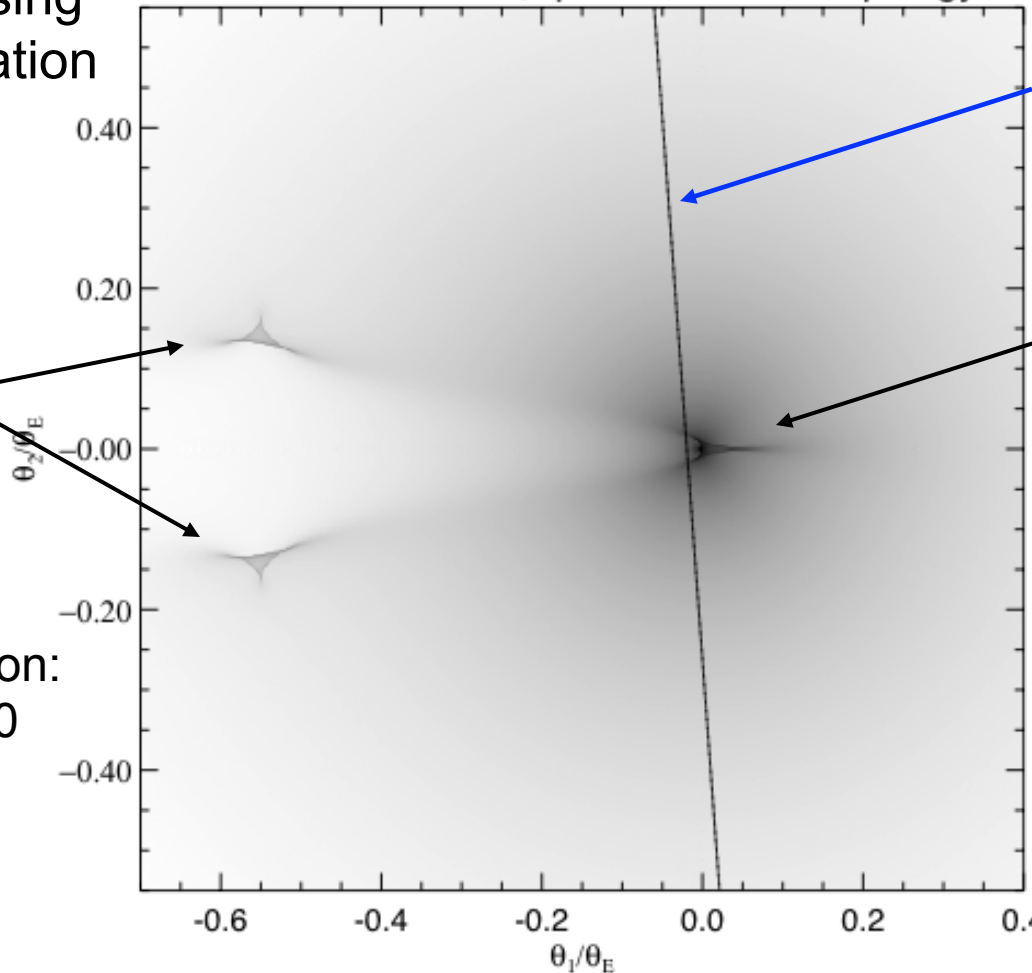
MOA-2009-BLG-319  
Miyake et al. (2011)

# Two Types of Planetary Signals

Microensing  
magnification  
map

OB05-071:  $d=0.759$ ,  $q=0.006$  caustic topology

minor image  
planetary  
caustics



The source trajectory is a nearly straight line across the magnification pattern.

central  
caustic

planet

Planetary caustics are larger and cause most planetary signals, but the central caustics are predictable, occurring at very high magnification. They offer the highest efficiency of planet detections for fixed telescope time.

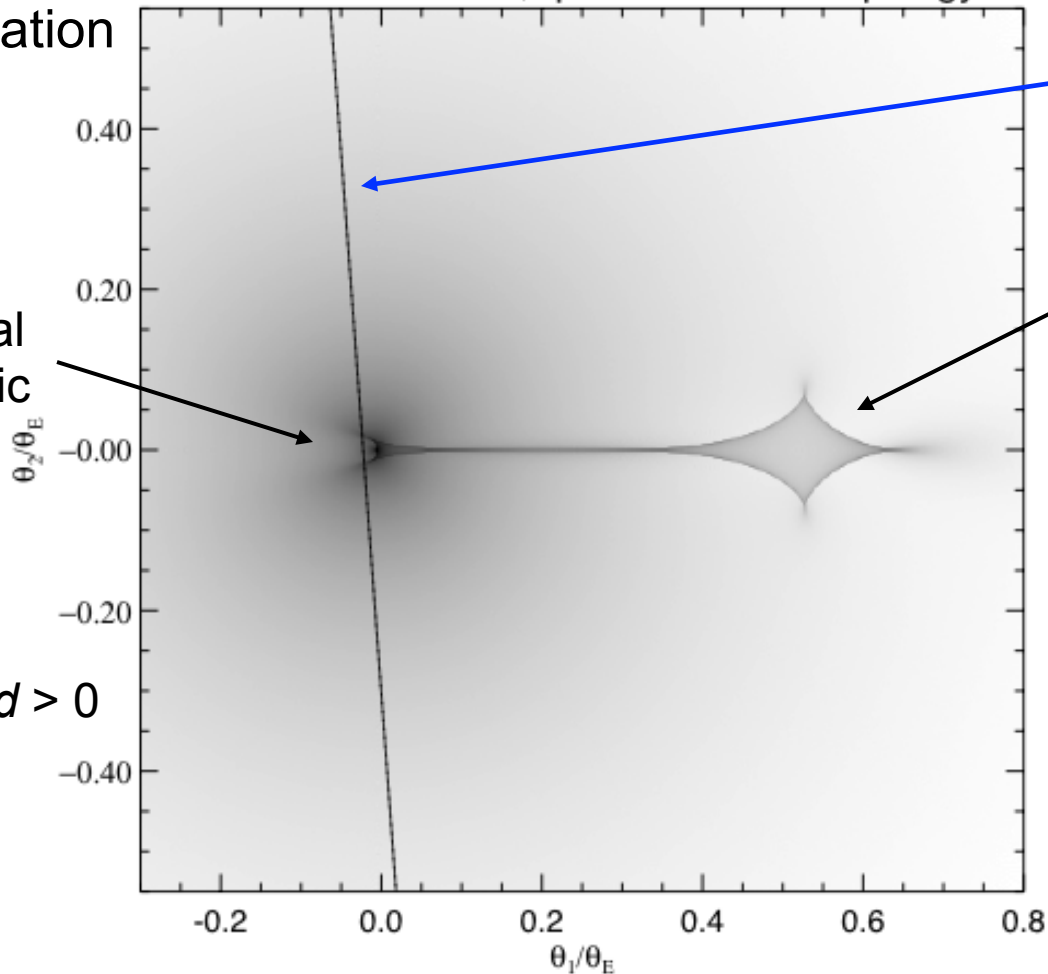
caustic location:  
 $s_c = d - 1/d < 0$

Detectable planetary signals due to image approach to planet (near planetary caustic), or at high magnification (near central caustic) - due to distortion of circular symmetry

# Two Types of Planetary Signals

Microlensing  
magnification  
map

OB05-071:  $d=1.299$ ,  $q=0.006$  caustic topology



central  
caustic

caustic  
location:  
 $s_c = d - 1/d > 0$

The source trajectory is a  
nearly straight line across  
the magnification pattern.

major image  
planetary  
caustic

planet

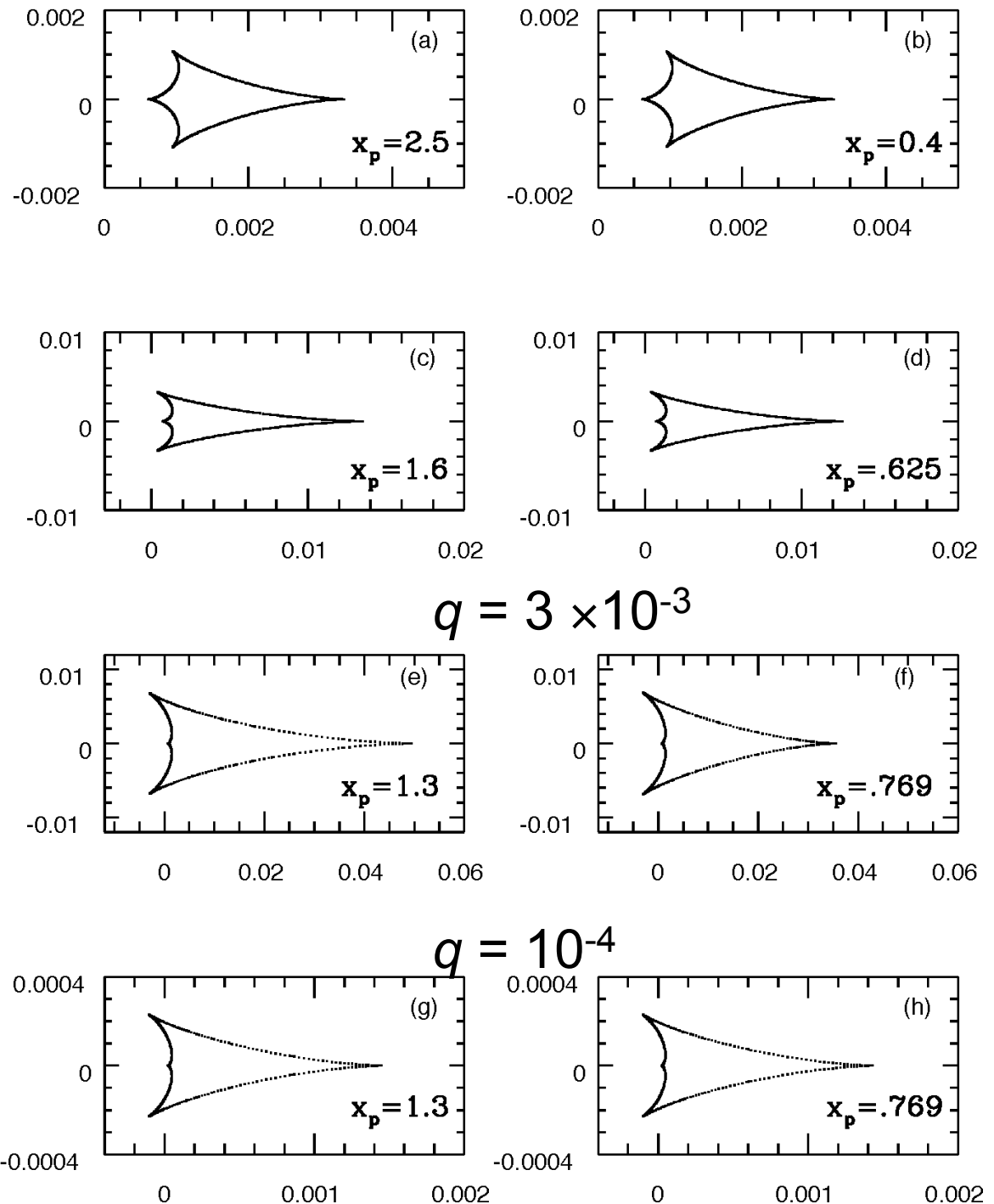
Planetary caustics are  
larger and cause most  
planetary signals, but  
the central caustics are  
predictable, occurring at  
very high magnification.  
They offer the highest  
efficiency of planet  
detections for fixed  
telescope time.

Detectable planetary signals due to image approach to planet (near planetary caustic), or at high magnification (near central caustic) - due to distortion of circular symmetry

# Central or Stellar Caustics

- $d \leftrightarrow 1/d$  symmetry
- as  $d \rightarrow 1$ , central caustic becomes large & weak
- “forward” single cusp is weaker than back-side cusps
- Since planets at any location produce a central caustic, high magnification events have good multi-planet sensitivity (Gaudi, Naber & Sackett 1998)

(Griest & Safizadeh 1998)



# Beyond the Point-Source Approximation

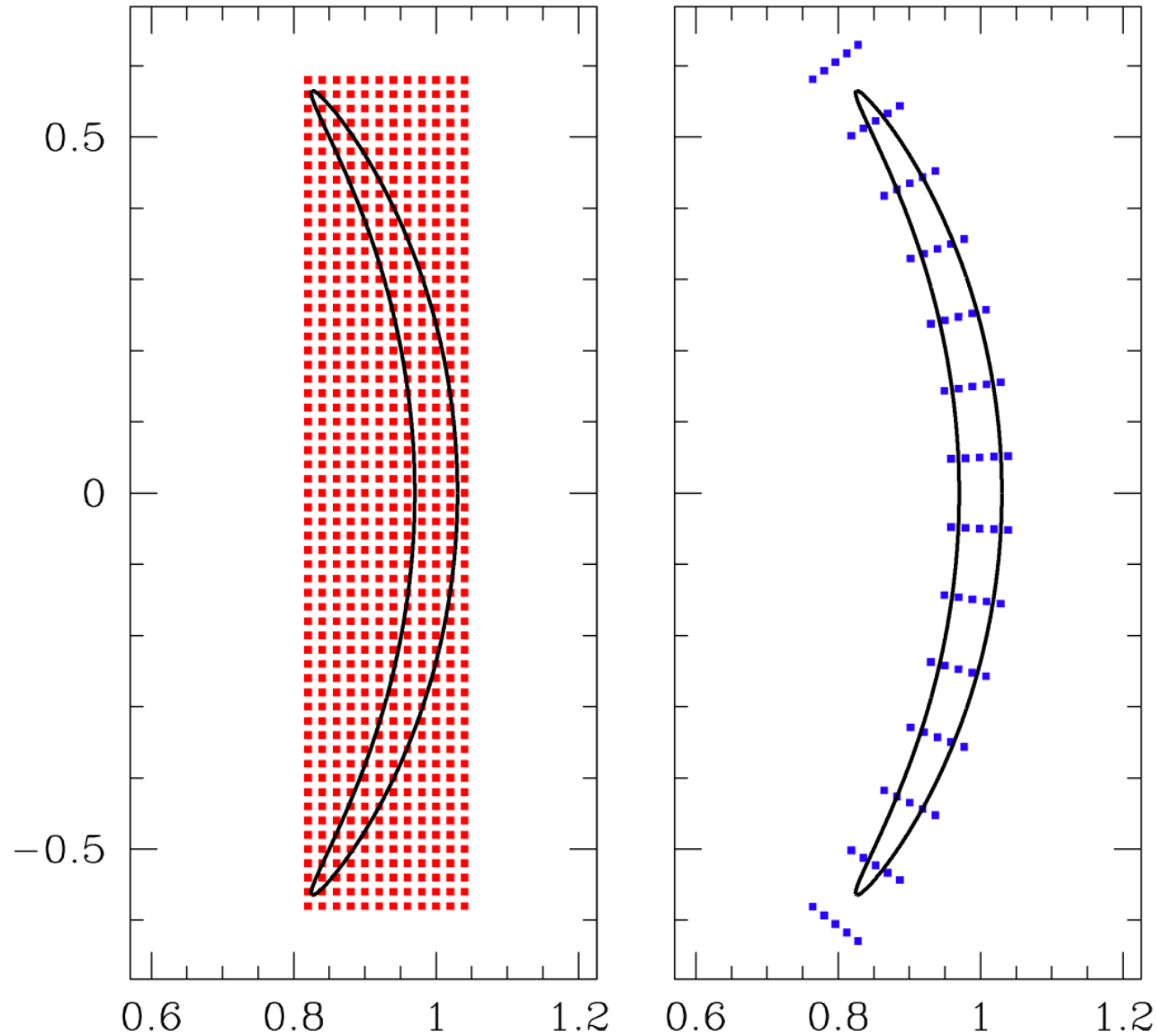
- Hexadecapole approx. (Pejcha & Heyrovsky 2009, Gould 2008)
  - Uses 13 point “grid” in the source plane
  - Cannot be used during caustic crossings
  - Not general, but fast
  - Best when combined with more general method
- Brute force ray-shooting (i.e. Wambsganss 1997)
  - Can be used for complicated static systems
    - i.e. many masses or continuous mass distribution
  - Becomes extremely slow for an orbiting lens system
- Stokes or Green’s Theorem (Dominik 1995, 1998; Gould & Gauchere 1997; Bozza 2010)
  - Very fast for uniform source
  - Competitive for realistic limb darkened sources
  - not yet implemented for  $n > 2$  lens masses – tracing image boundaries is difficult
- Direct integration of point-source formula over source plane
  - Highly inaccurate due to caustic singularities (tried by Griest)

# Beyond the Point-Source Approximation 2

- Image Centered Ray-Shooting (Bennett & Rhie 1996; Bennett 2010)
  - First general method for binary lens systems with finite sources
  - Used to show that microlensing can detect exo-Earths
  - use point source approximation except when the source is close to a caustic or image is close to a caustic curve
- Shoot rays from point-source image centers plus any partial images where the disk (but not the center of the source) crosses a caustic
  - grids grow until the grid boundary is outside the image
  - For a high magnification static lens system, we can save the rays shot close to the Einstein ring.
  - Polar coordinate and limb-darkening integration improvement
  - Only (current) practical method for fast orbiting triple lens systems, i.e. circumbinary planetary system OGLE-2007-BLG-349L

# Ray-Shooting Grids

- High magnification events are the most time consuming to calculate due to highly elongated images
- Polar coordinates can sample the long image axis with  $< 1/16$  of the grid points of a Cartesian coordinate system.
- High mag events have more extreme axis ratios, typically 100:1



# High Precision: 2<sup>nd</sup> Order Numerical Integration

Building blocks of 2<sup>nd</sup> order schemes (Numerical Recipes, Press et al.)

Trapezoidal rule:

$$\int_{x_1}^{x_2} f(x) dx = h \left( \frac{1}{2} f_1 + \frac{1}{2} f_2 \right) + O(h^3 f'')$$

Mid-point rule:

$$\int_{x_{1/2}}^{x_{3/2}} f(x) dx = hf_1 + O(h^3 f'')$$

# Integrating Over Limb-darkened Images

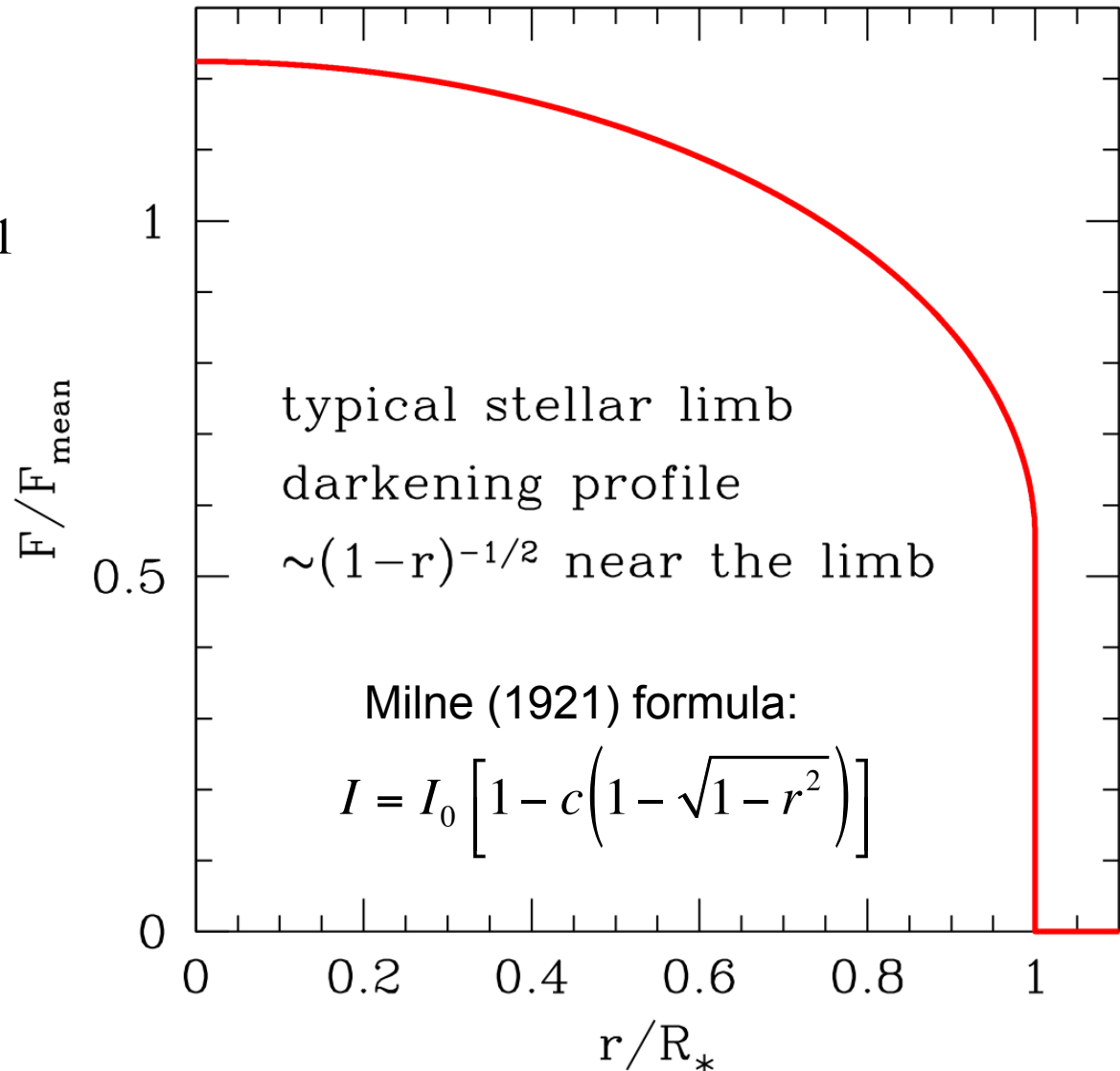
- But

$$\left( \frac{(x_{\max} - x_{\min})^3 f''}{N^2} \right) = \infty$$

both  $f'$  and  $f''$  diverge at  $r \sim 1$

for  $f \sim (1 - r)^{1/2}$

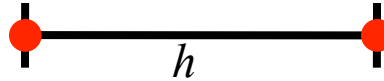
- This ruins the 2nd order accuracy of the differencing scheme
- Of course, we integrate in the image plane where the stellar profile is distorted, but the  $(1-r)^{1/2}$  behavior remains near the limb
- Bennett (2010) 2<sup>nd</sup> order scheme speeds calculation by  $>10$  for high mag events



# Numerical Integration of Limb-darkened Images

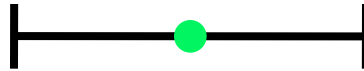
Building blocks of 1-dimensional 2<sup>nd</sup> order numerical integration schemes

trapezoidal rule



$$\int_{x_1}^{x_2} f(x) dx = h \left( \frac{1}{2} f_1 + \frac{1}{2} f_2 \right) + O(h^3 f'')$$

midpoint rule

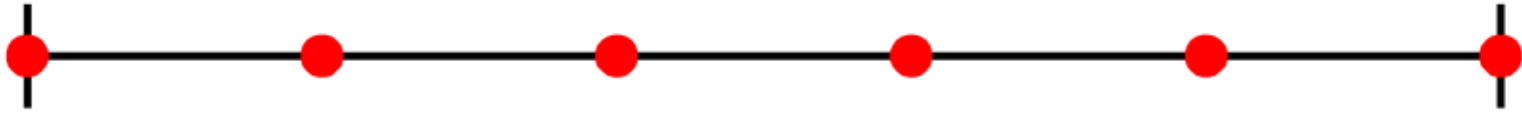


$$\int_{x_{1/2}}^{x_{3/2}} f(x) dx = h f_1 + O(h^3 f'')$$

Standard 1-dimensional integration schemes can be built from these simple formulae (see e.g. *Numerical Recipes* by Press et al.)

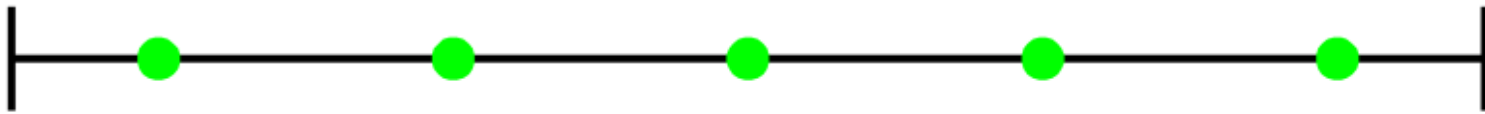
Build a scheme of 2<sup>nd</sup> order or higher accuracy

# Numerical Integration of Limb-darkened Images



extended trapezoidal rule

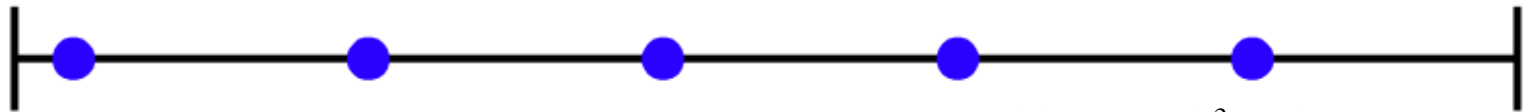
$$\int_{x_1}^{x_N} f(x) dx = h \left[ \frac{1}{2} f_1 + f_2 + f_3 + \dots + f_{N-1} + \frac{1}{2} f_N \right] + O \left( \frac{(x_N - x_1)^3 f''}{N^2} \right)$$



extended midpoint rule

$$\int_{x_{1/2}}^{x_{N+1/2}} f(x) dx = h [f_1 + f_2 + f_3 + \dots + f_{N-1} + f_N] + O \left( \frac{(x_{N+1/2} - x_{1/2})^3 f''}{N^2} \right)$$

For lensing calculations, we must calculate the grid points before we find the boundaries



$$\int_{x_a}^{x_b} f(x) dx = h_1 f_1 + h [f_2 + f_3 + \dots + f_{N-1}] + h_N f_N + O \left( \frac{(x_b - x_a)^3 f''}{N^2} \right)$$

$$h_1 = x_{3/2} - x_a \quad h_N = x_b - x_{N-1/2}$$

modifying the boundary step size would seem to restore 2nd order accuracy

# 1-Dimensional Integral of Limb Darkened Source

- Normally, we assume that the integrand is approximated by a power law in  $(x - x_L)$  where  $x_L$  is the position of the limb
- But, a limb darkened source is better approximated by a power law in  $\sqrt{x - x_L}$
- Require that the difference scheme is exact for low order power law functions in  $\sqrt{x - x_L}$  instead of  $(x - x_L)$
- Standard 2<sup>nd</sup> order schemes have error terms that scale as  $\sim h^{3/2}$  and are actually order 1.5
- A relatively simple scheme works best
- Formally higher order schemes are sometimes worse

# An Attempt at a 2<sup>nd</sup> Order Scheme

This is formally 2<sup>nd</sup> order accurate for a “linear” limb darkening profile:

$$\int_{x_L}^{x_{3/2}} f(x) dx = h \left( \frac{1}{2} + \delta \right) \left[ (1 - b) f_L + b f_1 \right] ,$$

where  $\delta = (x_1 - x_L) / h$  , and

$$b = \frac{2}{3} \sqrt{\frac{\delta + \frac{1}{2}}{\delta}}$$

but the  $b$  gets very large for  $\delta \sim 0$ , so this formula is applied only for  $b \geq b_c$  where  $b_c \sim 0.15$  has been determined to be optimal empirically

This method does turn out to be 2<sup>nd</sup> order in some cases, but in other cases  $\sigma \sim h^{3/2}$ , but precision is improved by a factor of  $\sim 10$

Computational overhead of finding the boundary is a factor of 1.5-2

# 2<sup>nd</sup> Order Integration Scheme for Limb Darkened Sources

- A relatively simple scheme cancels

$$\int_{x_L}^{x_{3/2}} f(x) dx = h \left( \frac{1}{2} + \delta \right) [(1 - b)f_L + bf_1]$$

where

$$b = \frac{2}{3} \sqrt{\frac{\delta + \frac{1}{2}}{\delta}}$$

- But  $b$  can get very large when  $\delta \rightarrow 0$
- Small  $\delta$  values can lead to large numerical errors
  - presumably due to large coefficients for higher order error terms

# Implement a Cut-Off

- For  $\delta < \delta_c$  use a lower order integration scheme

$$\int_{x_{L1}}^{x_{L2}} f(x) dx = h (A_1 f_{L1} + B_1 f_1 + f_2 + \dots + f_{N-1} + B_2 f_N + A_2 f_{L2})$$

with coefficients given by

$$A_i = \left( \frac{1}{2} + \delta_i \right) (1 - b_i) \Theta(\delta_i - \delta_c) + \frac{\delta_i}{3} \Theta(\delta_c - \delta_i)$$

$$B_i = \left( \frac{1}{2} + \delta_i \right) b_i \Theta(\delta_i - \delta_c) + \left( \frac{2}{3} \delta + \frac{1}{2} \right) \Theta(\delta_c - \delta_i)$$

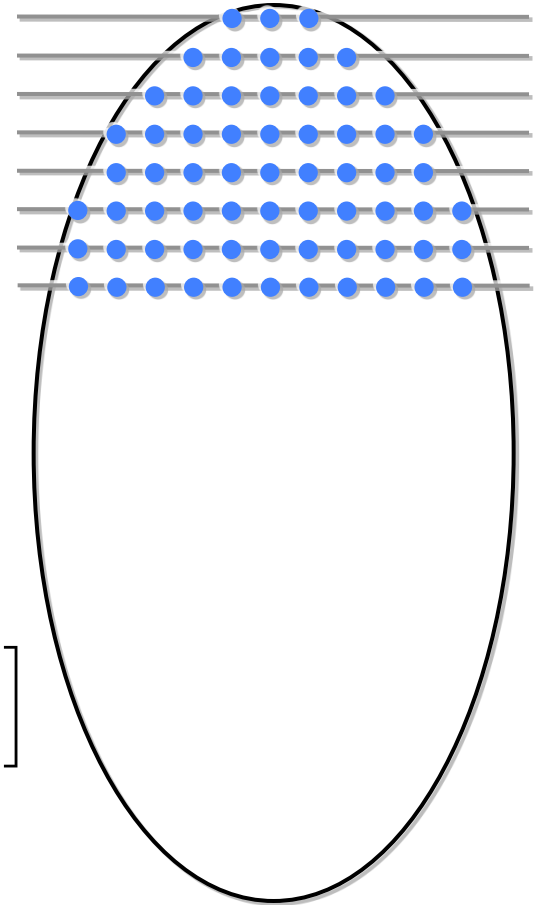
- The cut-off means that the differencing method is formally only order 1.5 accurate, but empirically, this works best.

# 2<sup>nd</sup> Dimensional Integration

- $y$  – direction
- Integrate over rows
- Integration over  $x$  removes the derivative singularity due to  $\sqrt{y - y_L}$  terms
- If  $F_i$  indicates the integral of the  $i$ -th row, the formula

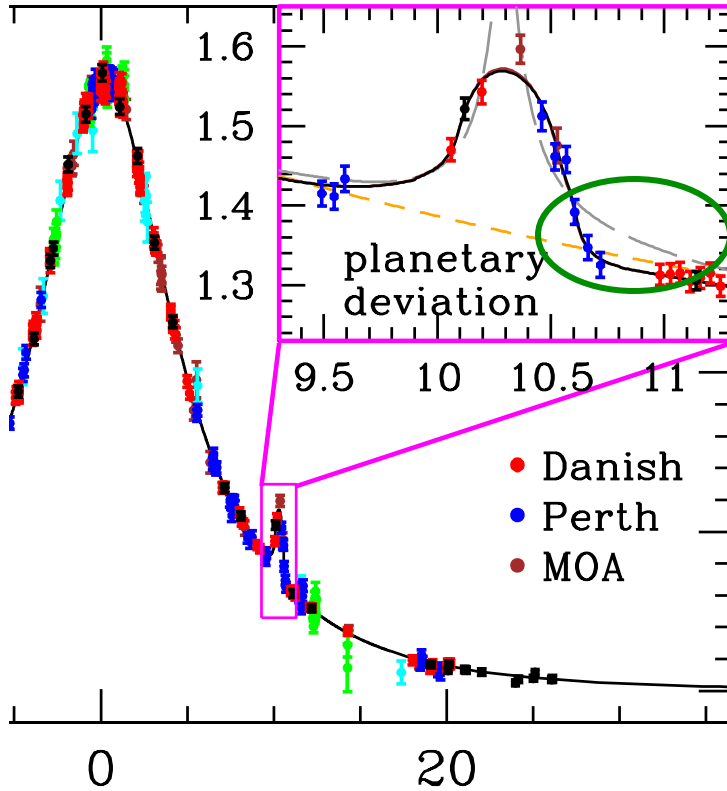
$$\int_{y_L}^{y_{5/2}} F(y) dy = h \left[ \left( \frac{3}{8} + \eta + \frac{\eta^2}{2} \right) F_1 + \left( \frac{9}{8} - \frac{\eta^2}{2} \right) F_2 \right]$$

makes the  $y$  – direction integral 2<sup>nd</sup> order accurate

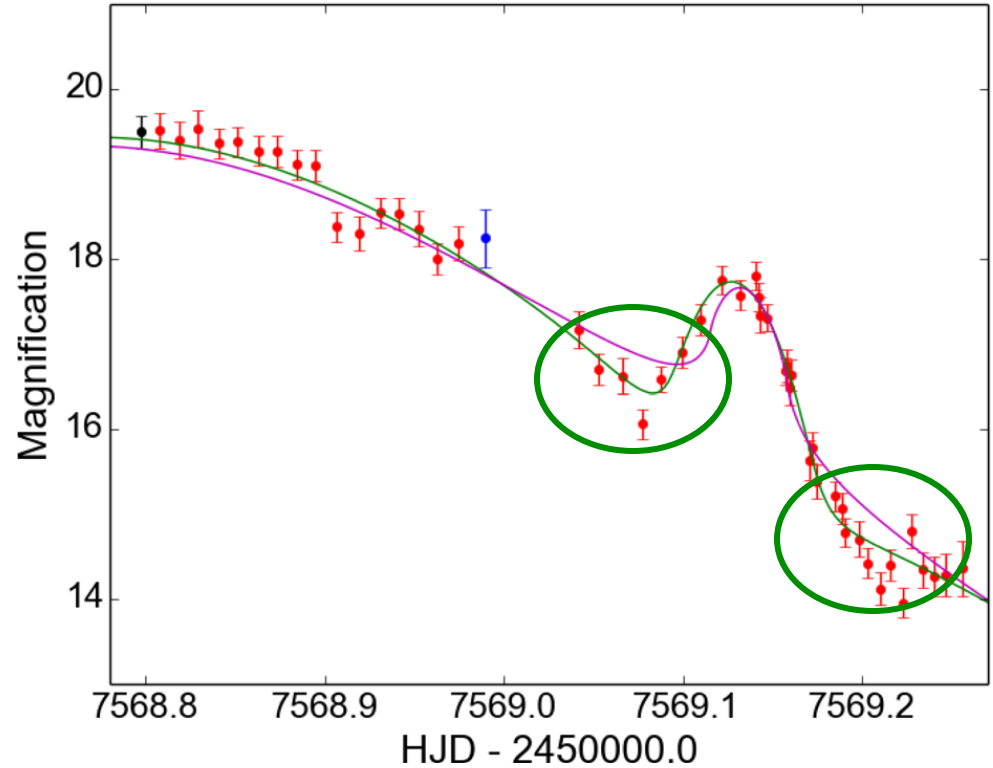


# Binary Lens vs. Binary Source

1<sup>st</sup> studied by Gaudi (1998)



OGLE-2005-BLG-390 (Beaulieu et al. 2006)

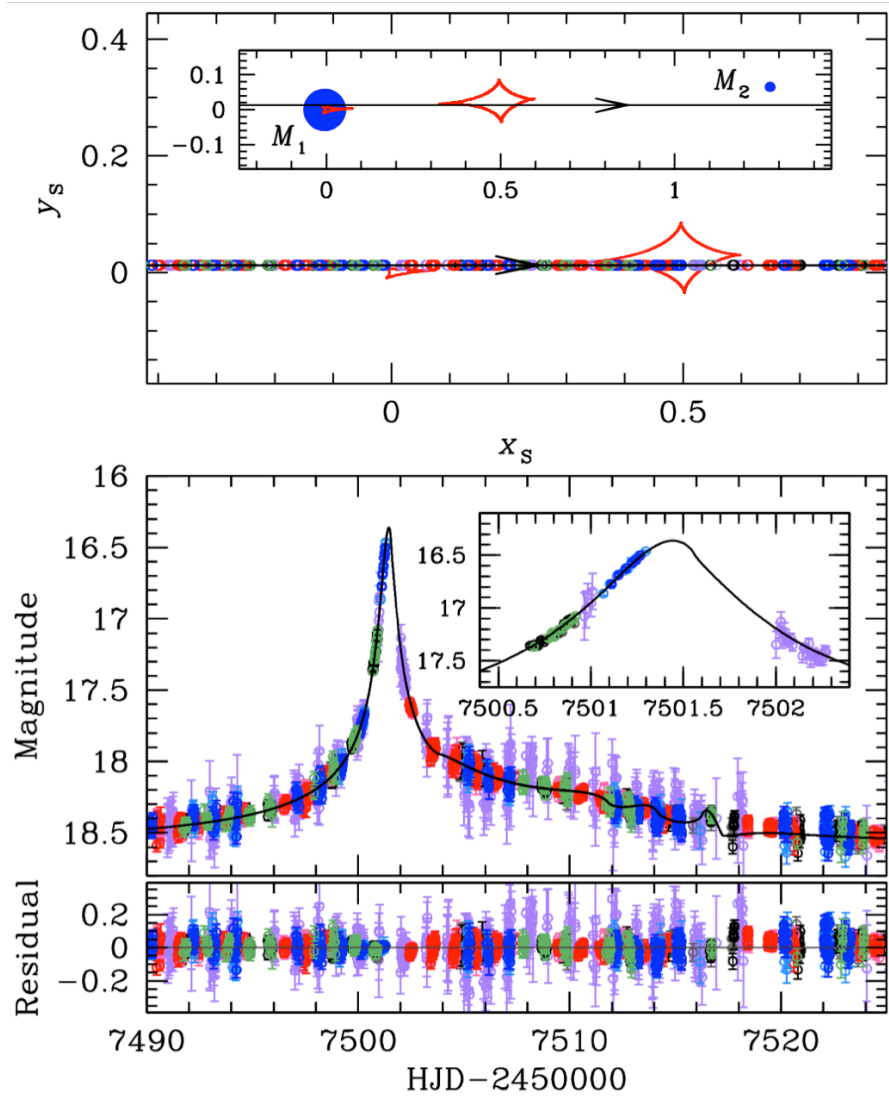


OGLE-2016-BLG-1195 (Bond et al. (2017))

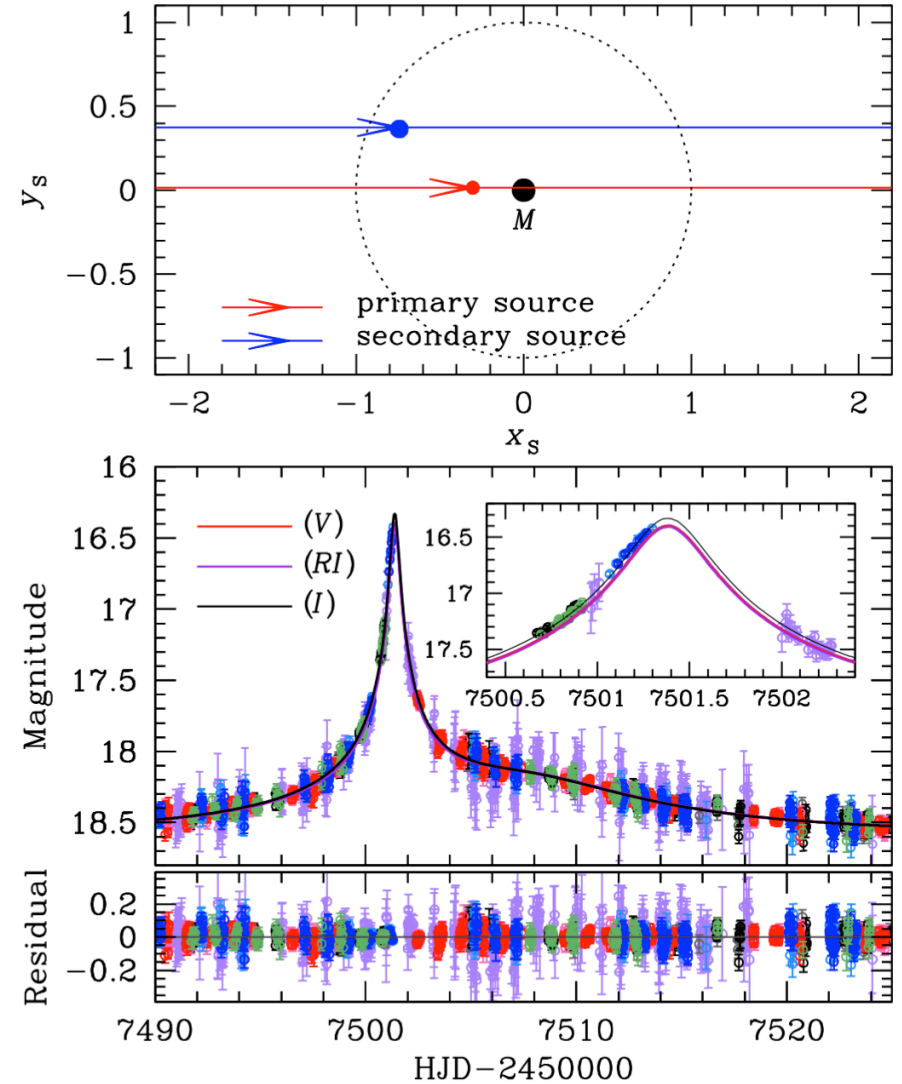
Higher magnification of faint secondary source can resemble a planetary signal.  
Observations of the light curve wings of the secondary bumps can rule out the binary source models.

# Binary Source Imitates a Planet

## OGLE-2013-BLG-0733



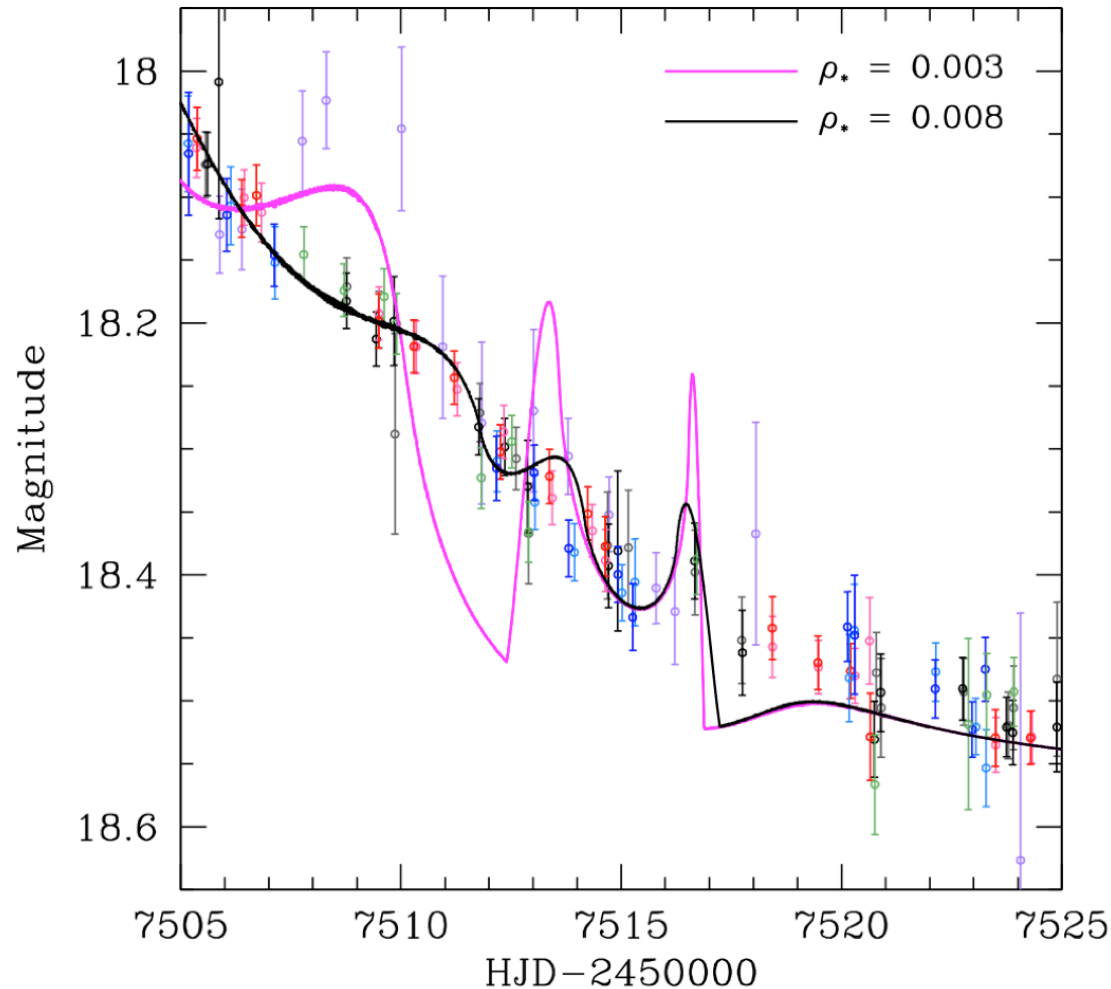
binary lens



binary source

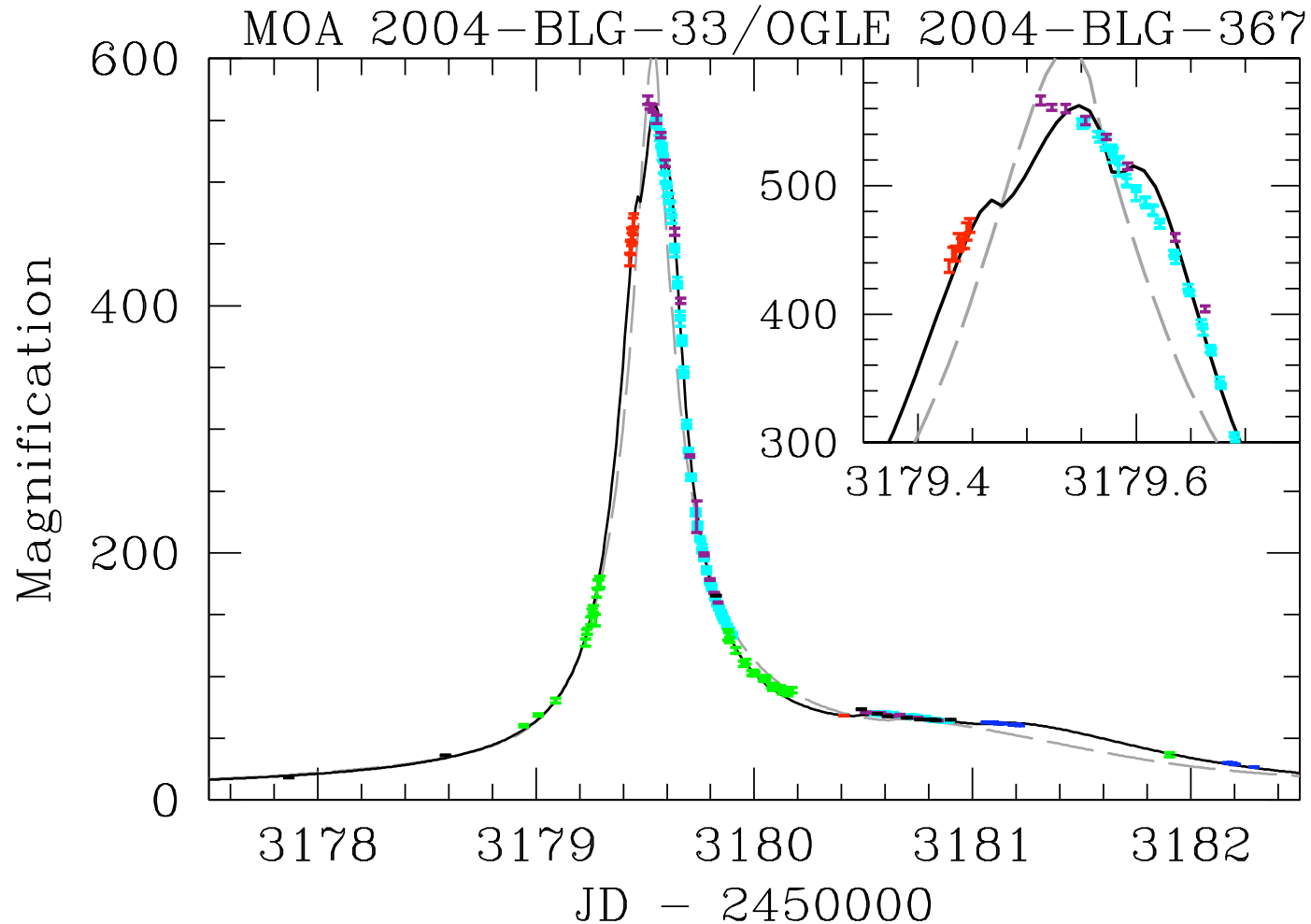
# Binary Source Imitates a Planet

## OGLE-2013-BLG-0733



binary lens model requires unusually large source to smooth sharp binary features, but it still doesn't quite fit the data

# Xallarap Confusion



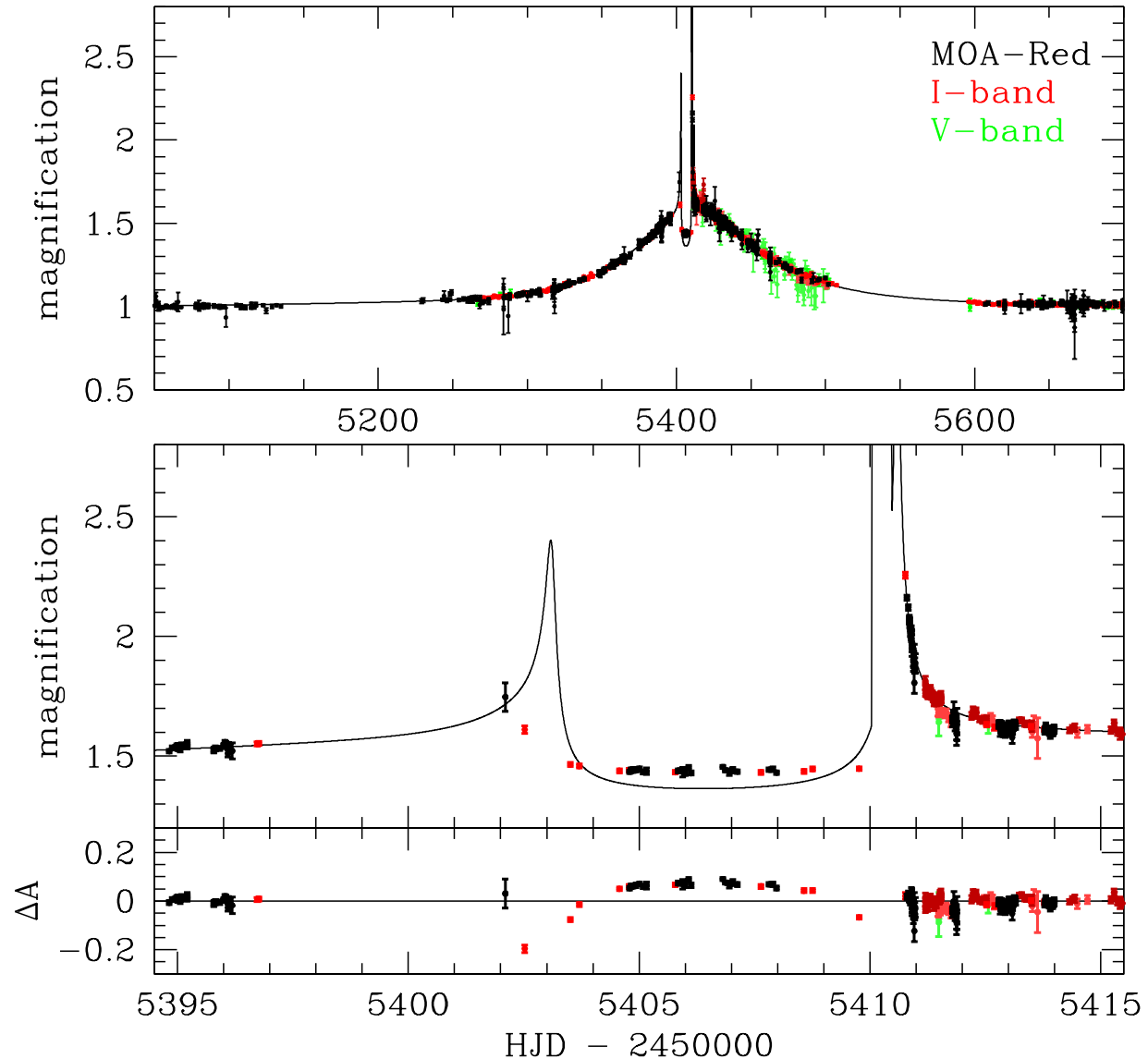
Triple lens model for MOA-2004-BLG-33, but short period source orbital motion fits better (Joe Ling, unpublished). Hint: sharp light curve features in model, but not data.

# MOA-2010-BLG-117: An Obvious Planet without a Good Binary Model

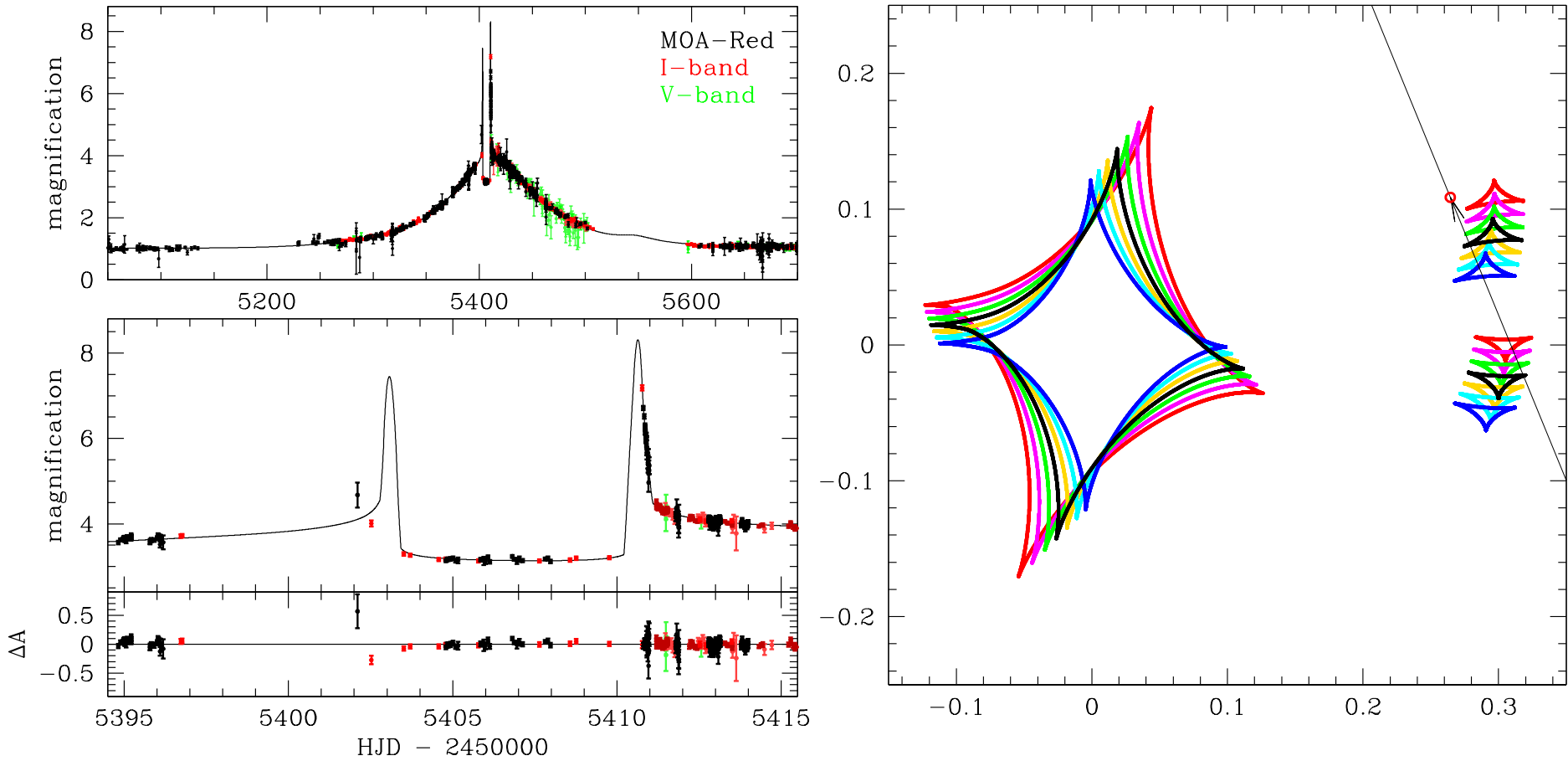
Light curve morphology indicates a planetary minor image caustic crossing event, but light curve doesn't fit.

De-magnification trough is too shallow.

Fill it in with another lens or another source.



# MOA-2010-BLG-117: Circumbinary Model



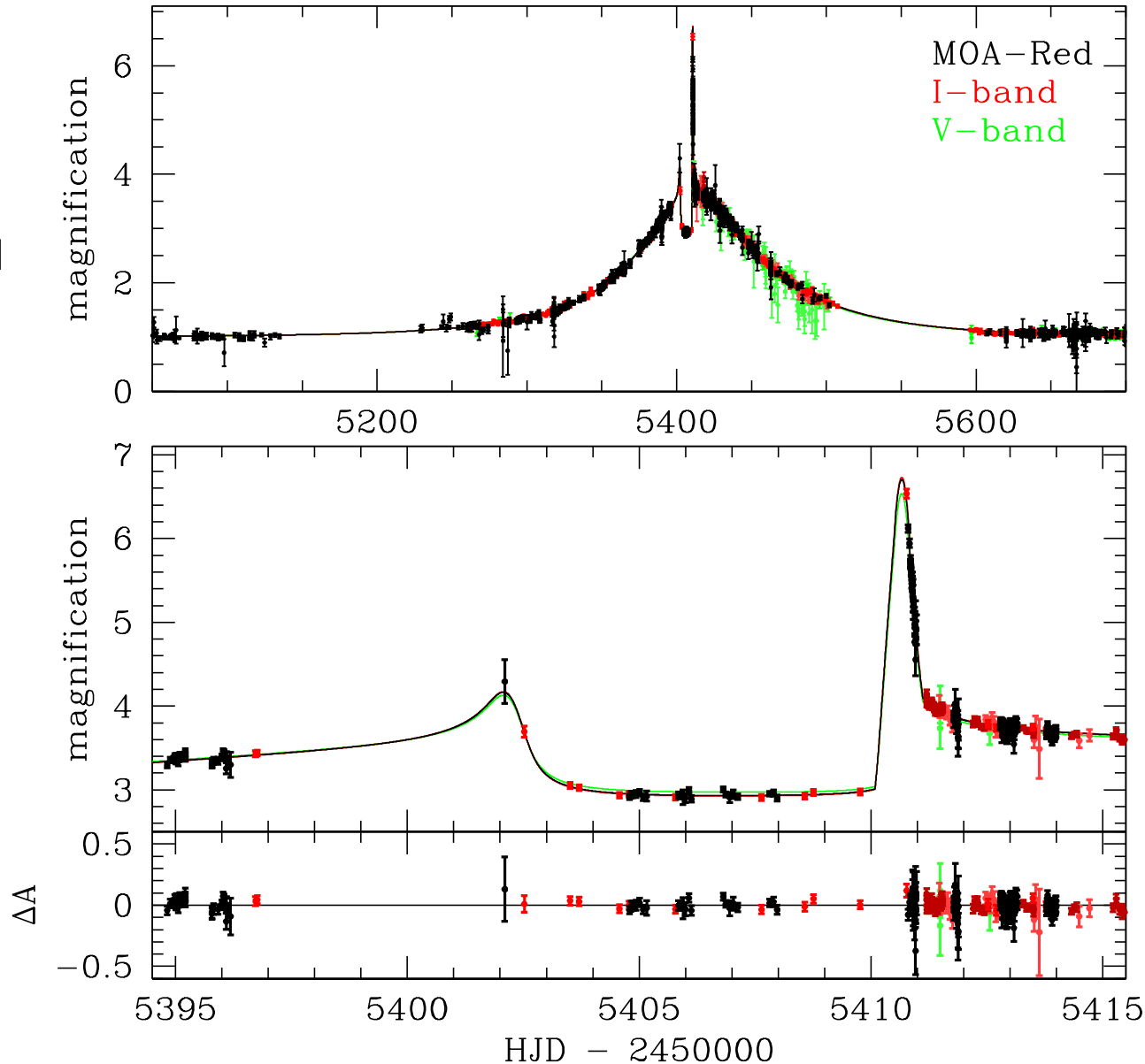
Circumbinary is a better fit – better than first attempts at binary source, but the cusp motion tracks the source at an implausibly large velocity,

# MOA-2010-BLG-117: Binary Source Model

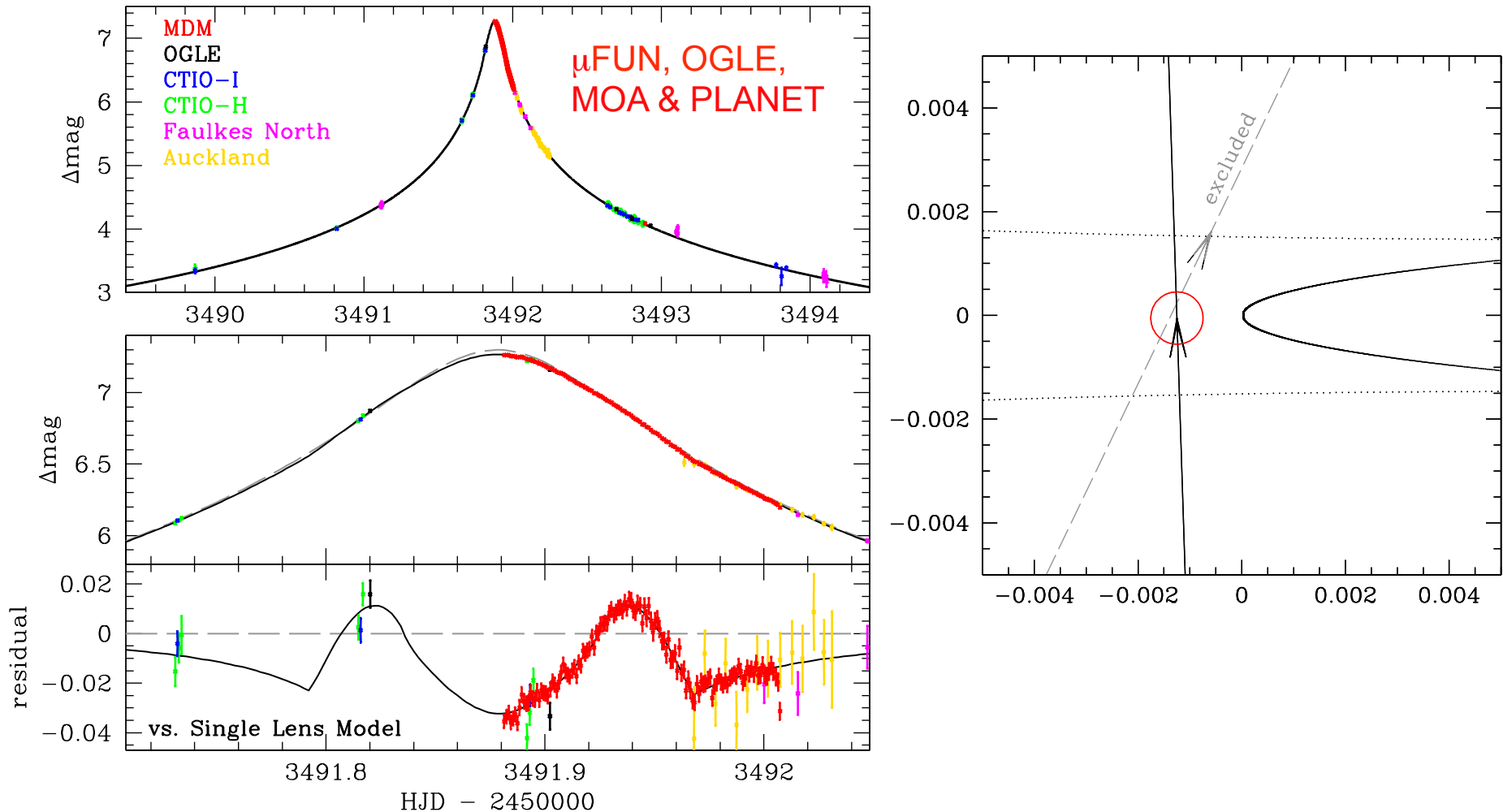
Source flux ratio was fixed to be consistent in the different data sets.

This removed local  $\chi^2$  minima and allowed a much better solution to be found.

Note the different light curves in different passbands.



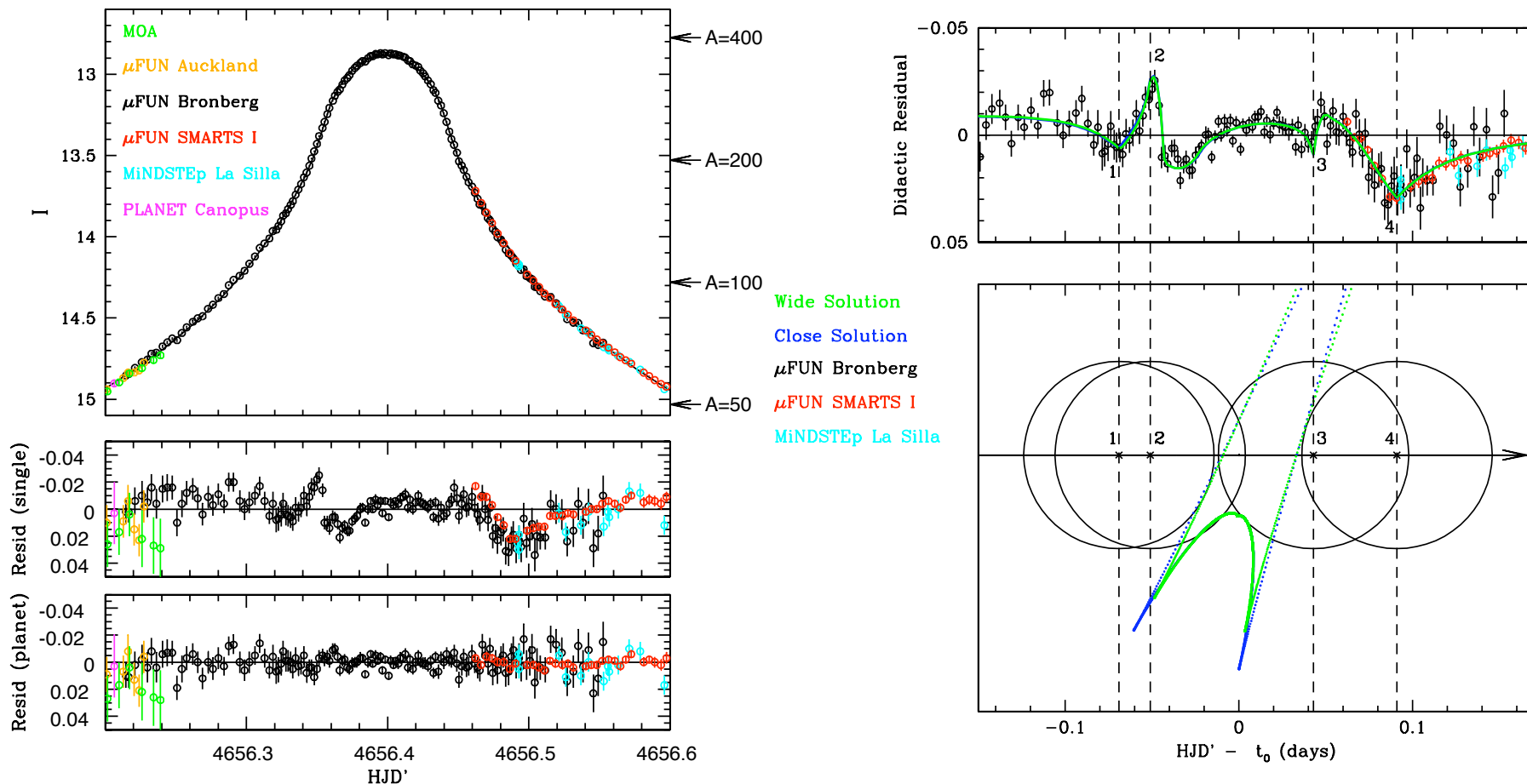
# Events Difficult to Detect by Inspection



Subtle, weak caustic crossing missed by  $\mu\text{FUN}$ , OGLE & PLANET for 8 months.

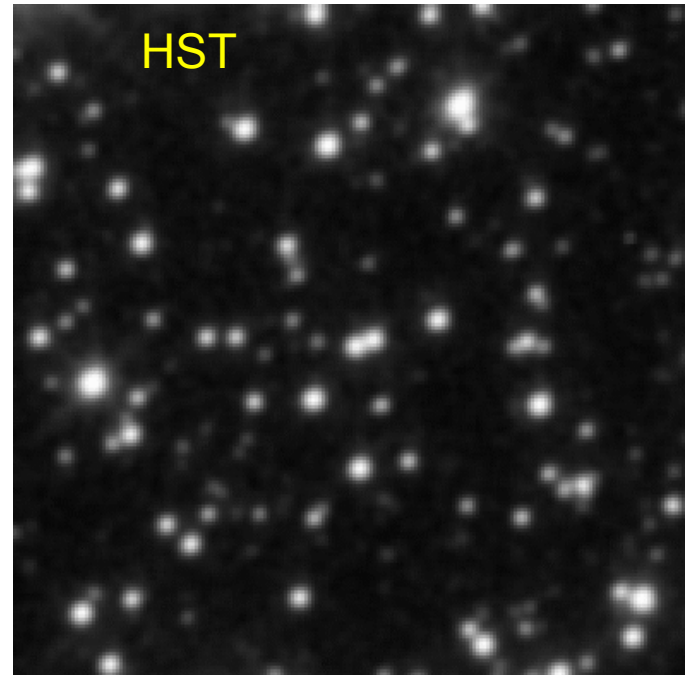
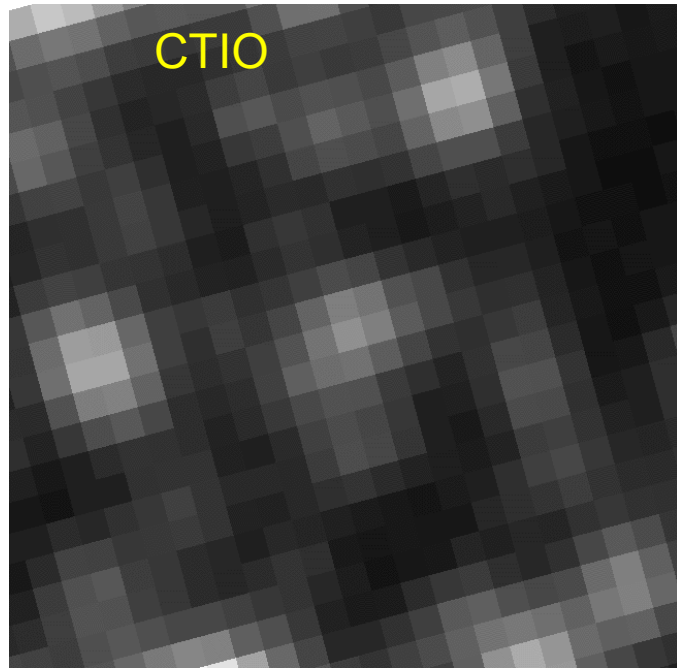
Signal noticed by Nick Rattenbury of MOA, which had no data.

# Events Difficult to Detect by Inspection (2)



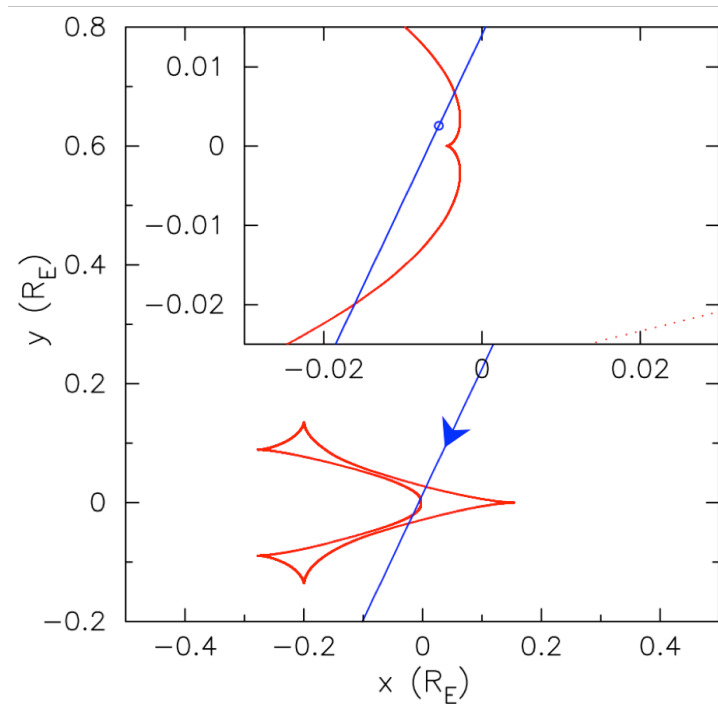
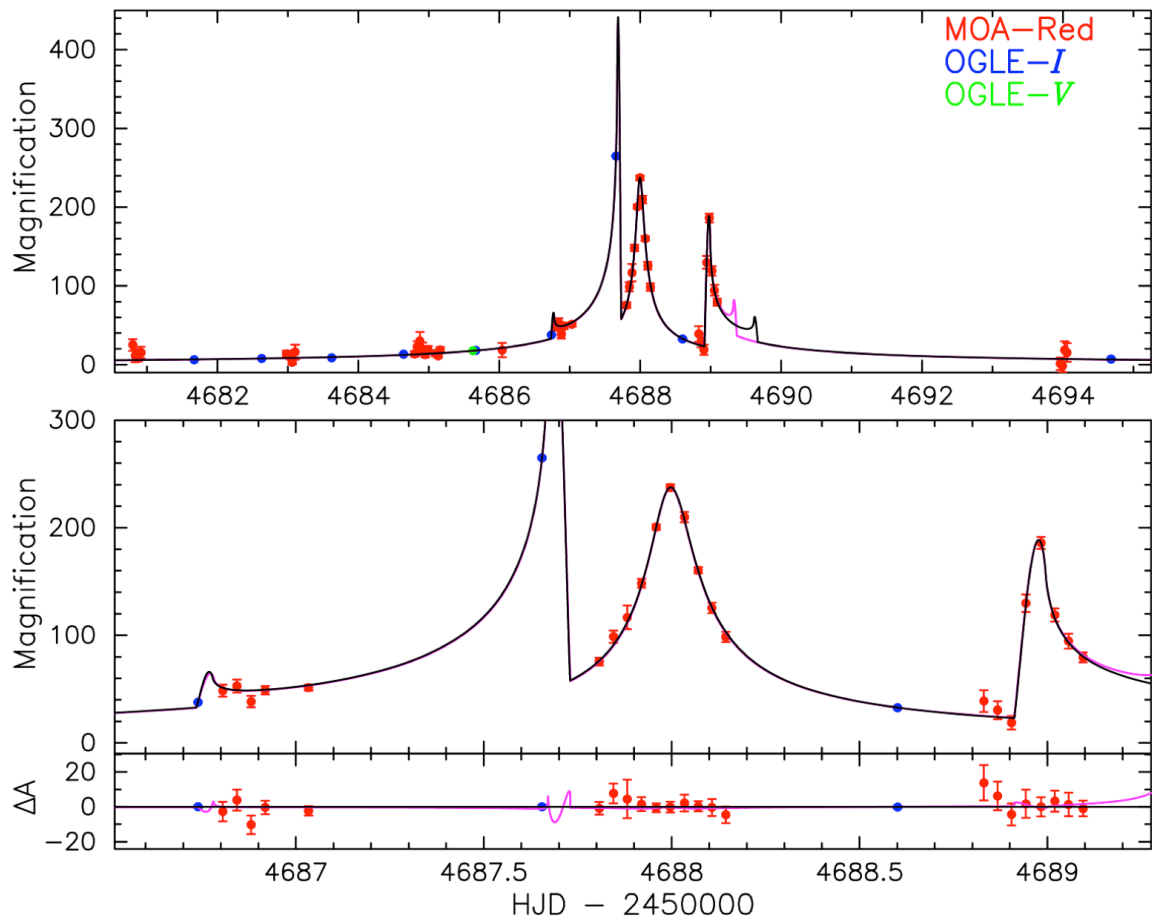
Like OGLE-2005-BLG-169, MOA-2008-BLG-310 (primarily) crossed the weak forward part of the central caustic, but the source radius was also larger than the caustic width

# Most Microlensing Events Have Unresolved Source Stars



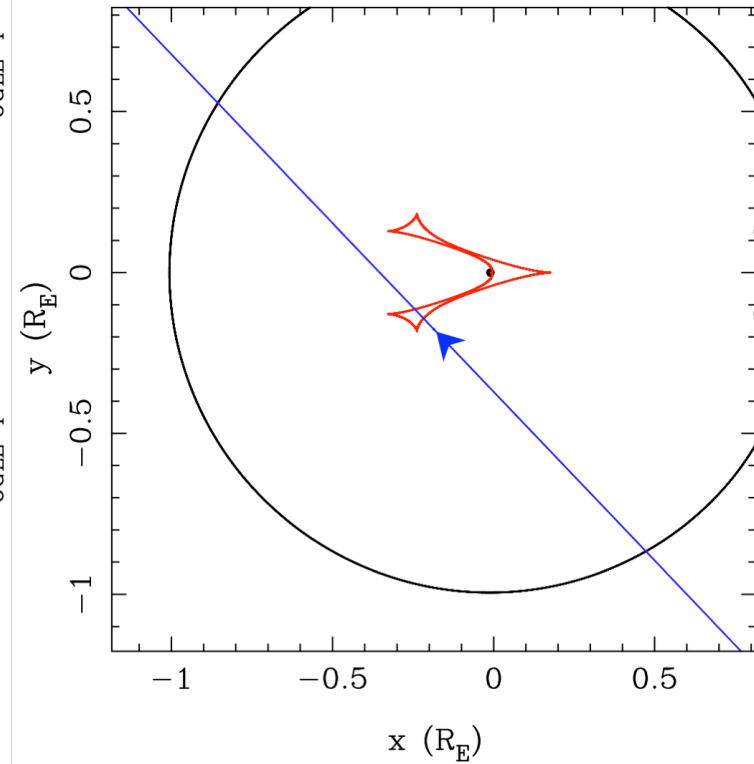
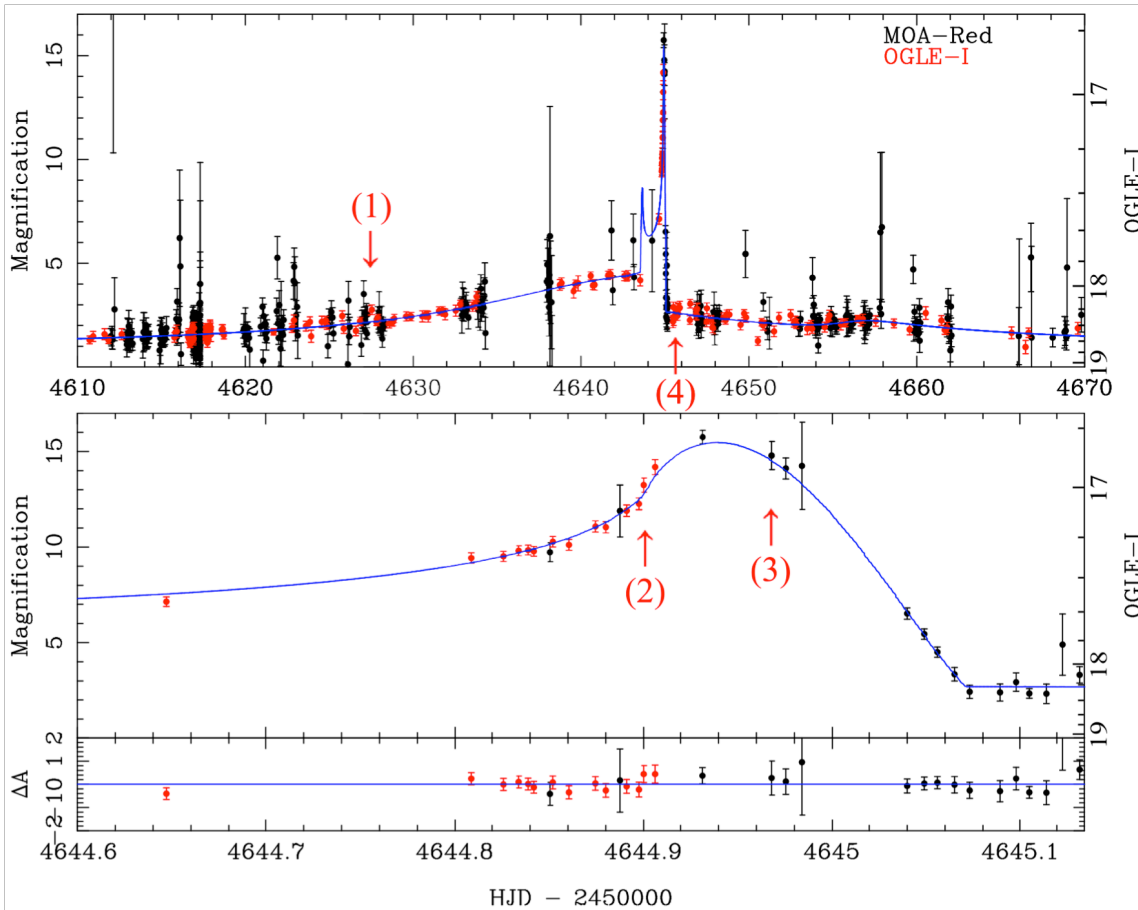
- But at high magnification (say  $A \geq 100$ ), they are resolved
- Several bright main sequence source stars per arc sec<sup>2</sup> .

# Events Difficult to Classify by Inspection



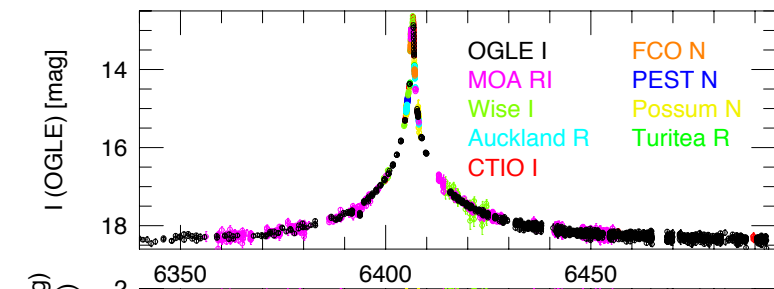
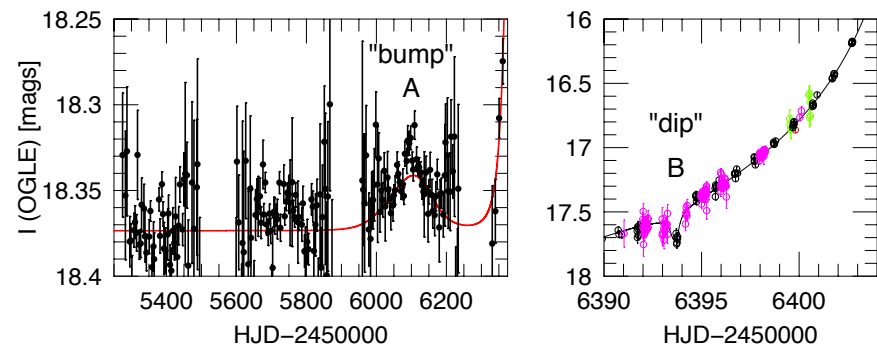
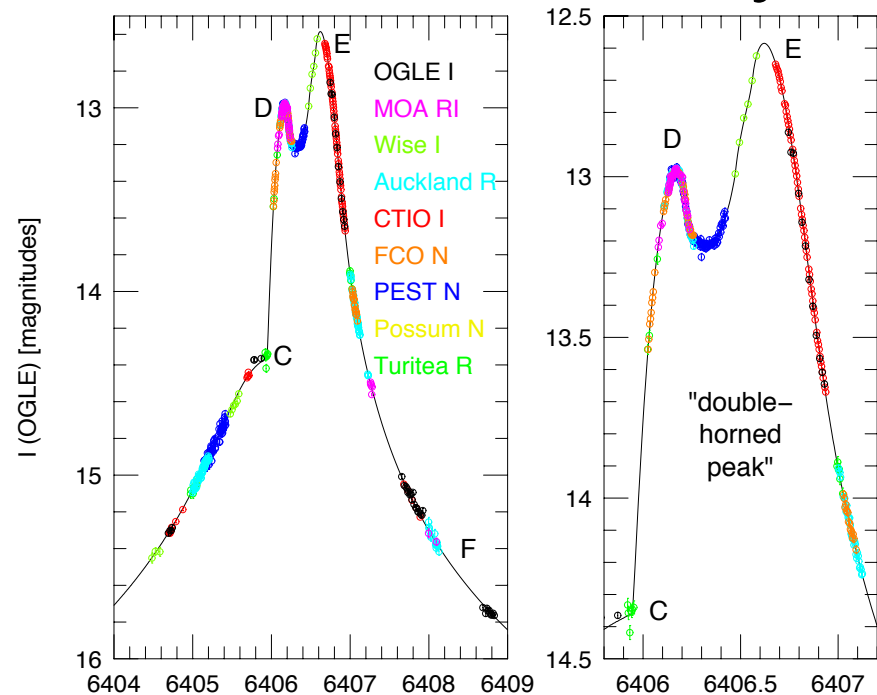
MOA-2008-BLG-379 not identified as planetary for 3 years until a systematic analysis of all MOA binary events. High mag event with faint source. Light curve is dominated by strong caustic crossing and cusp approach features on the “back” side of the central caustic

# Events Difficult to Classify by Inspection

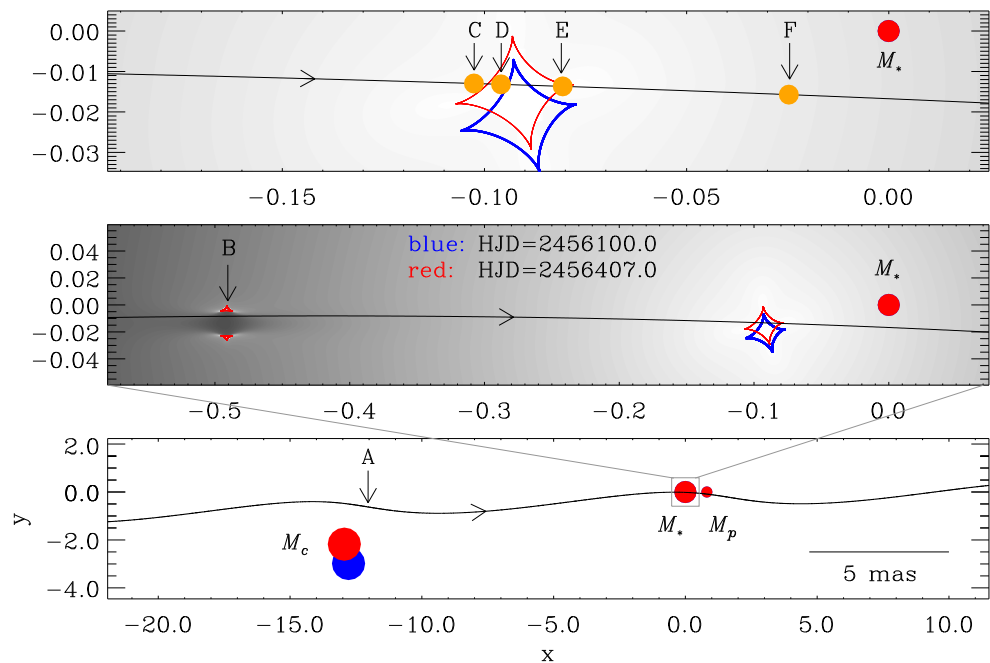


OGLE-2008-BLG-355 not identified as planetary for 3.5 years until a systematic analysis of all MOA binary events. Moderate mag event with an  $I = 20$  source. Light curve is dominated by strong caustic crossing and cusp approach features on the “back” side of the central caustic

# Planet in Binary: OGLE-2013-BLG-0341



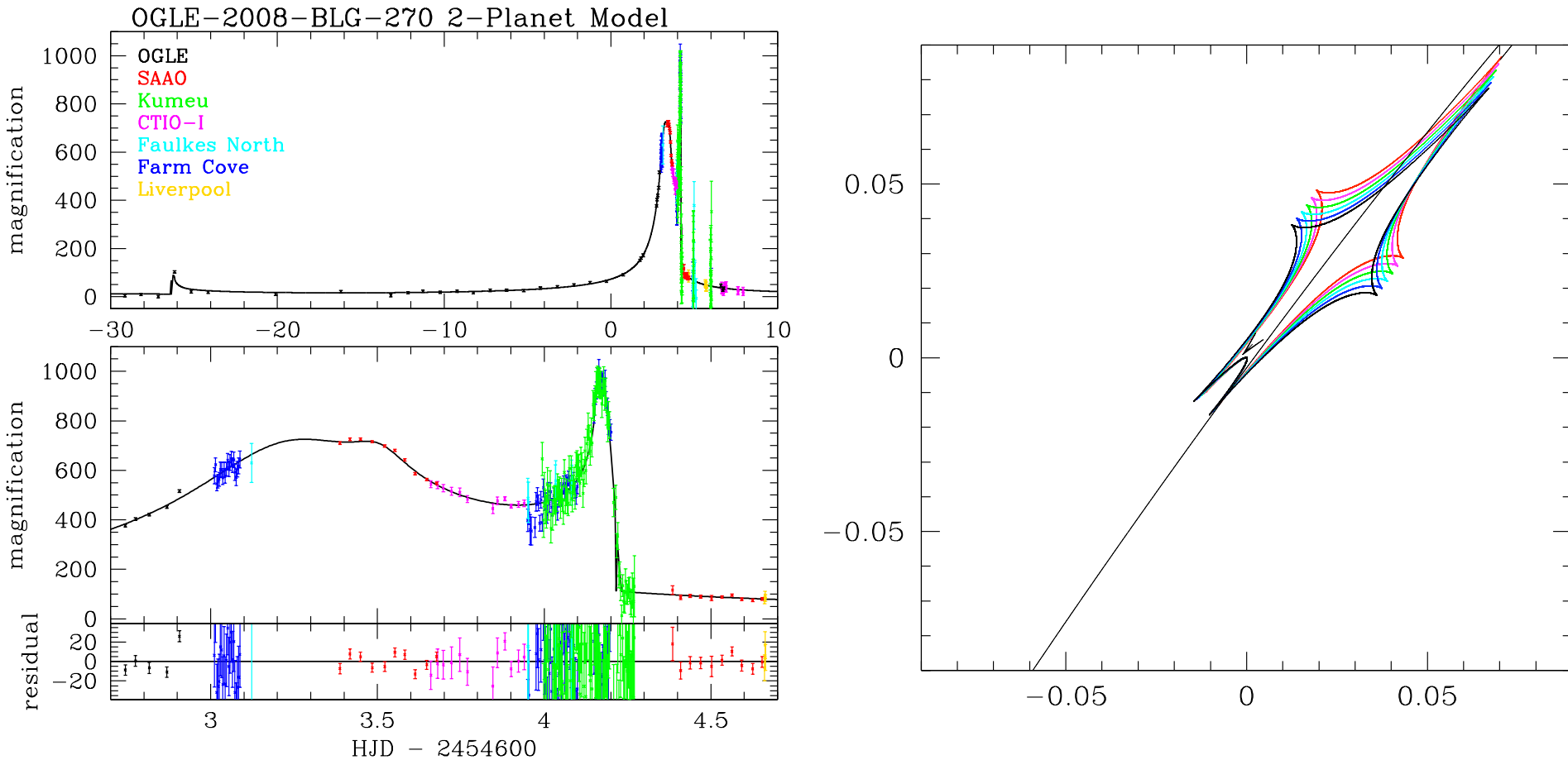
Close Model has  $s_3/s_2 = 5.1$



Very lucky to have planetary caustic signal (< 1%), but planetary signal can be detected without planetary caustic detection.

**Have we missed other planets in binary systems?  
Undiscovered planets?**

# Mystery Event: OGLE-2008-BLG-270

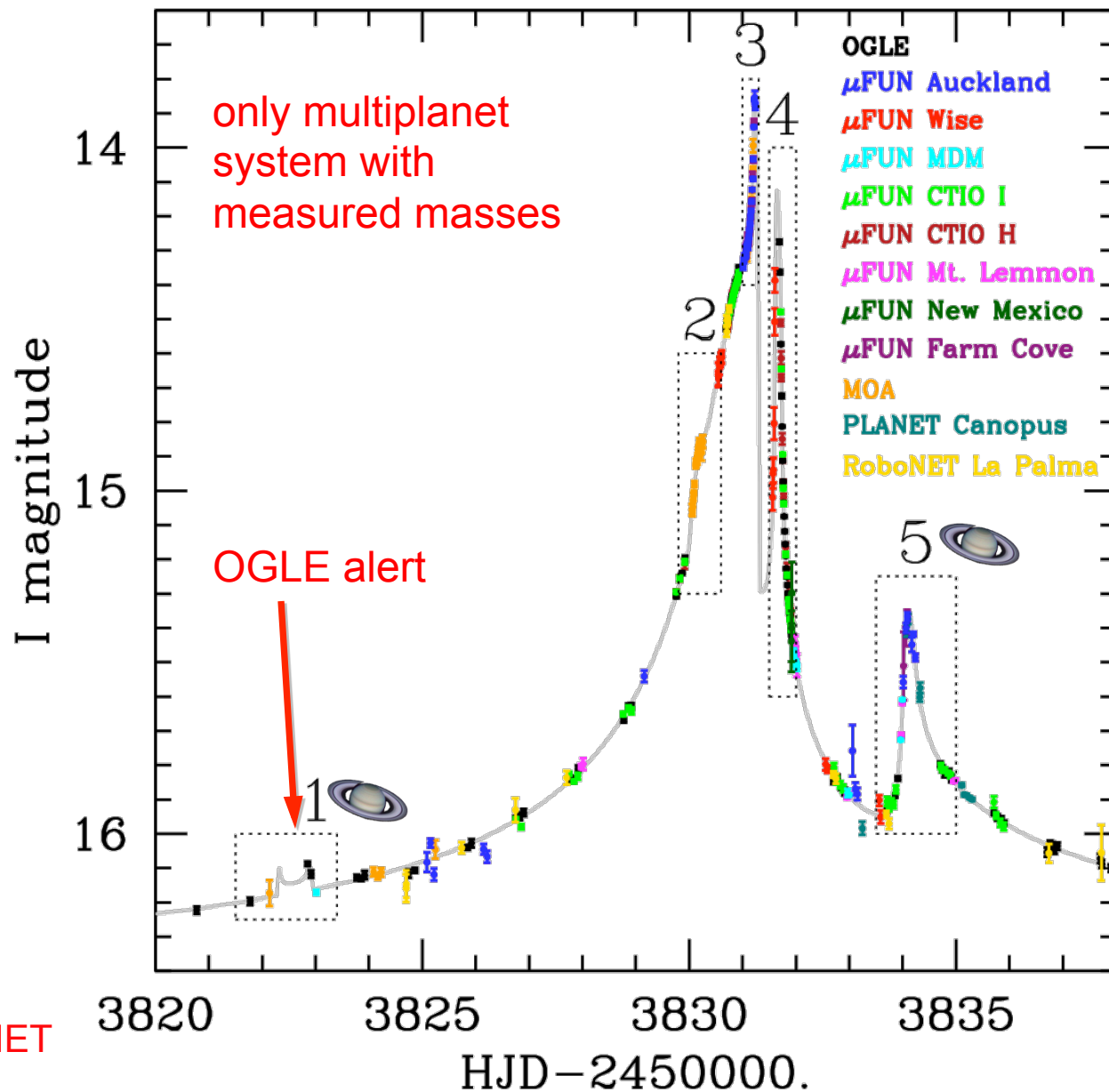


Likely triple lens system with orbital motion, but best known fit is not a good fit, and nearly tangential caustic crossing implies a  $> 2 M_{\text{solar}}$  lens star.

High dimensional model parameter space is difficult to search.

# Double-Planet Event: OGLE-2006-BLG-109

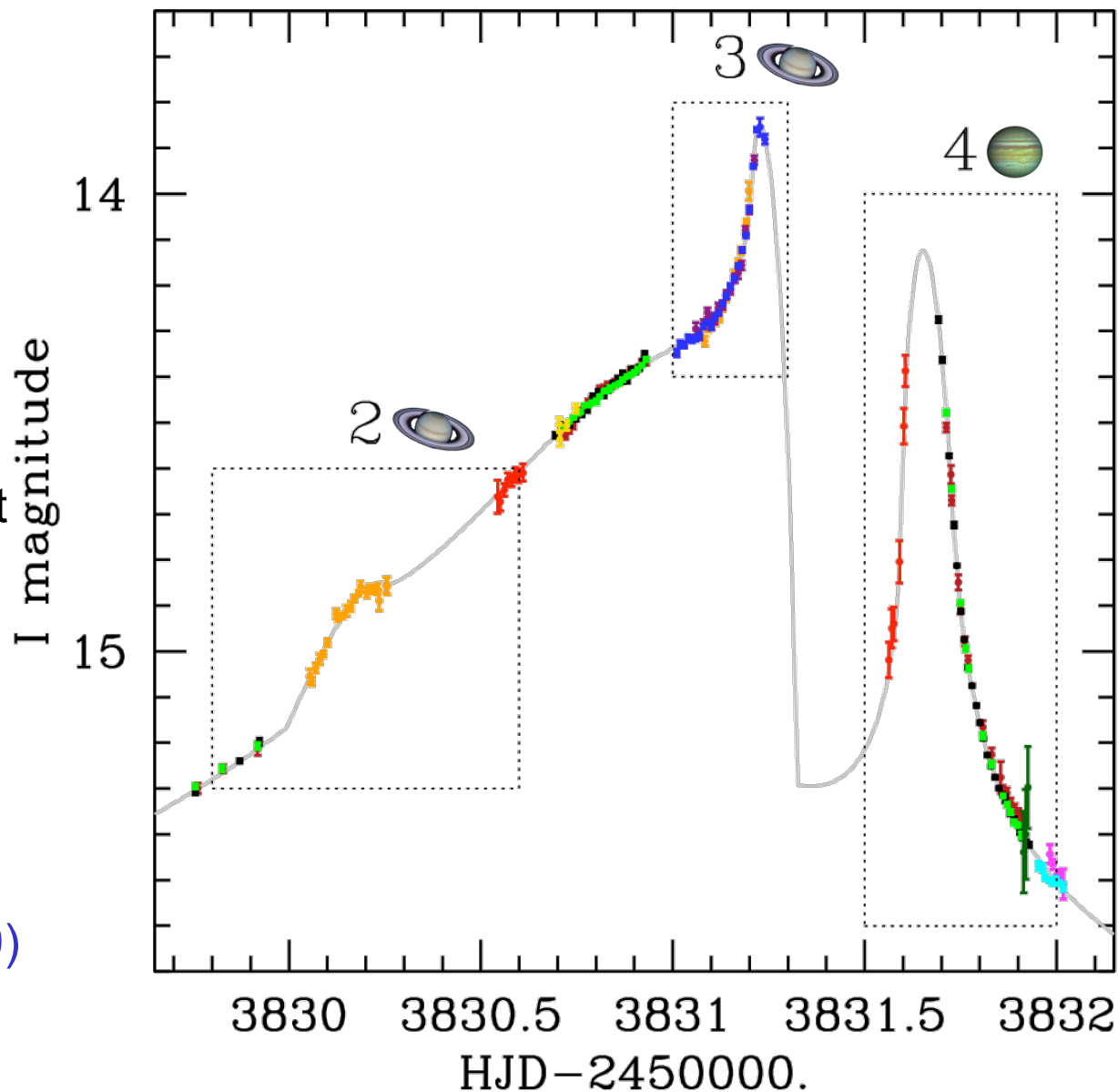
- 5 distinct planetary light curve features
- OGLE alerted 1<sup>st</sup> feature as potential planetary signal
- High magnification
- Feature #4 requires an additional planet
- Planetary signals visible for 11 days
- Features #1 & #5 require the orbital motion of the Saturn-mass planet



# OGLE-2006-BLG-109 Light Curve Detail

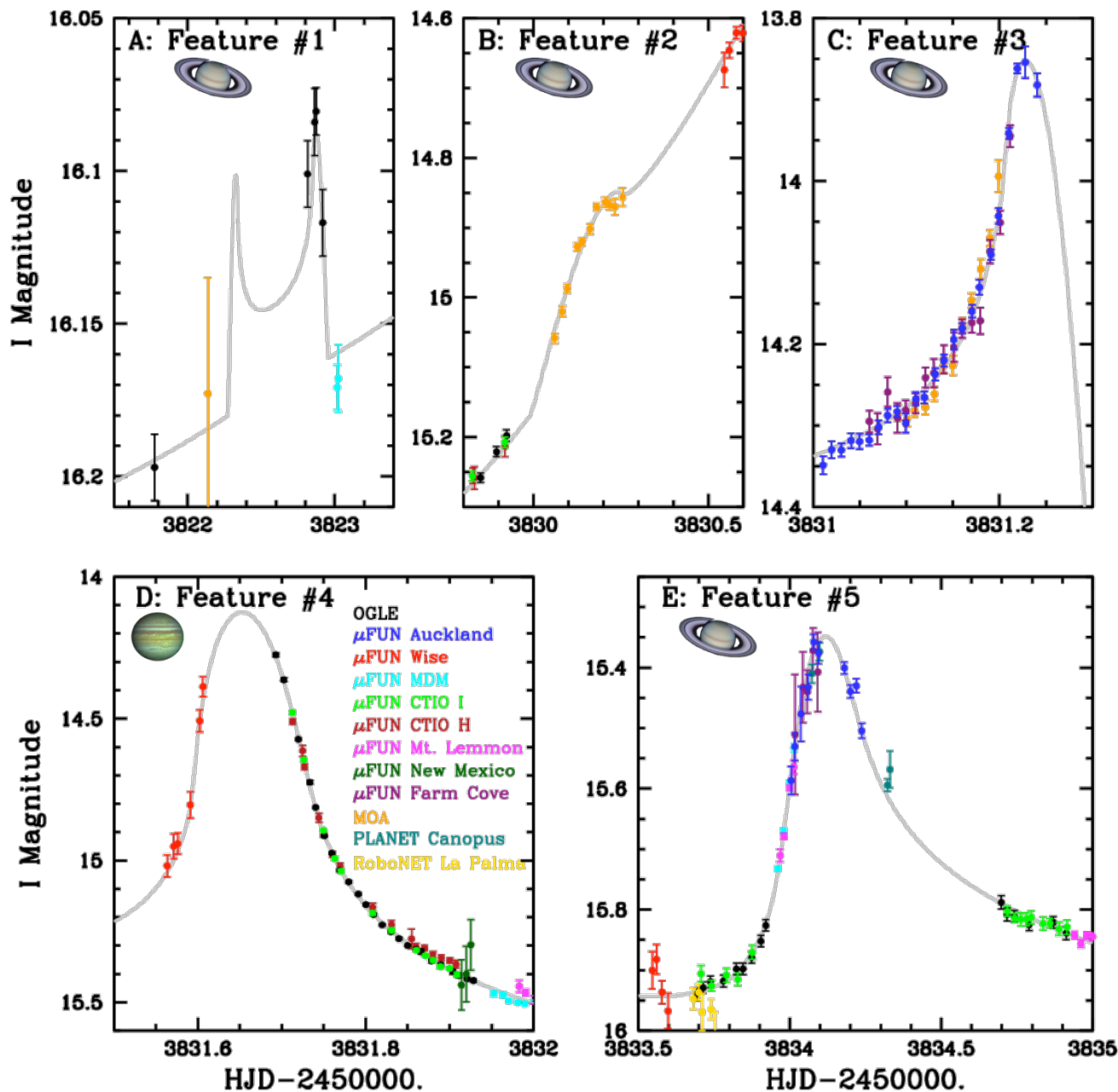
- OGLE alert on feature #1 as a potential planetary feature
- $\mu$ FUN (Gaudi) obtained a model approximately predicting features #3 & #5 prior to the peak
- But feature #4 was not predicted - because it is due to the Jupiter - not the Saturn

Gaudi et al (2008)  
Bennett et al (2010)

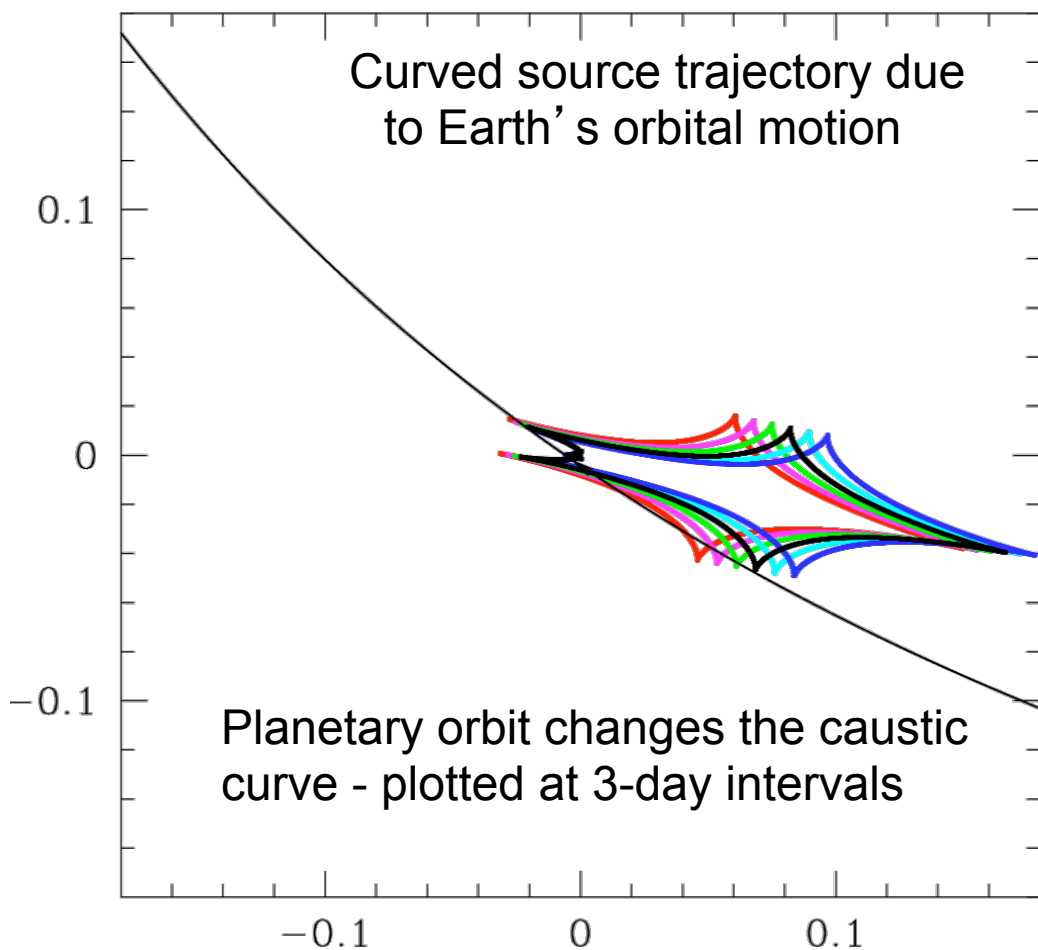


# OGLE-2006-BLG-109 Light Curve Features

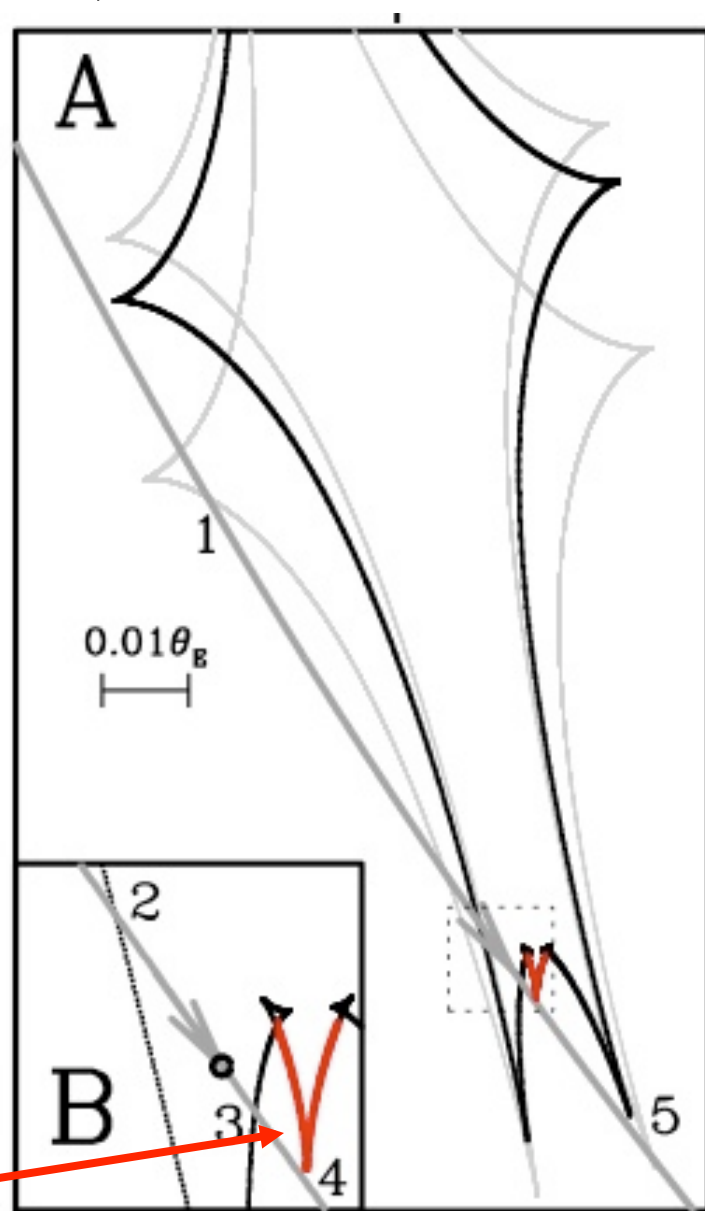
- The basic 2-planet nature of the event was identified during the event,
- But the final model required inclusion of orbital motion, microlensing parallax and computational improvements (by Bennett).



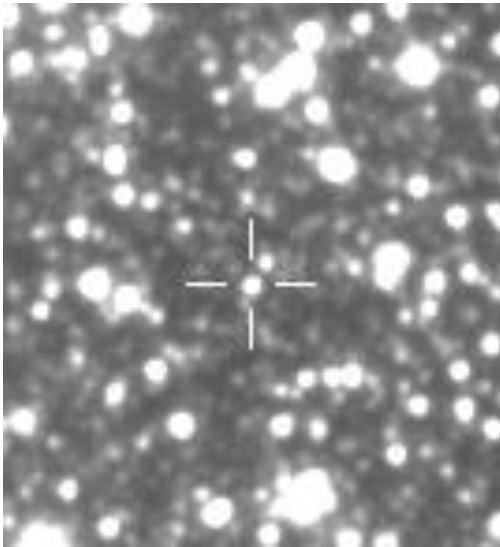
# OGLE-2006-BLG-109Lb,c Caustics



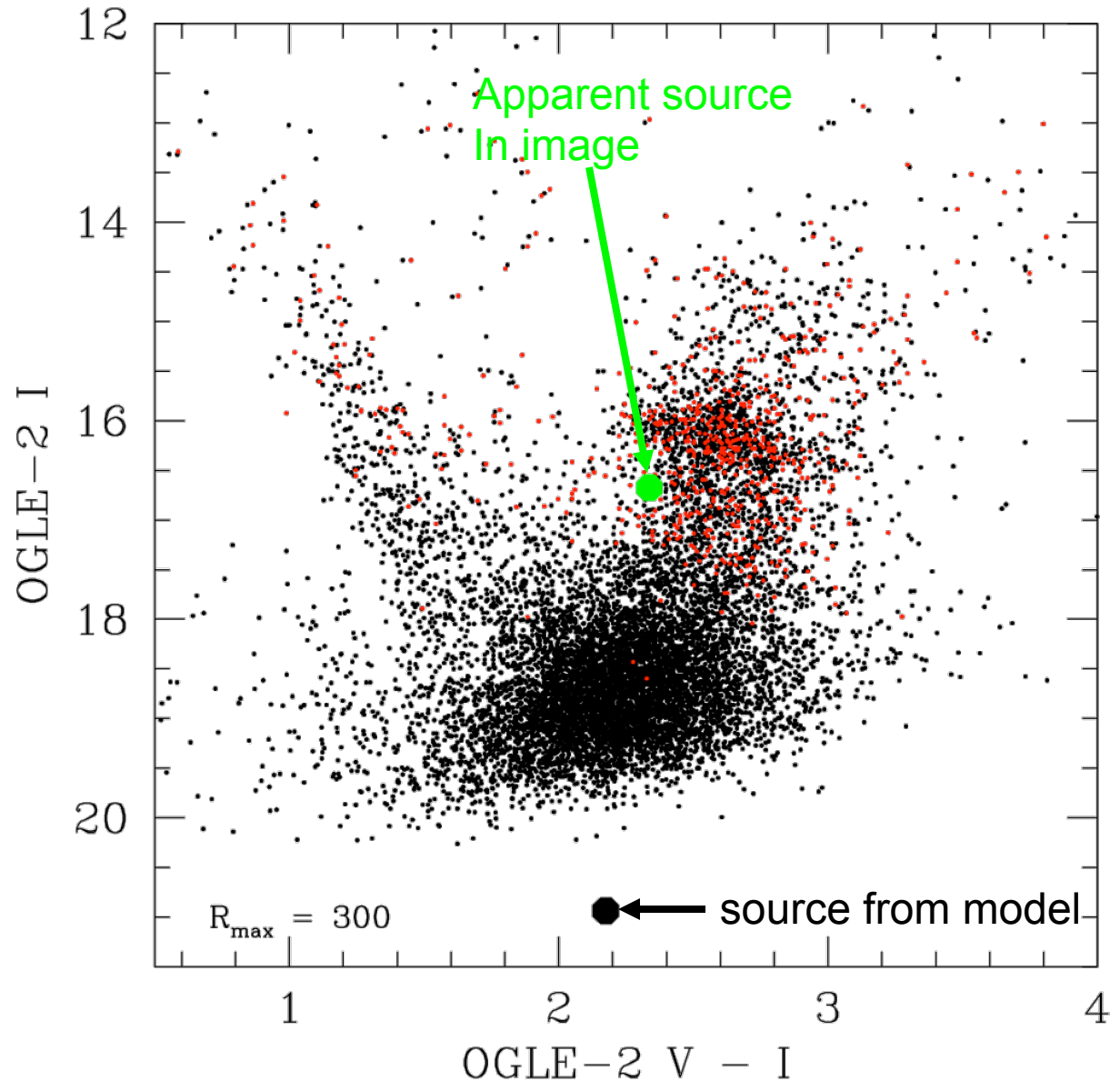
Feature due to Jupiter



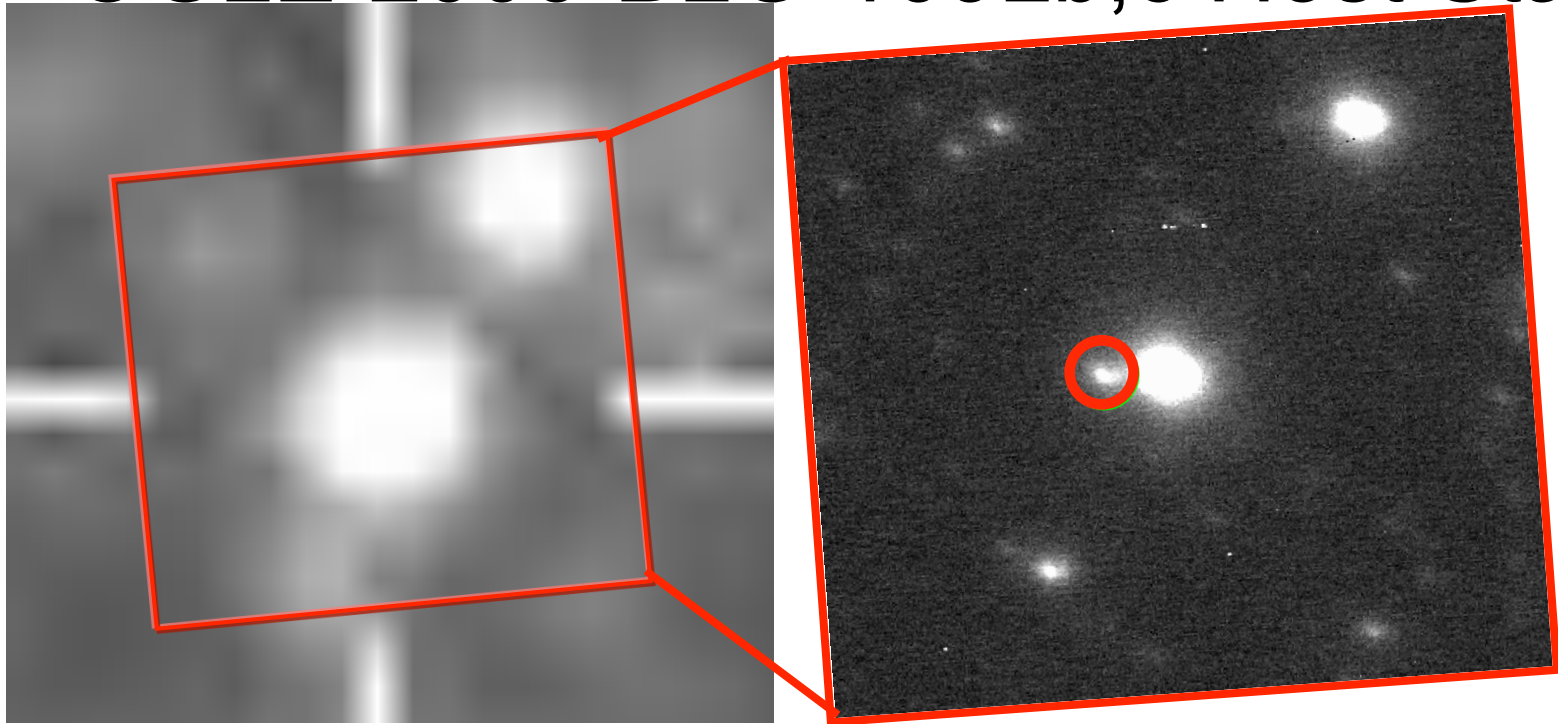
# OGLE-2006-BLG-109 Source Star



The model indicates that the source is much fainter than the apparent star at the position of the source. Could the brighter star be the lens star?



# OGLE-2006-BLG-109Lb,c Host Star



- OGLE images show that the source is offset from the bright star by 350 mas
- B. Macintosh: Keck AO images resolve lens+source stars from the brighter star.
- But, source+lens blend is 6 $\times$  brighter than the source (from CTIO H-band light curve), so the lens star is 5 $\times$  brighter than source.
  - H-band observations of the light curve are critical because the lens and source are not resolved
- Planet host (lens) star magnitude  $H \approx 17.17$ 
  - JHK observations will help to constrain the extinction toward the lens star

# First Multiplanet System with Measured Masses

Host star mass:  $M_L = 0.52^{+0.18}_{-0.07} M_\odot$  from light curve model.

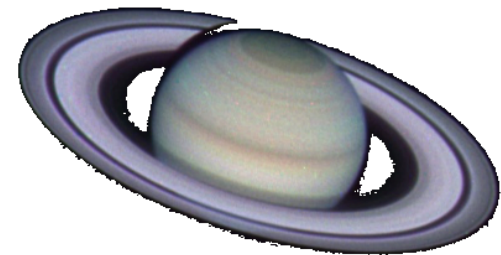
- Apply lens brightness constraint:  $H_L \approx 17.17$ .
- Correcting for extinction:  $H_{L0} = 16.93 \pm 0.25$ 
  - Extinction correction is based on  $H_L - K_L$  color
  - Error bar includes both extinction and photometric uncertainties
- Lens system distance:  $D_L = 1.54 \pm 0.13$  kpc

Host star mass:  $M_L = 0.51 \pm 0.05 M_\odot$  from light curve and lens H-magnitude.

Other parameter values:

- “Jupiter” mass:  $m_b = 0.73 \pm 0.06 M_{\text{Jup}}$
- semi-major axis:  $a_b = 2.3 \pm 0.5 \text{ AU}$
- “Saturn” mass:  $m_c = 0.27 \pm 0.03 M_{\text{Jup}} = 0.90 M_{\text{Sat}}$
- semi-major axis:  $a_c = 4.5^{+2.2}_{-1.0} \text{ AU}$
- “Saturn” orbital velocity:  $v_t = 9.5 \pm 0.5 \text{ km/sec}$
- eccentricity:  $\varepsilon = 0.15^{+0.17}_{-0.10}$
- inclination:  $i = 63 \pm 6^\circ$

# Full Orbit Determination for OGLE-2006-BLG-109Lc



- Full calculation using Markov chains run at fixed acceleration.
- Include only Hill-stable orbits
- results:

$$M_{LA} = 0.51 \pm 0.05 M_{\odot}$$

$$M_{Lc} = 0.27 \pm 0.03 M_J$$

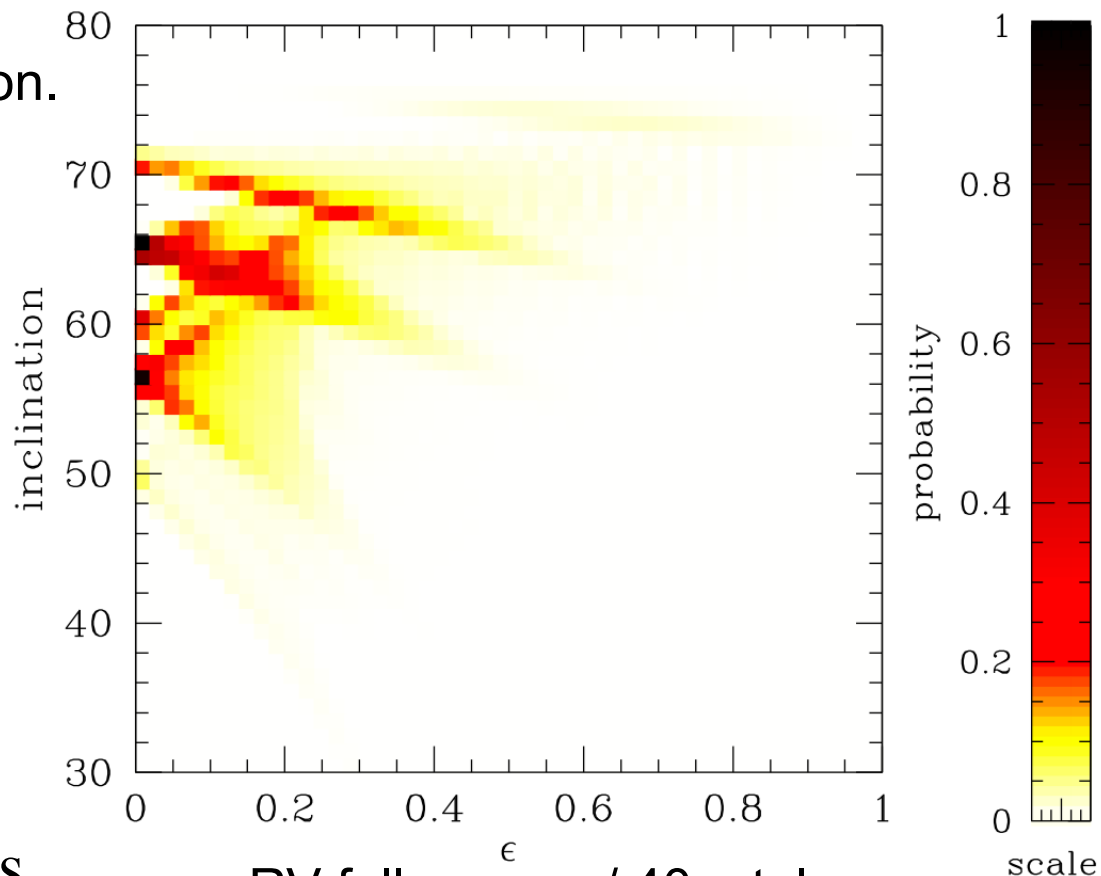
$$M_{Lb} = 0.73 \pm 0.07 M_J$$

$$a_{Lc} = 4.5^{+2.2}_{-1.0} \text{ AU}$$

$$a_{Lb} = 2.3 \pm 0.5 \text{ AU}$$

$$\text{inclination} = 64^{+4}_{-7} \text{ degrees}$$

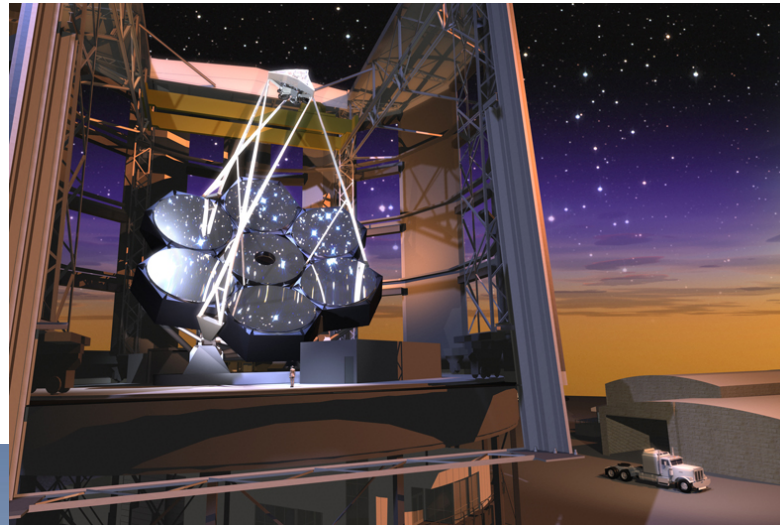
$$\varepsilon = 0.15^{+0.17}_{-0.10}$$



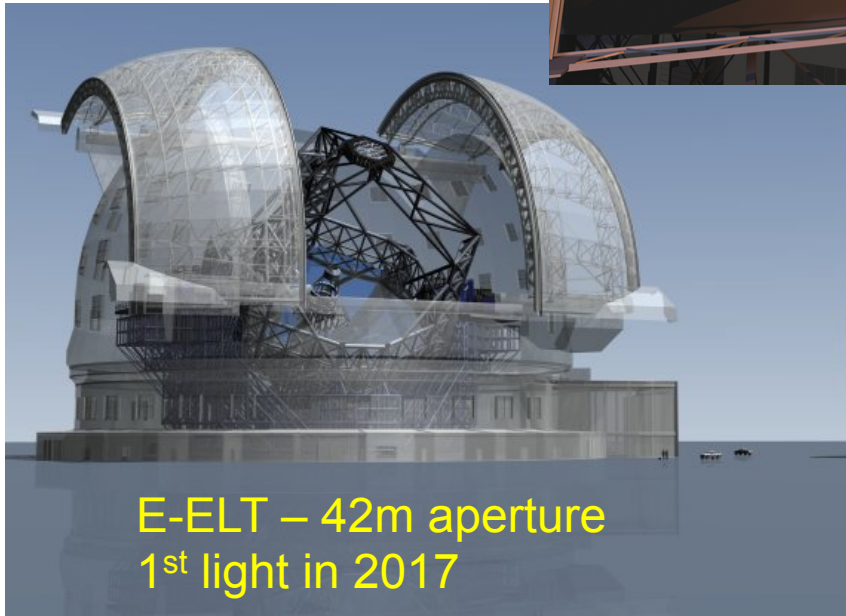
- RV follow-up w/ 40m telescope

$$-K = 19 \text{ m/sec} \quad (H = 17.2)$$

# Future Doppler Radial Velocity Confirmation



GMT - 22m aperture  
1<sup>st</sup> light in 2017



E-ELT – 42m aperture  
1<sup>st</sup> light in 2017



TMT – 30m aperture  
1<sup>st</sup> light in 2017

A high throughput, high resolution spectrograph on a 22-40m aperture telescope can measure the 19 m/s RV signal

